11-2016

Understanding the Differences Between Neuronal Calcium Sensor Proteins: A Comparison of Neurocalcin Delta and Hippocalcin

Jeffrey M. Viviano
Rowan University

UNDERSTANDING THE DIFFERENCES BETWEEN NEURONAL CALCIUM SENSOR PROTEINS: A COMPARISON OF NEUROCALCIN DELTA AND HIPPOCALCIN

Jeffrey M. Viviano, B.S

A Dissertation submitted to the Graduate School of Biomedical Sciences, Rowan University in partial fulfillment of the requirements for the Ph.D. Degree.

Stratford, New Jersey 08084

November 2016

Table of Contents

Acknowledgements

Throughout my six-year tenure at Rowan University, there have been many people who have aided me in the completion of my PhD. I feel that the education I received at Rowan University will help me attain my goals in life of becoming an independent scientist. Representing the school, I must thank Dr. Worrad, Dr. Hock, and the rest of the GSBS staff who have aided me in completing my thesis work, and providing an exceptional learning environment.

First and foremost, I must thank my P.I., Dr. Venkateswar Venkataraman. His laboratory has set me up with a fantastic project, which has yielded multiple publications. I have enjoyed our in-depth discussions of scientific material. In addition, I greatly appreciate how he has allowed me to try new experiments, explore new ideas, and find my own niche within the project. I found that our similar personalities and ability to challenge each other allowed not only myself and the project to grow, but has also helped me to think critically. Most of all, I appreciate how he has always treated me like a family member, and not like another employee.

I cannot fully express how helpful Dr. Anu Krishnan has been to my advancement. From running the laboratory every day, to teaching me new techniques, her guidance has been greatly appreciated. Her contribution to my growth as a scientist cannot be understated. In addition, I must thank her for having a kind heart and always treating me like one of her own children.

My committee has been an essential part of my growth as a scientist. Dr. Anikin, Dr. Temiakov, Dr. Nagele, and Dr. Moss have each greatly contributed to my

growth as a scientist, providing insight through discussions and other resources. In particular, I must thank my committee chair, Dr. Anikin, who has provided me with much scientific support, including aiding in the design of novel experiments and in teaching me new techniques. Additionally, I would like to thank Dr. Nagele, who has provided me much guidance as a young scientist.

I must thank my lab mates over the past six years, Hao Wu and Jingyi Zhang. Not only have they provided me emotional support inside the laboratory, but outside of the laboratory as well. Our adventures include traveling to New Orleans and hiking in Shenandoah National Park. These adventures have helped make the years even more enjoyable. In addition to this support, Hao and Jingyi have always provided me a strong sounding board for scientific discussion and discovery.

I would be remiss if I did not thank my parents Mike and Donna, as well as my brother Ross Viviano. From a young age my family has always supported my love of science, whether it be providing me with an endless supply of scientific books, taking me fossil hunting, or building a museum in our basement. My family has always encouraged me to follow my passion and I am forever grateful for everything they have provided for me.

I feel extremely fortunate to be part of a class with so many talented people. My classmates provided much support throughout the difficult course work. In particular I must thank Shuang "Steve" Wu who always gave me someone to talk to at lunch, and a partner to study with, and Yaroslav Morozov who aided me with experiments.

At Rowan University I was fortunate enough to meet my fiancée, Cassandra

DeMarshall. She has provided me much emotional and mental support throughout the years. I am extremely grateful to have met someone with a great mind to discuss science when it is necessary, and someone with such a caring heart with which to enjoy life. I feel extremely fortunate because I have met someone who I can relate to at every level. I cannot wait to see what our future together brings.

Abstract

Many neuronal functions, including learning and memory are driven by changes in intracellular Ca^{2+}concentrations. The Neuronal Calcium Sensor (NCS) family of proteins is responsible for mediating the response to calcium. They are typically comprised of 4 EF hands; of which EF 2, 3, and 4 bind calcium.

Hypothesis: NCS proteins carry out unique, non-overlapping functions, and that specific characteristics of the family can be mapped to precise regions of the proteins.

Results: The effect on the following properties were investigated primarily on two highly similar NCS proteins, Neurocalcin Delta (NCALD) and Hippocalcin (HPCA): (1) Response to calcium was determined through two independent methods: change in tryptophan fluorescence and migration on a native polyacrylamide gel (CIMSA); (2) size exclusion chromatography, (3) Calcium binding, (4) Guanylate Cyclase stimulations and (5) sequence analysis. These results lead to the conclusion that specific aa locations are hyper-variable and pivotal in determining how the proteins respond.

Chapter 1. Introduction

1.1.1 The Neuronal Calcium Sensor Family of Proteins

Calcium is a critical signaling molecule in many neuronal functions such as vesicular trafficking, synaptic transmission, and programmed cell death. Changes in intracellular levels of calcium are critical in determining neuronal responses [5-7]. These neuronal responses underlie the physiological processes such as emotions, thought, sleep, and memory [5, 6]. Alterations in these processes lead to disorders such as Alzheimer's disease, insomnia, autism, dystonia, or narcolepsy [8-11]. Changes in calcium concentrations are critical for neurotransmitter release [12]. Therefore, signaling pathways that are designed to sense changes in intracellular calcium are particularly honed by evolution in neuronal cells.

The Neuronal Calcium Sensor (NCS) family of proteins governs the cellular response to calcium signals. They are contained within the super family of proteins that are characterized by the presence of the calcium-binding EF-hand motif. Distant members of this family include Calmodulin and the S100 super family [13, 14]. The members of the NCS family are encoded by 14 distinct genes: Frequenin (FRQN), Visinin-like Protein 1 (VSNL1), Hippocalcin-like Protein 1 (HPCAL1), Hippocalcin-like Protein 4 (HPCAL4), Neurocalcin delta (NCALD), Hippocalcin (HPCA), K-Channel Interacting Proteins 1 through 4 (KChIP1-4), Guanylate Cyclase Activator Proteins 1 through 3 (GCAP1-3) and Recoverin (RCVRN) [15]. Multiple splice-variants have been identified for several of the NCS members. This highly conserved family is typically 190-200 amino acid residues long, and share more than 45%

sequence identity (reviewed in: [16]). This family of proteins is characterized by 4 EF-hand motifs which are helix-loop-helix structures that bind calcium [17]. The EF hands are distributed between the N and C-terminal lobes of the protein. EF-1 and EF-2 are located in the N-terminal half of this protein, while EF-3 and EF-4 are in the C-terminal half of the protein [18]. For most of the NCS members, EF-2-4 bind calcium, while EF-1 is non-functional with respect to binding calcium, due to a conserved Cys-Pro mutation.

Proteins of the NCS family were initially isolated in the neurons of different species where they carry out critical functions. For example, loss of function of specific members has been demonstrated to cause loss of memory formation in nematodes [19] and mice [20], while others are linked to inherited visual degeneration [21-23]. In many instances, the defect has been traced to the loss of ability to sense and respond to changes in calcium in the neuron [21, 24-26], which is the primary functional feature of this family of proteins. However, many of these proteins are also expressed outside the nervous system and interact with a variety of targets in multiple cell types (some excellent reviews are: [5, 6, 18, 27]), suggesting that the calcium-dependent modulation by these proteins is not restricted to neurons. Many of the individual members have also been characterized extensively at the biochemical and molecular level [28-31].

NCS members have a N-terminal myristoylation site, where they are known to be myristoylated by the enzyme N-myristoyl transferase. The covalently linked myristoyl group allows for the interaction with lipid bilayers, and facilitates

interaction with other membrane proteins [6]. This myristoylated N-terminus facilitates the translocation from the cytosol to the membrane [18, 32], and has been demonstrated to be critical for targeting NCS proteins to specific membrane locations[33, 34]. In this manner, the modification allows the proteins to respond spatially to a calcium signal. In addition, some NCS members have been shown to be modified by palmitoylation [35] at the N-terminus.

The N-terminal myristoyl group is a critical component of the calcium myristoyl switch mechanism, which is the method by which NCS proteins respond to calcium. This mechanism was first described with the resolution of the structure of Recoverin [36], and has been identified in several other NCS members [37-39]. In the absence of calcium, the N-terminal myristoyl group is sequestered in the protein's hydrophobic core. This prevents the fatty acid from interacting with the intracellular membrane and, perhaps, other binding partners such as guanylate cyclases. Upon the binding to calcium, the NCS protein's structure reorients by rotation around a hydrophobic core. This structural response causes the myristoyl group to extrude from the core of the protein and interact with additional partners [40, 41]. The structure (and therefore, the function) of these proteins oscillates between the calcium-bound and calcium-free state, while the transition is the calcium-myristoyl switch (reviewed in: [5, 42, 43]). For several NCS proteins, the binding of calcium induces changes in structure that may be detected, even under denaturing conditions on SDS polyacrylamide gel [30, 44-46].

Many members of the NCS family interact with guanylate cyclases [6, 45, 47-53]. Guanylate cyclases, or mGCs, are a class of transmembrane proteins, which catalyze the conversion of guanosine triphosphate (GTP) to 3',5'-cyclic guanosine monophosphate (cGMP). cGMP is a critical signaling molecule in the regulation of calcium homeostasis because it binds to cGMP gated calcium channels and modulates the influx of extracellular calcium [52]. The regulation of homeostatic calcium levels is necessary for many neuronal processes, but in particular for vision, and has been shown to be crucial for light adaptation in photoreceptors [54, 55].

1.2.1 The Sub Families of the Neuronal Calcium Sensor 1 (NCS1)

The 14 gene-coding members of the NCS family can be broken into five distinct sub families. NCS1 (Frequenin) and Recoverin are single members of their own subfamilies. GCAP-1, GCAP-2, and GCAP-3 make up the GCAPs, or the Guanylate-Cyclase Activating Proteins. The Potassium Channel-Interacting Proteins (KChIPs) family is comprised of KChIP1, KChIP2, KChIP3 and KChIP4. The final subfamily of Neuronal calcium sensor proteins is the Visinin-Like Proteins (VILIPs), which are made up of the members Neurocalcin Delta, Hippocalcin, VSNL1, HPCL1 and HPCL4. Each subfamily has common physiological characteristics and a shared structure, which ultimately derives function.

1.2.2 Neuronal Calcium sensor 1 (NCS1)

Neuronal Calcium sensor 1 (NCS1), or Frequenin in humans, is the archetypical NCS protein, and is observed in early eukaryotes [19, 56]. In *C. elegans,* NCS1 was demonstrated to not only be crucial for memory formation, but also that over expression of this NCS protein was able to increase memory [19]. In vertebrates, NCS1 has been shown to be critical for both nerve growth and synaptic transmission [57]. This clear role in neurons links NCS1 to several neurodegenerative diseases, including schizophrenia and bipolar disorder [58]. Point mutations in the EF-3 hand of NCS1 have been linked to autism [11, 59, 60] and the R102Q mutation impairs the type of calcium response NCS1 exhibits, perhaps through altering the duration of interaction between NCS1s and its partners [61].

1.2.3 Recoverin

Recoverin makes up the second branch of the NCS family. It was the first NCS protein to be discovered [36] and its structure was the first to detail the calcium-myristoyl switch mechanism [6, 43]. Unlike other members, Recoverin has only two functional calcium-binding EF hands, EF-2 and EF-3. Recoverin is localized primarily in the retina and plays role in light adaptation and phototransduction [62-64]. Recoverin has also been shown to indirectly regulate cGMP levels by inhibiting Rhodopsin kinase when it binds to calcium [18]. This NCS protein has been shown to be a marker of cancer-associated retinopathy [65, 66].

1.2.4 Guanylate-Cyclase Activating Proteins (GCAPs)

The third branch of NCS family is called Guanylate-Cyclase Activating Proteins (GCAPs). There are three main genes, which make up the GCAP sub-family: GCAP-1, GCAP-2 and GCAP-3 [56]. GCAPs are expressed only in photoreceptor cells of the retina [18]. In the photoreceptors, the GCAPS activate retinal Guanyl-cyclase at low calcium concentrations. The regulation of the GCAPs has been well studied, demonstrating binding to both magnesium and calcium. Upon binding magnesium, GCAPs activate rod outer segment membrane guanylate cyclase (ROSGC) activity, and inhibit the activity when calcium is bound [67-69]. Studies have highlighted how the GCAPs are kept in a more stable apo form when bound to magnesium [70].

All members of the GCAP family are expressed in the same cells at the same time [5]. In addition, all three members bind to, and activate the same target. This would suggest redundancy; however this is not the case. Each of the GCAP members has demonstrated differing affinities for calcium [6, 49, 71]. This suggests that the genes are not redundant, rather each of the GCAPs responds over varying calcium ranges.

This non-redundancy is supported by physiological evidence. GCAP 1 and 2 have mouse knockouts. These mice demonstrated increased sensitivity to light, as well as a decreased recovery due to a flash response [5, 48, 72]. Additionally, over expression of GCAP-1 could compensate for GCAP-2 deficient mice [48]. However, in mice lacking a functional GCAP-1, over expression of GCAP-2 was

not able to restore the light sensitive function, again supporting the non-redundant functions of the GCAP family [71].

The GCAPs have been linked to various retinal diseases, including retinal dystrophy, a condition that leads to loss of vision [73]. A Y99C mutation in GCAP-1 was identified in a family which had a hereditary form of retinal dystrophy [21]. This mutation leads to a constitutively activated form of the protein where the Y99C mutation impairs calcium dependent activation, causing GCAP-1 to activate ROSG-C1, regardless of the free calcium levels [24, 74]. This constant activation of ROSG-C1 can ultimately lead to cone degradation.

1.2.5 Potassium Channel-Interacting Proteins (KChIPs)

The KChIP subfamily of NCS proteins is comprised of the members KChIP1, KChIP2, KChIP3 and KChIP4, of which each member has multiple splice variants [75]. They were originally named for their ability to interact and regulate the Kv4 class of potassium channels [76] and aid in its trafficking [35, 77]. In addition, the KChIPs can interact with T-type and L-type calcium channels. KChIPs, like Recoverin, and unlike the other NCS proteins, bind 2 calcium ions [38, 78]. They are, however, myristoylated like the rest of the NCS family [18, 53], as well as harboring a site for palmitoylation [35].

This class of NCS proteins has a unique property; they bind to and interact with the DNA motif DRE, or Downstream Regulatory Element [79]. By binding to both DNA transcription factors, the KChIPs regulate the expression of several

genes[80]. It has been demonstrated that KChIP1, KChIP2, KChIP3 and KChIP4 can all bind to the DRE DNA motif and prevent transcription [76].

The multiple regulatory roles of the KChIPs are further attenuated by several regulatory methods. Many times, multiple KChIPs are co-expressed, however, some splice variants are expressed in specific tissues [81, 82], like that of KChIP 2 (KV4.2 and KV 4.3), which are expressed exclusively in the heart [58]. Other KChIP members differentiate themselves by their sub-cellular localization. KChIP 1.2, for example, uses the myristolated N-terminus to target intracellular vesicles [34, 83]. Palmitoylation of KChIP 2.3 and 3.1 allows for effective trafficking of Kv4 channels. Other KChIPs are localized only in the cytosol [35, 77]. In addition, the different KChIP variants regulate Kv4 channels in a distinctive manner [84, 85]. The regulation and differentiation of the KChIPs highlights the multiple methods that the family delineates functions and attunes calcium specific responses.

1.2.6. Visinin-Like Proteins (VILIPs)

The Visinin-Like Proteins or VILIPs are the last class of NCS proteins. This class is the least studied and has five members: Neurocalcin Delta, Hippocalcin, VSNL1, HPCL1 and HPCL4. This family is highly conserved with identities of 67-94% between members [86]. Each member has a non-functional EF-1 hand and binds 3 calcium ions [5, 6, 18, 86, 87]. This sub family is expressed in neurons of the brain, as well as peripheral organs, and may be co-expressed in the same cells at the same time [88].

VSNL1, also known as VILIP1, was the first Visinin-Like Protein to be discovered [88]. VSNL1 modulates cAMP levels via interaction with adenylyl cyclase [89, 90]. VSNL1 has also been shown to interact with α4β2 nicotinic acetylcholine receptors (nAChR) [89]. Recently VSNL1 has been implicated as a potential biomarker for general calcium deregulation [91], leading to neuronal disease. More specifically, there appears to be a critical role for VSNL1 deregulation and Alzheimer's disease. It is down regulated in Alzheimer's disease brains, showing decreased staining in pyramidal and non-pyramidal neurons, but higher staining extracellularly. VSNL1 co-localizes with other Alzheimer disease hallmarks like amyloid plaques and extracellular tangles [92-94], and its levels in the cerebrospinal fluid can be used to monitor the progression of the disease [95-97].

Hippocalcin-like 4, (HPCAL-4) or VILIP-2, shares a 89% homology with VSNL1[86], however, unlike VSNL1, not much is known about its role in calcium regulation. Despite its high similarity with VSNL1, HPCAL-4 is expressed primarily in the dentate gyrus of the hippocampus [98]. Functionally, it has been shown to have a role in calcium regulation by binding to, and inactivating P/Q-type Ca^{2+} channel (CaV2.1) [99].

Hippocalcin-like protein 1 (HPCL1) or VILIP3 is another member of the VILIP family, which is also not well characterized [5, 6, 86], but is thought to share many properties with hippocalcin [31]. Studies have highlighted its ability to bind calcium as well as magnesium [100] and its possible role as a modulator of MAP kinase [31]. It is expressed in the cerebellum, primarily in Purkinje cells, and the hippocampus [101, 102]. HPCL1, like VSNL1, co-localizes with Alzheimer disease

hallmarks in the brain, indicating its potential usefulness as a biomarker of neurodegenerative disease [92].

1.2.6.1 Neurocalcin Delta

Neurocalcin Delta, or NCALD, is of interest due to preliminary results from laboratories that have shown NCALD, to display a strong circadian rhythm. Little is known about NCALD; it is expressed throughout the central and peripheral nervous system, but also in other tissues, including the kidneys, liver, skin, and testes [103]. Biochemically, NCALD has been shown to interact with two membrane Guanylate cyclases: ROS-GC1, in the Ganglion cells of retina, and ONE-GC, in olfactory receptor neurons [16, 30, 104-106]. There is no functional knockout known to date. It is hypothesized to be involved in cytoskeletal rearrangement, due to its ability to interact with actin and tubulin. It has also been shown to interact with clathrin upon the elevation of calcium, suggesting that NCALD may be involved in the control of clathrin-coated vesicular traffic in the trans-Golgi network [107].

NCALD has been implicated in several diseases, which may help explain the physiological role of the protein. Recently, patients with a partial deletion of NCALD have been identified. The interstitial deletion in 8q22.2-q22.3 leads to a disease characterized by seizures, intellectual disability, and autistic behavior [59, 108]. In addition, NCALD has been shown to be down regulated in several different tumor types [109, 110], again suggesting a role in cell growth [107].

1.2.6.2 Hippocalcin

Hippocalcin (HPCA) was originally purified from the hippocampus [111] and has been demonstrated to be critical for long term potentiation of memory (LTP). Mice that lack HPCA function have demonstrated impaired long-term memory [20], visual learning, and creating spatial memories [112]. Recently, mutations in the HPCA gene have been demonstrated to be associated with autosomal recessive primary-isolated dystonia [113]. The molecular mechanisms underlying these physiological roles for HPCA remain to be elucidated.

Some of the biochemical data on the proteins that HPCA interacts with and the processes ~~that~~ they affect exposes some of its proposed roles. First, HPCA interacts with potassium channels to modulate hyperpolarization of the hippocampal neurons, contributing to long-term potentiation [111, 114] and potentially, dystonia [113]. HPCA interacts with membrane Guanylate cyclases such as Olfactory Neuro-Epithelial Guanylate Cyclase (ONE-GC) [45, 115] and Rod Outer Segment membrane Guanylate Cyclase type 1 (ROS-GC1) [30], which it activates in a calcium-dependent fashion. A role in preventing the unwarranted apoptosis of neurons has been demonstrated with Neuronal Apoptosis Inhibitor Protein (NAIP) interaction [116]. Finally, translocation to the membrane can be driven by its interaction with creatine kinase beta isozyme in a calcium-dependent fashion [117]. Proteomic analyses indicate that several cytoplasmic proteins may associate with HPCA in a calcium-dependent manner [118].

1.3.1 NCALD vs. HPCA

Unlike the other NCS proteins, it is not abundantly clear how the VILIP members differentiate themselves. VILIP3 and Hippocalcin have similar expression [101, 102], while VILIP-2 does not [119]. It is thought that different VILIPs have varying affinities for calcium [120-122] ranging from 200 nM to 10 μM [86]. It is also possible that the differences in these proteins are how they respond to calcium, rather than the calcium response range. Because this is unknown, the VILIP subfamily makes an excellent subject for the study of how evolution has driven the differentiation of functions in NCS proteins.

To better study how this occurs, two candidates were chosen, NCALD and HPCA. NCALD shares an 88% identity (95% similarity) with HPCA. Both of these VILIPS, are 193 residues long, have a myristolated N-terminus, and 4 EF hands in which the first hand is not functional. The addition of calcium causes the proteins to cycle from the cytosol to the membrane [5, 42, 43]. NCALD and HPCA are often expressed in the same cells, at the same time in mammals (reviewed in: [6]). In addition, they interact with some of the same partners, like ROS-GC1 and ONE-GC [16, 30, 104-106].

All of these factors would typically mean that these two proteins are likely redundant, however, this is not the case because of the existence of the HPCA knockout mouse. The HPCA knockout expressed a phenotypic loss of LTP. When the animals were tested, there was no change in other NCS protein levels, showing that NCALD cannot compensate for HPCA [20]. In addition, diseases related to mutations in these proteins are distinct point mutations in which HPCA causes a form of

dystonia, while a partial loss of NCALD in patients leads to a disease that causes seizures, intellectual disability, and autistic behavior [59, 108].

It is, therefore, clear that these two proteins have evolved to carry out distinct functions. The focus of the following work is to determine what makes NCALD and HPCA unique, in hopes to better understand how evolution has driven the differentiation of functions in NCS proteins.

Chapter 2. Rationale

Calcium signaling is critical for the proper functioning of neurons. Since a single ion can cause multiple reactions, including memory formation, synaptic firing, or cell death, it is critical for the cells to be able to detect and respond to a specific range of calcium. The Neuronal Calcium Sensor (NCS) protein family carries out this "sensing" and subsequent response. In order to better understand what makes NCS proteins unique, the following study will primarily focus on two members: HPCA, which is well characterized, and NCALD, whose function is still unknown.

Hypothesis: NCS proteins, namely NCALD and HPCA, carry out unique, non-overlapping functions related to their specific structures.

In order to test this hypothesis, the NCS members NCALD and HPCA will be compared. They are members of the VILIP subfamily of NCS proteins and share an 88% identity (reviewed in: [6]), but have evolved to carry out distinct functions. In the VILIP family of proteins it is not clear how the members differentiate themselves despite their high similarity. In order to properly examine what makes NCALD and HPCA unique, three goals must be met.

First, we need the ability to express, isolate, and purify large quantities of the NCS family proteins. By isolating pure protein, *in-vitro* experiments can be conducted to better understand how the NCS family works. This *in-vitro* experimentation is critical in the case of NCALD, where no mouse knockout exists because the loss of NCALD appears to be embryonic lethal.

Next, we need to identify assays that are capable of differentiating the proteins. Because all the NCS family members bind calcium, stimulate similar partners, and are of a similar size and composition, it is critical to identify methods to differentiate them. Parameters using classic methods like tryptophan fluorescence, size exclusion chromatography, sequence analysis, and ROS-GC stimulation will be used to help differentiate the NCS members. In addition, newly developed methods using native gel analysis will be highlighted.

Finally, once we can work with pure proteins and can differentiate between the NCS proteins, we can apply these tools to answer physiological questions. There are three major questions this work will highlight in order to answer the aforementioned hypothesis: 1) The role of dimerization in NCALD, 2) the role of the EF-1 region in the NCS family, and 3) how point mutations in HPCA lead to dystonia.

Chapter 3. Materials and Methods

3.1 Construct Creation and Mutagenesis:

Rat NCALD, HPCA or the GCAPs coding region was amplified by PCR and inserted into the bacterial expression vector pET 21d between NcoI and HindIII sites. The expressed protein is without tags. To generate different mutants, pET 21d plasmid encoding the rat NCS proteins was used. Point mutations were created using the QuikChange II XL Site-Directed Mutagenesis kit from Agilent Technologies. All constructs were confirmed via sequencing

To create the dimer mutants,the following mutagenic primers were used:

S19 to N Primers:

Fwd (AGGACTTACTGGAAAACACAGACTTCACAGAG),

K102 to M Primers:

Fwd (GCTGGAGCAGAAGCTGATGTGGGCCTTCAGCATGTATG,) and

A119 to E Primers :

Fwd (CGGCTACATCAGCAAGGAAGAAATGCTGGAGATTGTGC).

Double mutants harboring K102M and A119 E as well as triple mutant with all three mutations (S19NK102MA119E) were also created by the same method.

To create the HPCA dystonia mutants the following primers were used..

T71N: Fwd (CAT GTC TTC CGC AAT TTT GAC ACC AAC -3'). N75K: Fwd 5'-(ACT TTT GAC ACC AAA GCG ACG GCA CCA -3').

3.2 Expression of recombinant myristoylated and non-myristoylated HPCA in *E. coli:*

The rat HPCA/pET 21d construct was transformed into *E. coli* ER2566 cells which co-expressed yeast N-Myristoyl Transferase (plasmid pBB131, a kind gift from Dr. Gordon). For the purification of the non-myristoylated form, *E. coli* cells without the N-Myristoyl Transferase were used for expression. Cells were inoculated from an overnight culture (1%) into 300ml of fresh LB medium containing ampicillin (50 μg/mL) and kanamycin (25 μg/mL) and grown at 37°C with shaking at 200rpm. Once an OD of 0.4 at 600nm was reached, 100 μg /ml myristic acid was added to generate the myristoylated form. Induction was facilitated by the addition of IPTG, which was added to a final concentration of 1mM after an OD of 0.6 was reached, consistent with previously published protocols [45, 123]. Cells were pelleted 3 hours after induction by centrifugation at 2500x g for 30 minutes and the pellet was frozen at –20°C until further use.

3.3 Bacterial cell lysis of HPCA containing cells:

The cells were suspended in a buffer containing 20mM Tris pH 8.0, 0.1M NaCl, 1mM PMSF and 0.2mM Benzamidine HCl. The suspension was then sonicated on ice at 30% power using a Branson 450 Sonifier 7x15 seconds with a 15-second rest between each burst, followed by centrifugation at 17000x g for 20min. The supernatant contained the soluble, fraction of HPCA and was directly used for purification. The pellet contained the inclusion bodies and was processed as described below.

3.4 Processing Inclusion bodies:

The inclusion bodies were resuspended in 12.5ml of 6M Guanidine HCl in 20mM Tris pH 8.0 containing 2mM DTT and were left to stir for 1 hour at room temperature. Following denaturation the inclusion bodies were spun at 17,000x g for 30min at 4^0C. The supernatant was then dialyzed against 4L of 20mM Tris HCl pH 8.0, 0.1 M NaCl overnight at 4^0C. The next morning the dialysate was spun at 17,000x g for 20min to remove the precipitated proteins.

3.5 Hydrophobic interaction chromatography (HIC) purification of HPCA:

Hydrophobic interaction chromatography was carried out on a phenyl sepharose column (1.5 mL) connected to an AKTA prime. 1mM $CaCl_2$ was added to either the soluble fraction or the dialysate and the samples were loaded on to the column pre-equilibrated with a buffer containing 20mM Tris pH 8.0, 0.1M NaCl and 1mM $CaCl_2$. The column was then washed with 15mL of buffer containing 20mM Tris pH 8.0, 0.1M NaCl and 1mM $CaCl_2$ followed by a second 15mL wash of the same buffer but without $CaCl_2$ and finally with a 15mL wash of 20mM Tris pH 8.0. HPCA was eluted from the column in 1.5mL fractions using 15mL of 20mM Tris pH 8.0 containing 5mM EGTA. Fractions containing the purified protein (identified by SDS-PAGE) were pooled and dialyzed overnight into 20mm Tris pH 7.5 at 4^0C.

3.6 Concentration of HPCA and Calcium depletion:

The dialysate (purified HPCA) was concentrated using (10KDa cutoff) Amicon Ultra 4 centrifugal filters and then washed with calcium depleted 20mM

Tris-HCl (pH 7.5) buffer. Calcium depletion of the buffer was carried out as described in [124] using Chelex resin. Protein concentration was determined by the Bio-Rad protein assay according to the manufacturer's protocols (Bio-Rad Laboratories Inc., CA, USA).

3.7 Polyacrylamide gel electrophoresis:

Previously established protocols were followed [30, 45, 105]. Briefly, proteins were separated by discontinuous SDS-(12%) PAGE (pH 8.8) at a constant voltage of 135V for 1 hr.

3.8 Western Blotting:

Western blotting was carried out with a 45 min transfer to nitrocellulose and HPCA was detected using a previously described polyclonal antibody [45] using the standard methods [30, 45, 105].

3.9 MALDI-MS:

Purified HPCA (5µg) was desalted using C4 ZipTip (Millipore Inc.). The protein sample was then mixed 1:2 with saturated 1,5-diaminonaphthalene in 50% acetonitrile and 0.1% TFA in water and spotted on the MALDI target plate. In-source decay (ISD) data was collected using Bruker MicroFlex LFR MALDI-TOF in positive linear mode. Mass range was set from 1000 to 7000 Da and the pulse ion extraction was set at 240ns. ISD spectra were analyzed with Flex Analysis software (Bruker).

3.10 Tryptophan fluorescence:

Fluorescence measurements were carried out on a Fluromax -3 spectrofluorometer. Tryptophan emission fluorescence spectra were recorded at 22°C from 0.1 ml samples with 4 µM HPCA in 20mM Tris pH 7.5. The excitation wavelength was set at 290 nm (bandwidth, 4 nm), and the emission wavelength was varied from 300 to 400 nm (bandwidth, 4nm). Samples were incubated with buffer containing increasing concentrations of calcium using calcium calibration buffers purchased from Molecular Probes by Life Technologies.

3.11 Native Gel Electrophoresis (CIMSA):

Purified proteins were separated by native discontinuous (12%) PAGE (pH 8.8) at a constant voltage of 165 V for 2.5 hrs in running buffer comprised of 25 mM Tris base and 190 mM glycine. The gels were 8 cm length, 10 cm width and 0.75 mm thickness. The gels were discontinuous, with stacking (4% acrylamide in 125 mM Tris-Cl, pH 6.8) and separating (12% acrylamide in 300 mM Tris-Cl, pH 8.8) components. The electrophoresis chamber (standard mini PROTEAN apparatus, Bio-Rad) was kept on ice to prevent overheating of the gel. Five □l□□1□□g/□l) of each of the proteins was mixed with 15□□l of buffer containing specific concentrations of the free divalent cation, obtained by mixing EGTA/EDTA and the divalent cation in appropriate proportions based on the program MAXCHELATOR [32]; for increments of calcium, calcium calibration buffers of increasing calcium concentrations from 0 □M to 39 □M were used. 5 □l of 6x Sample buffer (Laemmli sample buffer without SDS) was added to all samples [125, 126].

After electrophoresis, proteins were visualized with Coomassie blue R250. The relative mobility value for each band was measured as the distance migrated by the band measured from the top of the gel in relation to the total gel length from scanned images using ImageJ. To determine the effect of calcium on a single protein, the mobility value at each calcium concentration was estimated in relation to that obtained at the maximal concentration of calcium (39 μM). Data compiled from several replicates were analyzed and presented as mean ± SE using Prism 6.0. Statistical significance between indicated groups was determined by two-tailed student's *t* tests.

3.12 Ferguson plot:

Native electrophoresis of individual NCS protein was carried out as described above on gels of varying acrylamide concentrations ranging from 9%-12%. Proteins were incubated with either 0 μM or 39μM free calcium with Calcium calibration buffers (Molecular Probes by Life Technologies) and were electrophoresed, for 2 hrs at 165V on ice. Relative mobility values were measured plotted as a function of log values of concnetration in Prism 5.

3.13 Guanylate cyclase activity assay:

Membranes of COS cells transfected with ROS-GC1 served as the source of the enzyme for guanylate cyclase activity assay. The activity was assayed as described previously [45]. Briefly, membranes were pre-incubated on ice with or without NCS protein in a reaction mix containing 10 mM theophylline, 15 mM phosphocreatine, 20

□g creatine kinase, 50 mM Tris–HCl, pH 7.5. Incubation was carried out in the presence or absence of calcium (10 □M). The total assay volume was 25 □l. The reaction was initiated by addition of the substrate solution (to a final concentration of 4 mM $MgCl_2$ and 1 mM GTP), followed by incubation at 37°C for 10 min. The reaction was terminated by the addition of 225 □l of 50 mM sodium acetate buffer, pH 6.2 and heating on a boiling water bath for 3 min. The mixture was spun down at 1100x g for 10 mins and the supernatant was used to measure the amount of cyclic GMP formed using DetectX direct cGMP immunoassay kit according to manufacturer's protocol (Arbor Assays).

3.14 Protein Charge Calculations:

Protein pI and charges were calculated using web-based program "ProteinCalculator" [65]. The accession numbers along with their gene symbols for the proteins referred to are: Calmodulin [P62158.2; CALM1], Frequenin [AAF01804.1; NCS1], Recoverin [NP_002894.1; RCVRN], Neurocalcin delta [NP_001035720.1; NCALD], Hippocalcin [BAA74456.1; HPCA], Visinin-like protein 1 [P62760.2; VSNL1], HPCL1 or VILIP3 [P37235.3; HPCAL1], HPCL4 [Q9UM19.3; HPCAL4], GCAP1 [P43080.3; GUCA1A], GCAP2 [Q9UMX6.4; GUCA1B], GCAP3 [NP_005450.3; GUCA1C], KChIP1 [Q9NZI2.2; KCNIP1], KChIP2 [Q9NS61.3; KCNIP2], KChIP3 [Q9Y2W7.1; KCNIP3], KChIP4 [Q6PIL6.1; KCNIP4] and Ovalbumin [AAB59956.1; OVAL].

3.15 Computation of sequence interrelationships:

The sequences of NCS proteins used for analyses are presented below and grouped according to the figures. They were:

Figure 4.1-1: Frequenin [AAF01804.1], Recoverin [NP_002894.1], Neurocalcin delta [NP_001035720.1], Hippocalcin [BAA74456.1], VSNL1 [P62760.2], HPCAL1 [P37235.3], HPCAL4 [Q9UM19.3], GCAP1 [P43080.3], GCAP 2 [Q9UMX6.4], GCAP 3 [NP_005450.3]), KChIP1 [Q9NZI2.2], KChIP2 [Q9NS61.3], KChIP3 [Q9Y2W7.1] and KChIP4 [Q6PIL6.1]

Figure 4.1-2 GCAP1 *Homo sapiens* [P43080.3], GCAP 2 *Homo sapiens* [Q9UMX6.4], GCAP 3 *Homo sapiens* [NP_005450.3]), GCAP1 *Bos taurus* [P46065.2], GCAP1 *Mus musculus* [NP_032215.2], GCAP1 *Gallus gallus* [AAB47111.1], GCAP1 *Danio rerio* [AAL05602.1], GCAP2 *Gallus gallus* [AAB47112.1], GCAP2 *Mus musculus* [NP_666191.1], GCAP2 *Bos Taurus* [NP_777211.1], GCAP2 *Danio rerio* [NP_571946.1], and GCAP3 *Danio rerio* [AAK95949.1]

Figure 4.1-3 Frequenin [AAF01804.1], Recoverin [NP_002894.], Neurocalcin delta [NP_001035720.1], Hippocalcin [BAA74456.1], VSNL1 [P62760.2], HPCAL1 [P37235.3], HPCAL4 [Q9UM19.3], NCS1 *Caenorhabditis elegans* [AAA85631.1], NCS1 *Danio rerio* [AAO34710.1], NCS1 *Xenopus laevis* [NP_001084088.1], NCS1 *Saccharomyces cerevisiae* [Q06389.2], and NCS1 *Drosophila melanogaster* [AAH04856.1]

Figure 4.1-4 KChIP1 [Q9NZI2.2], KChIP2 [Q9NS61.3], KChIP3 [Q9Y2W7.1], KChIP4 [Q6PIL6.1], KChIP1 isoform 3 [NP_001030010.1] denoted as

KChIP1.3, KChIP2 isoform 2 [NP_775283.1] denoted as KChIP2.2, KChIP 3 isoform 2 precursor [NP_001030086.1] denoted as KChIP3.2, and KChIP 4 isoform 5 [NP_001030175.1] denoted as KChIP4.5 in Figure 4.

For the sequence analysis in Figure **5.4-1** the following sequences were used:, Neurocalcin delta [NP_001035720.1], Hippocalcin [BAA74456.1], Recoverin [NP_002894.1], Frequenin [AAF01804.1], VSNL1 (VILIP1) [P62760.2], HPCAL1 (VILIP3) [P37235.3], HPCAL4 (VILIP-2) [Q9UM19.3], GCAP1 [P43080.3], GCAP 2 [Q9UMX6.4], GCAP 3 [NP_005450.3]), KChIP1 [Q9NZI2.2], KChIP2 [Q9NS61.3], KChIP3 [Q9Y2W7.1] and KChIP4 [Q6PIL6.1].

All alignments were performed using ClustalX 2.1 with the default setting: Gap opening 10, Gap extension 0.1, Protein weighted matrix –Gonnet 250 [29]. The unrooted tree was compiled using NJPlot [30] and enhanced in Adobe Illustrator. For the construction of phylogenetic trees, the NJ Bootstrapping method with a random number generator seed set at 111 and 1000 reiterations was used. The tree was displayed with NJ Plot [30] and enhanced with Adobe Illustrator.

3.16 Tissue expression analysis:

The analyses were carried out *in silico*. Expression at mRNA as well as protein level was analyzed. Two different databases - Genevestigator [127] and BioGPS [128] –were used to obtain mRNA expression profiles across different human tissues (brain, heart, liver, lung and skin) for indicated proteins.

Protein expression level in whole human brain and liver was obtained for indicated proteins from two independent databases: (a) Human Protein Atlas

database[129-131], which is based on immunohistochemical analyses, and scores expression levels as negative (0), weak (1), moderate (2) or strong (3), and (b) PaxDB [132], which compiles standardized and integrated data on protein expression levels based on MS/MS. The data from the Human Protein Atlas was also utilized to investigate the relative expression levels of the indicated proteins within different neurons of the human brain.

3.17 Inductively Coupled Plasma (ICP) Spectroscopy:

The concentration of calcium in components used for native gel electrophoresis was determined by ICP spectroscopy. Chelex-treated water served as a blank. Briefly, samples were diluted into 10 mL of 5% nitric acid in ICP grade water rated at 18.2 MΩ cm. The quantity of calcium present was estimated as parts per billion (ppb) and converted into molarity.

3.18 Cell Culture:

COS7 cells were cultured in DMEM medium with 1g/L glucose, L-glutamine and sodium pyruvate (CORNING), supplemented with 10% fetal bovine serum from Hyclone, at 37 °C in 5% $CO_{2.}$.

3.19 Translocation Assay:

COS7 cells grown to 75% confluence were transfected using calcium phosphate buffer (2X HEBS buffer (HEPES 50 mM, NaCl 280 mM and Na_2HPO_4 1.5 mM, pH 7.05) with either an expression plasmid for wild type hippocalcin (pcDNA3-

Hippocacin-ECFP) or the two mutants (T71N and N75K) or the control vector (pcDNA3-ECFP). After 24 hours the cells were moved to a TokaiHit on-stage incubator attached to a Nikon C1 laser confocal microscope. The cells were treated with 6 mM Histamine to increase intracellular calcium levels and live imaging was performed.

3.20 Size exclusion chromatography:

Purified samples were analyzed on a Superdex 75 (gel filtration) column on an AKTA Purifier. Analyses were carried out in the presence of 20mm Tris pH 7.5, 150mm NaCl and either 0.2 mM calcium (+ Calcium) or in the presence of 2.0 mM EGTA (- Calcium). The data shown is a representative experiment of at least 4 independent runs, which included at least 2 independent preparations and 2 independent clones for each construct.

3.21 Direct calcium binding assay

The experiment was carried out as previously described [133]. Briefly, purified proteins were separated on an 12% SDS-PAGE and then transferred to nitrocellulose. The blot was then washed 3x in imidazole buffer (10mm imidazole pH 6.8, 60mm KCl, and 1mm $MgCl_2$). The blots were then incubated for 20 min at room temperature with 4μci ^{45}Ca in imidazole buffer. The blots were washed 2x with dH20, followed by 2x washes of 50% ethanol, and then imaged using the phosphoimager.

Chapter 4: Results

4.1 Evolutionary Interrelationships and Insights into Molecular Mechanisms of Functional Divergence: An Analysis of Neuronal Calcium Sensor Proteins

Portions of this work were previously published in:

***Viviano J*, Wu H**, Venkataraman V. Evolutionary Interrelationships and Insights into Molecular Mechanisms of Functional Divergence: An Analysis of Neuronal Calcium Sensor Proteins. J Phylogen Evolution Biol (2013) : 117. doi:10.4172/2329-9002.1000117*

As a first step towards analyzing the link between evolutionary and functional diversity, we investigated the relationship among the NCS family members in the human genome. Several additional sequences (truncated or splice variants or without additional documentation) were left out of the analysis. There were 14 members of the NCS family: Frequenin (also known as NCS1), Recoverin, Kv Potassium-Channel Interacting Proteins types 1 through 4 (KChIP 1-4), Guanylate Cyclase Activating Proteins types 1 through 3 (GCAP 1-3), Visinin-like Protein type 1 (VILIP1; gene ID VSNL1), Neurocalcin Delta (NCALD), Hippocalcin (HPCA) and hippocalcin-like proteins type 1 and 4 (HPCAL1 & HPCAL4). The result presented in Figure 4.1-1 shows that these members generate three major groups, which we have identified as GCAPs, VILIPs and KChIPs (indicated by shaded areas in Figure 4.1-1). Frequenin and recoverin were out grouped consistent with earlier analysis from other laboratories [6, 8].

The grouping is also consistent with known functions of the members in each: All GCAPs are intimately linked with the maintenance of the autoregulatory feedback loop in phototransduction [55, 134, 135] through their interaction with membrane guanylate cyclase (mGC) [5, 55]; GCAP1, in addition, may also contribute to olfaction [136]. Some members of the VILIP group also share this ability to modulate mGC activity [29, 30, 45, 87, 105, 137, 138]. However, in addition to mGC, each member of the VILIP group is known to interact with multiple targets, generating perhaps the most functionally diverse group among the three[5, 6, 28]. The KChIPs were initially identified as modulators of potassium currents[139]. It has now been demonstrated that all KChIPs share DNA-binding ability also [140]. Interestingly,

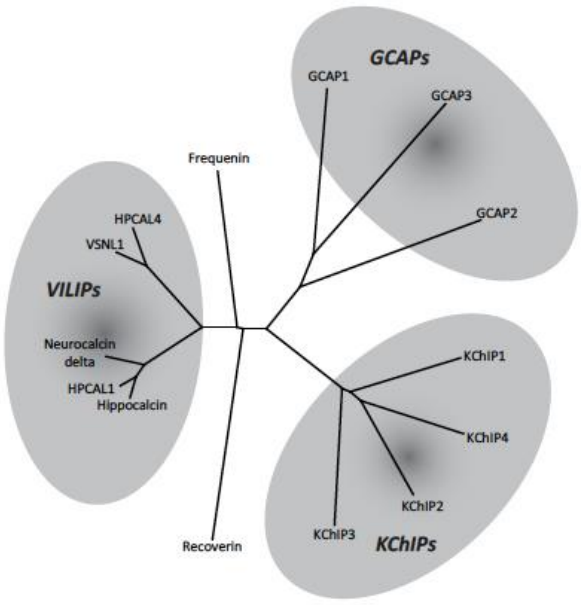

Figure 4.1-1: Computation of sequence interrelationships among the NCS Family of proteins. The sequences of all known members of the NCS family identified in the human genome (excluding the splice variants) were aligned. The sequences used and the generation of the unrooted tree is described in the "Methods" section. The three major groups that are evident from the alignment are marked and labeled.

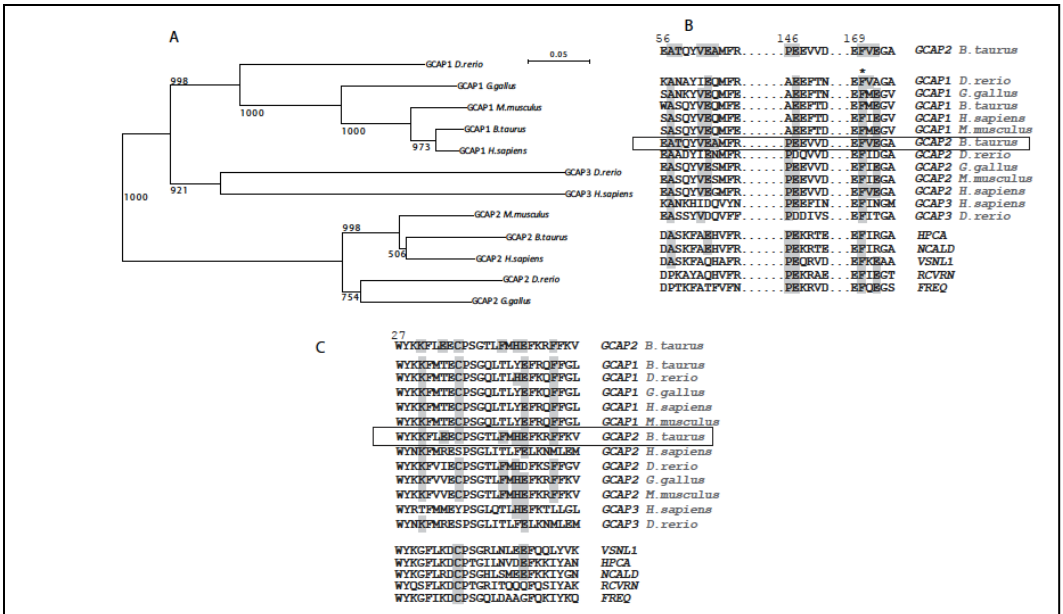

Figure 4.1-2: Analysis of GCAP2/ROS-GC1 interactive domains. (A) A phylogenetic tree depicting the interrelationship among GCAP proteins across several species was created as described in "Methods" and is presented. (B) Regions of GCAP2 that were identified to be involved in binding to ROS-GC1 are depicted. The region of the bovine GCAP2 (used in the study) encompassing the residues is presented in the top row. Amino acid residues are numbered at the top for guidance. Alignment of all GCAPs, including species orthologs, is provided below. Alignment of the corresponding regions from other proteins is presented as the third block. All sequences used are listed in the "Methods". Amino acid residues shaded in grey were identified to form the GCAP2/ROS-GC1 interface [53]. Those that are completely conserved within the GCAP family are indicated with asterisks. (C) Sequence alignment of GCAP proteins across species and representative members from the VILIP group. Amino acid residues in the EF1 region of GCAP2 previously identified to be involved in ROS-GC1 interactions [52] are shaded in grey. The region of interest is presented in the top row, with some amino acid residues numbered.

between the two outgrouped members, frequenin activates mGC [138] but recoverin does not; instead, it regulates rhodopsin kinase [42] and contributes to the feedback loop in phototransduction [141, 142]. Thus, members of the GCAP and VILIP groups

as well as the outgrouped frequenin share the ability to modulate mGC activity. Further details of this shared function are presented below.

4.1.2 Intricacy of NCS/mGC interactions

A closer investigation reveals an extraordinarily intricate relationship between the NCS protein modulators and mGCs. There are seven genes in the human genome that encode mGCs. Of the seven, the one encoded by GUCY2D (also known as ROS-GC1/RetGC1) is modulated by GCAP1, GCAP2, GCAP3, and NCALD [30, 105]; (reviewed in: [5, 42, 55, 142]. As an additional level of intrigue, the GCAPs inhibit mGC activity at calcium concentrations greater than 500 nM, while NCALD stimulates it ([30, 105]; reviewed in:[55, 142]*).* All the above proteins also modulate the GUCY2F product (ROS-GC2/ RetGC2) in a similar fashion, albeit at differing efficiencies as assessed by fold-change in activity and EC_{50} values [55, 142]. Frequenin [138] and HPCA [45] activate the olfactory guanylate cyclase (ONE-GC/GC- D) at elevated calcium concentrations; interestingly, so does GCAP1 [136]. VSNL1, on the other hand, activates the product of NPR2B (atrial natriuretic peptide receptor type B/GC-B) [29, 87, 137]. The overlapping specificities of NCS proteins to one cyclase, the ability of one NCS protein to modulate different cyclases and opposing responses to elevated calcium are all observed in this interaction, which is spread between two groups and the two outliers. Information on the binding site on some NCS proteins necessary for their modulation of mGC is also available. Therefore, we chose to analyze this function in terms of evolutionary interrelationships among these proteins. Two laboratories have independently mapped

amino acid residues on GCAP2 that mediate its interaction with ROS-GC1 [51, 143]. Similar information is available for NCALD, which regulates ROS-GC1 in an opposite fashion compared to GCAP2 in their calcium-loaded states [105]. A correlation between the molecular interactions leading up to functional divergence and phylogenetic relationships among these proteins are presented below.

4.1.3 GCAP2 modulation of ROS-GC1

For these analyses, results from two different laboratories were used.

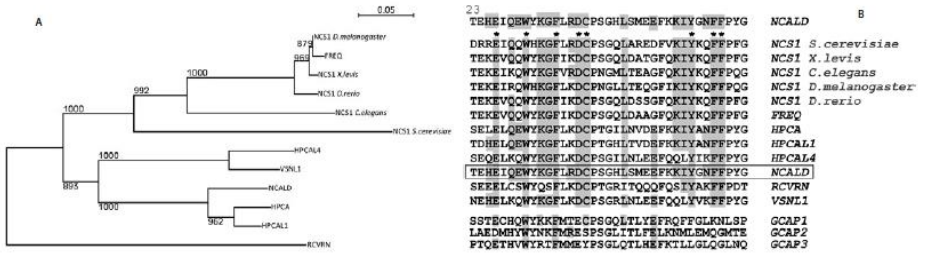

Figure 4.1-3: Analysis of NCALD/ROS-GC1 interactive domains. (A) A phylogenetic tree of the proteins of the VILIP group along with recoverin and frequenin (NCS-1) across several species was created after Clustal alignment as described in "Methods". (B) Residues that are involved in NCALD/ROS-GC1 interactions were identified [46]. The region of interest in bovine NCALD is presented in the top row, with some amino acid residues numbered. Alignment of the corresponding region from all VILIPs (including species orthologs), recoverin and frequenin is provided below. Alignment of the region from GCAPs is presented as the third block. All sequences used are listed in the "Methods". Those that are completely conserved within the VILIP family are indicated with asterisks.

Pettelkau *et al*. [51] have identified residues on GCAP2 that are in close proximity to and, presumably, form the contact points with ROS-GC1.This was accomplished

through a combination of chemical cross-linking, photo-affinity labeling and MS. Based on these studies, a model for the calcium-loaded GCAP2 interaction with ROS-GC1 is also proposed involving specific amino acid residues in the interface. Ermilov *et al*. [143] identified residues on GCAP2 necessary for calcium-dependent regulation of ROS-GC1 using a completely different approach. Between the two studies, residues on GCAP2 that are critical for the interaction as well as modulation of ROS-GC1 have been mapped. Given that all GCAPs interact with ROS-GC1, along with at least one member of the VILIPs, it was of interest to investigate the presence of these identified residues within the GCAP group and, then, compare with the VILIP group members. The results are presented in Figure **4.1**-2. As a first step, several orthologs for GCAP1 and GCAP2 from different vertebrate species as well as the two known orthologs of GCAP3 were aligned as described in Methods and the results are presented (Figure 4.1-2A). It is noted that for GCAP3 these are the only reported sequences available although it has been suggested that it is expressed in multiple species. None of the GCAPs are completely conserved among the species, variation does exist between species and the grouping is as expected: sequences for each of the GCAPs from different species cluster together (Figure 4.1-2A). Are they divergent on the amino acid residues that interface with ROS-GC1? An alignment of all GCAP sequences (species indicated in *italicized font*) with the amino acid residues spanning the interface is presented in Figure 4.1-2B. In addition, they are aligned with members from the VILIP group. It is noted that all members of the VILIP groups are conserved across the vertebrate species (data not shown).

On GCAP2, two areas of interaction were identified [51]: one that spans the EF1 hand and the other, the EF4 hand. The bovine form of GCAP2 was used in these experiments. The amino acid residues in the region are presented in the top row of Figure 4.1-2B and numbers for some amino acid residues are provided on top for guidance. The residues identified to be at the interface are shaded in grey. They are: A57, T58, V61, E62, A63 (all in EF1), P146, E147, F170, V171 and E172 (all in EF4). How are these residues conserved during the divergence of GCAPs and VILIPs? A57 is highly conserved in GCAPs as well as most VILIPs but is replaced by a Pro residue in recoverin and frequenin. Ala is not likely to interact, but its presence may allow other interactions to occur. Neither of these proteins interacts with ROS-GC1 ([138]; reviewed in:[42]). Therefore, could this residue be critical for ROS-GC1 interaction? Interestingly, HPCA and VSNL1, which are shown to interact with mGCs other than ROS-GC1, have preserved A57. Is it possible that these NCS proteins also interact with ROS-GC1? In order to answer that question, the conservation of residues at other positions was investigated. T58 is not conserved even in species orthologs of GCAP2. Given that GCAPs have been shown to operate across species (GCAP) from one species can modulate ROS-GC1 from another species [144], it is unlikely that this residue is critical for interaction. V61 and E62 are conserved in most GCAPs or replaced by Ile or Asp residues across the GCAPs. This suggests that both of the sites are likely to be the amino acids utilized for mGC activation in GCAPs. In VILIPs, there is an Ala at position corresponding to V61 and, therefore, supports a GCAP- specific role for this residue. On the other hand, E62 is preserved in HPCA and NCALD. Considering that VILIPs and GCAPs have opposite

effects on mGC stimulation ([30, 105]; reviewed in: [55, 142]), could V61 be the reason for this functional divergence? Like T58, A63 is not conserved even within GCAP2 orthologs and, therefore, is likely not an interaction site [53].

The amino acid residues in EF4 that are located in the interface are: P146, E147, F170, V171 and E172 [51]. P146 is interesting because it is conserved throughout the NCS family but is substituted with an Ala in all species orthologs of GCAP1, suggesting that the presence of Ala allows for critical interactions which contribute to the unique properties of GCAP1 such as binding at a different site [50]. E147 is almost completely conserved, with only the GCAP2 and GCAP3 proteins in *D. rerio* bearing a conserved substitution of Asp at the corresponding position. F170 is completely conserved (indicated with an asterisk; Figure **4.1**-2B). Position corresponding V171 is highly variable even between the same proteins in different species with substitutions ranging from presumably conserved ones such as with an Ile to Met and positively charged Lys and Gln. There are two completely opposite inferences that may be drawn: (a) it is possible that this position may govern parameters of interaction of individual members with ROS-GC1, in which case mutation of these residues would affect the interaction of the protein with ROS-GC1 or (2) this residue may play no role, in which case mutation would have no effect. The last identified residue on GCAP2 is E172. Conservation at this position shows an interesting pattern; a negatively charged residue is present in this position in all GCAPs except GCAP3 and *D. rerio* GCAP1; this also holds true for the VILIPs, except for HPCA and NCALD, where a positively charged Arg is found. Thus, the

phylogenetic analyses have enabled to distinguish the role of amino acid residues identified at the GCAP2 interface with ROS-GC1: some are unlikely to play an important role either because they are not conserved at all (T58, A63) or completely conserved among all examined NCS sequences (F170). The possibility still remains that theses residues co-evolved to interact with unique partners. Further predictions could be made about residues that may determine NCS-specific interaction (Ala at P146 for GCAP1, Arg at position corresponding to E172 for HPCA and NCALD, V61 and E62 for GCAPs) and would enable more incisive experimental design to test these predictions.

A completely different approach was taken by Ermilov *et al*. [143] using site-directed mutagenesis and analyzing the effects on biological activity to map amino acid residues within the EF1 hand of GCAP2 that mediate its calcium-dependent regulation of ROS-GC1. Unlike the previous approach [51], the emphasis is on residues that contribute to the regulation of ROS-GC1. Several residues were investigated for a possible contribution to mGC regulation - K30, E33, C35, F41, H43, E44 and F48. Interestingly, all residues identified by this approach, reside within EF1 region, unlike the previous study, which identified residues in both EF1 and EF4 (Figure 4.1-2B). The residues on bovine GCAP2 identified by Ermilov *et al*. [143] are shaded grey in Figure 4.1-2C. An alignment of all GCAP sequences as well as representative VILIPs are also depicted. Conserved residues are shaded in grey. Analyses of sequence divergence as before, lead to the following conclusions regarding the mapped region: F41 is GCAP2-specific and may be critical for the

specificity of GCAP2 interaction with ROS-GC1; a similar argument could be made for H43, except that the residue is not preserved in the human orthologs. However, experimentally, mutations of these residues affect the ability of GCAP2 to activate mGC [143]. K30 is present in all GCAPs except GCAP3, suggesting that its role is common at least between GCAP1 and GCAP2. The observation that the K30G mutation showed decreased activation, therefore, is less likely due an effect on specific GCAP2/ROS-GC1 interaction and is more likely due to an effect on overall protein function common between GCAP1 and GCAP2. F48 is also conserved in all GCAPs except GCAP3 and, notably, the human GCAP2 ortholog. The scenario with C35 is identical to that of F48. However, C35 is also conserved in the VILIPs, suggesting that the residue may not be involved in unique GCAP2/ ROS-GC1 interaction. E44 is conserved in all members analyzed except the two out grouped members: recoverin and frequenin. The final site thought to be involved in mGC activation by GCAP2 is E33. Interestingly the sequence alignment shows that this site is variable even between species. We predict that E33 contributes little to ROS-GC1 activation, since it is not conserved even among species orthologs of GCAP2. Not surprisingly, the prediction is supported by experimental data [143].

In summary, evolutionary interrelationships were used to analyze amino acid residues determined to be at the GCAP2/ROS-GC1 interface or critical for activation of ROS-GC1 by GCAP2. As a result, residues could be predicted to fall into one three classes: (i) those that have little role in the interaction, (ii) those that are likely to contribute to the specificity of the NCS/ROS-GC1 interaction, and (iii) those that

could contribute to the total protein structure rather than specific interactions. Notably, some of these predictions have been substantiated by experimental data.

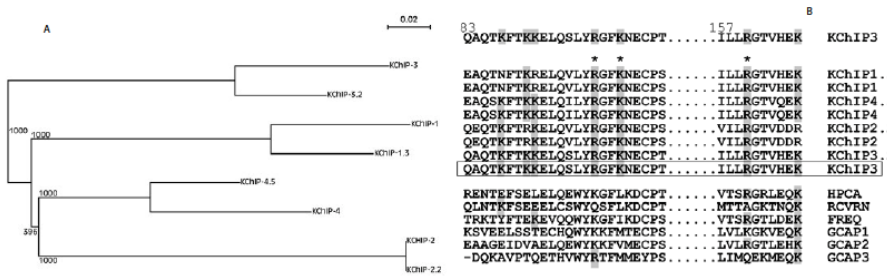

Figure 4.1-4: Analysis of KChIP/DRE sequence interactions.(A) A phylogenetic tree created from a Clustal sequence alignment of the KChIP family of proteins along with isoforms of each variant is presented. The sequences used and the generation of the phylogenetic tree is described in the "Methods" section. (B) Sequence alignment of the NCS proteins corresponding to the region identified in KChIPs to interact with DRE sequence [48]. The region of interest in KChIP3 is presented in the top row, with some amino acid residues numbered. Those that are completely conserved within the KChIP family are indicated with asterisks. Alignment of the corresponding regions from other proteins is also presented

4.1.4 NCALD activation of ROS-GC1

NCALD is a member of the VILIP group (Figure 4.1-1) and brings about activation when it binds to ROS-GC1 in its calcium-loaded state [30, 105]. Analysis of the VILIP group members across species is of interest in itself: several members such as NCALD, HPCA, FREQ and VSNL1 are conserved across vertebrates. The VILIP member in lower organisms is identified as NCS1 and has been included in the alignment (Figure 4.1-3A). All VILIPs that stimulate mGC activity do so in their

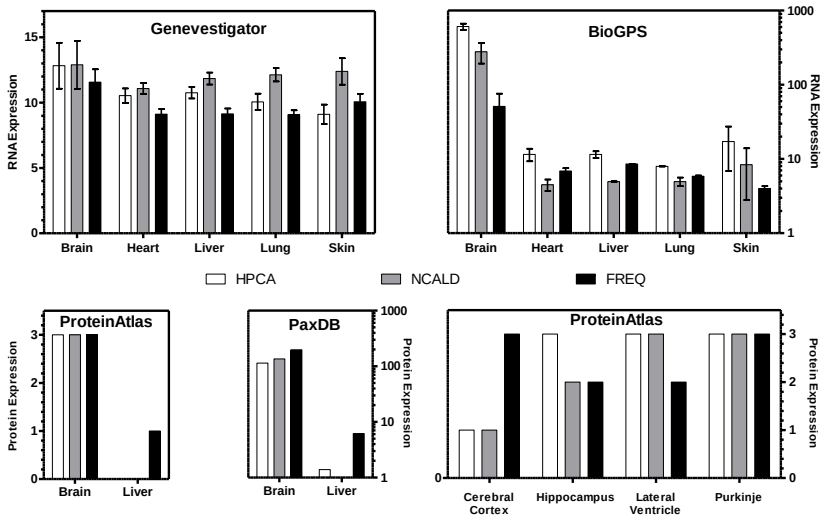

Fig. **4.1-5** Expression profile of three NCS proteins:

(A) mRNA expression profiles across different human tissues (brain, heart, liver, lung and skin) for indicated proteins were obtained from Genevestigator and plotted across the y axis. Level of expression is represented by signal intensity on Human Genome 47k Array. Mean±SEM is displayed. (B) mRNA expression profiles for the same tissues with probe sets identical to the ones used in (A) were acquired from BioGPS. Mean±SEM of expression values from Affymetrix chips related to fluorescence intensity across tissues were plotted on a logarithmic scale. (C) Protein expression level in human brain and liver quantitated immunohistochemically was scored as negative (0), weak (1), moderate (2) and strong (3) by Human Protein Atlas and plotted in y axis. (D) Standardized and integrated data on protein expression level based on MS/MS data was obtained from PaxDB for the same tissues as in (C) and plotted on a logarithmic scale (E) Protein expression level in different neurons of the brain (Cerebral Cotex, Hippocampus, Lateral Ventricle and Purkinje) were compiled in the Human Protein Atlas database based on immunohistochemical analyses and scored as negative (0), weak (1), moderate (2) and strong (3). Data for the proteins of interest are presented.

calcium-loaded state [30, 45, 105, 137]. Information on the residues on the NCS protein that may mediate the function is available only for NCALD: Venkataraman *et al*. [105] have identified residues on NCALD that may be critical for the interaction through a combination of biological assays, peptide competition and direct binding assays. The residues thus identified and localized to the EF1 hand region of NCALD are: H25, E26, Q28, E29, W30, K32, G33, F34, R36, D37, C38, L43, E47, K50, I51, Y52, N54, F55 and F56. They are identified by shading in the top row in Figure 4.1-3B. Comparison of residues that are conserved among VILIPs against those conserved in GCAPs (Figure **4.1**-3B) reveals interesting patterns. Several residues are completely conserved across VILIP members even in lower organisms. These are E26, W30, F34, D37, C38, Y52, F55 and F56 (indicated by asterisks; Figure **4.1**-3C). At corresponding positions in GCAPs, only E26 (D26 in GCAP2), W30 and F34 are conserved. This would lead to the prediction that these residues are important for overall protein integrity, while the rest of the conserved residues contribute to a VILIP-specific function. Furthermore, this function is most likely conserved all the way from lower eukaryotes to vertebrates. The vertebrate VILIPs all activate mGCs in their calcium-loaded state [30, 45, 105, 137]. If this is the preserved function, the results would indicate that the function would be conserved in lower eukaryotes too. On the other hand, it may be a function waiting to be discovered. Further experimental analyses would enable validating one of the alternative scenarios.

The extraordinarily high conservation among VILIPs prompted the question whether these could be redundant proteins. Experimental evidence from loss-of-

function scenarios [19, 20, 23, 47] and the fact that they are completely conserved across vertebrates argue that it is not the case. This leads to two possibilities: (a) their expression is separated by space and/or time, or (b) despite the conservation, they are sufficiently divergent and perform critical functions. In order to distinguish between these two possibilities, we used a data-mining approach to scan the expression of three members of the VILIP family - two closely related members of the VILIP group (HPCA and NCALD) and an outgrouped member (FREQ) (Figure 4.1-1). mRNA expression levels across tissues based on microarrays, were integrated by two different websites (Genevestigator and BioGPS). The data for NCALD, HPCA and FREQ are compiled and presented in Figure 4.1-5 A and Figure 4.1-5 B. The results indicate that all three are expressed in the same tissue, although the expression levels might be different. Similar conclusions are reached at the protein level based on data compiled from Human Protein Atlas (Figure 4.1-5 C) and PaxDB (Figure 4.1-5 D). However, in liver, FREQ is expressed at a lower level while HPCA and NCALD are absent. Even among neurons from different regions of brain, Purkinje neuron shows a comparable expression level across all three proteins, while the presence of FREQ in cerebral cortex, HPCA in Hippocampus and HPCA/NCALD in lateral ventricle are more abundant compared to the rest. These results (Figure 4.1-5) argue that there is no spatial or temporal separation of the expression of the analyzed NCS proteins, either at the mRNA or at the protein level. Furthermore, in the brain, they seem to be co-expressed in different neuronal subtypes, albeit at different levels. This would support a non-overlapping, perhaps critical, function for each tested NCS protein. Thus, the approach presented in this study, we feel, will be particularly beneficial in

delineating the functional divergence among members of this group, which exhibit a high degree of evolutionary conservation. We would predict that the functional divergence is mediated by residues that lie outside of the region that interacts with ROS-GC1, which appears to be highly conserved (Figure 4.1-3B).

4.1.5 Interaction of KChIPs with the downstream regulatory element

Compared to GCAPs and VILIPs, members of the KChIP group are less well characterized and are not known to modulate mGC; their primary shared function appears to be interaction with Kv channels [139]. Only 4 genes have been documented in the human genome, although several splice variants have been reported. An alignment of the known KChIP genes and several of their splice variants is depicted in Figure 4.1A. For the purpose of our analyses of this closely-preserved unique group, we chose a function that every KChIP is believed to carry out: namely, binding to the Downstream Regulatory Element (DRE) [6, 140]. Residues that mediate this interaction were identified through experimental analyses to be K87, K90, K91, R98, K101, R160 and K166 (shaded grey in Figure 4.1-4B). Sequence divergence analyses across members of the three groups were carried out along with some variants chosen at random. Surprisingly, KChIP2 and KChIP 2.2 are completely conserved, suggesting the possibility that one sequence was perhaps reported more than once. With regard to molecular insight into the KChIP interaction with DRE, however, the analyses were beneficial once again. K87 is replaced by Asn in KChIP 1 and its variant; R98 and R101 are completely conserved in all KChIPs (indicated by asterisks; Figure 4.1-4B), while the others exhibit a conserved substitution (Arg for

Lys) (Figure 4.1-4B). When compared to members from other groups, R160 and K166 are conserved throughout and, therefore, are less likely to contribute to the specific interaction [145]. K87 is preserved in recoverin, which does not bind to DRE [140], suggesting that the presence of K87 alone is not enough to drive DRE binding. A conserved substitution (Lys) is observed in most members at position corresponding to R98 in KChIPs decreasing the likelihood of the residue being critical for the specific interaction. Thus, the prediction would be that the remaining residues – K90, K91 and K101 - are the ones that determine the DRE-binding function in KChIPs. Of the three, only K101 remains to be experimentally validated [140].

4.2 Single-column purification of the tag-free, recombinant form of the neuronal calcium sensor protein, hippocalcin expressed in Escherichia coli

Portions of this work were previously published in:

*Krishnan A, **Viviano J *,** Morozov Y, Venkataraman V. Single-Column Purification of the Tag-free, Recombinant Form of the Neuronal Calcium Sensor Protein, Hippocalcin Through a Single Column after Expression in E. coli. Protein Expr Purif. 2016 Mar 18. pii: S1046-5928(16)30040-7. doi: 10.1016/j.pep.2016.03.005*

*Krishnan A, **Viviano J *,** Morozov, Y, Venkataraman, V. Data on the Identity and Myristoylation State of Recombinant, Purified Hippocalcin Data in Brief, 2016 May 20;8:78-81. doi: 10.1016/j.dib.2016.04.024.*

Whether investigations are aimed at elucidating the calcium-dependent changes in the protein itself, or at the downstream interacting partners of HPCA, it is important to be able to obtain the pure protein in sufficient amounts. In this report, we detail how to purify recombinant, tag-free HPCA at high purity from *E.coli* in a single step, incorporating hydrophobic interaction chromatography, which has been used to purify other NCS proteins [45, 146]. This optimized method provides a high yield of active, physiologically relevant protein.

Recombinant HPCA was expressed in *E.coli* ER2566 cells under the control of a lac promoter inducible by IPTG as described in the Materials and Methods section. Purification was carried out using a single phenyl sepharose column on an AKTA Prime and monitored by absorption at 280 nm. Figure 4.2-1A shows the purification profile of HPCA with A_{280} as a function of volume. The fractions are indicated by numbers as an additional inset on the X-axis. Briefly, the whole cell lysate was loaded onto the column and majority of the proteins were eluted in the flow through (Fraction 1). Fractions 2, 3 and 4 represent washes with buffers

containing 20mm Tris with decreasing concentrations of salts. Fractions 5-11 show the elution of HPCA with the calcium chelator EGTA (Fig. 4.2-1; demarcated

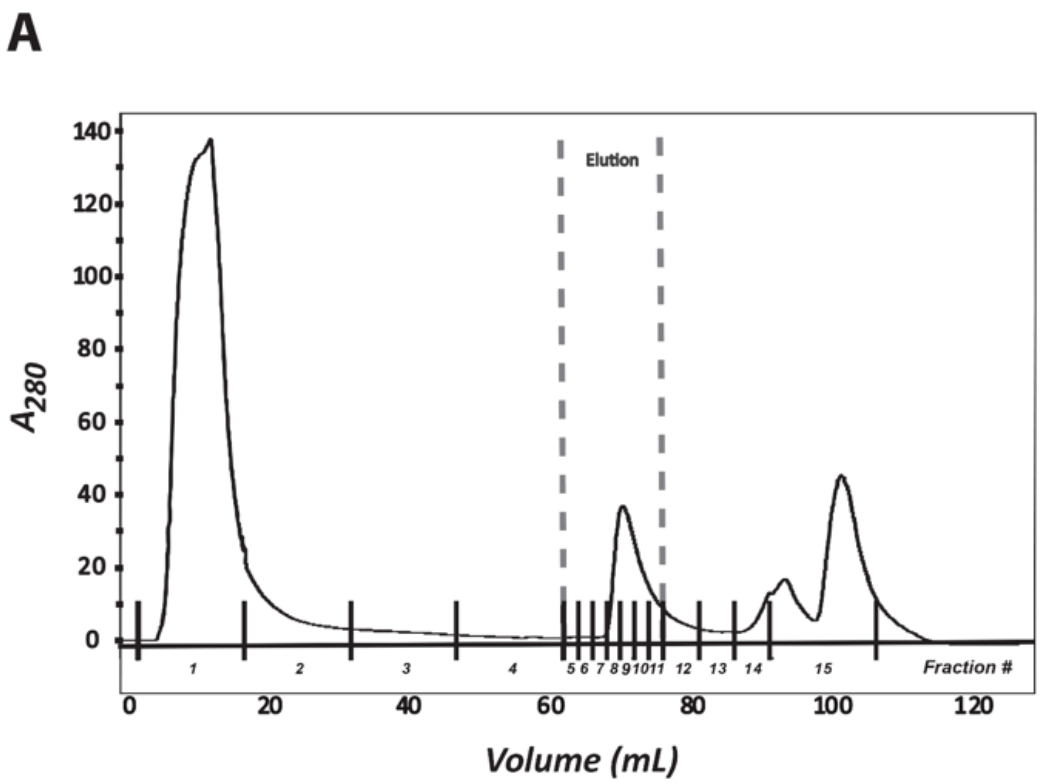

Figure 4.2-1 - Purification of HPCA through a single column. Purification profile from AKTA prime on phenyl sepharose column. Absorbance at 280nm is plotted as a function of volume (mL) on X-axis. An inset is provided to indicate fraction numbers. Fraction 1 contains the unbound protein; Fractions 2 through 4 are 15mL washes with buffers of decreasing salt concentrations as described in "Materials and Methods". Elution of HPCA was accomplished with EGTA (2mL fractions from 5 through 11). Cleaning of the column was through passage of water (fractions 12-14) followed by urea (Fraction 15). The column was then regenerated with water (Fraction 16).

A

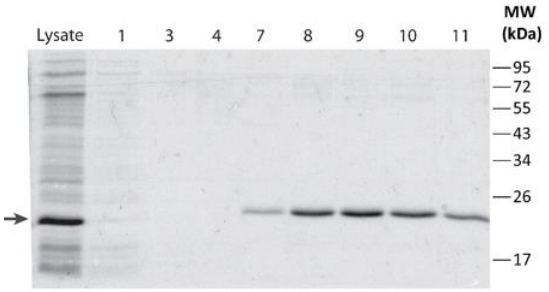

B

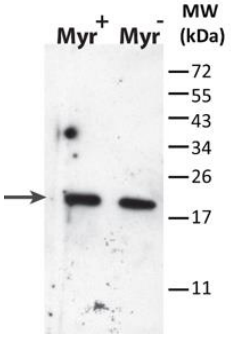

Figure 4.2-2 – Analysis of purified HPCA through a single column.
(A) SDS PAGE analysis of fractions. Fractions from purification were electrophoresed on SDS-PAG as described in "Materials and Methods" and a representative image is presented. Lanes are labeled with the fraction numbers from figure 4.2-1. Total lysate (Lysate) was also included. Arrow indicates the position of the band corresponding to the protein. (B) Western Blot analyses. Myristoylated (Myr^+) and non-myristoylated (Myr^-) forms of HPCA were independently purified and analyzed as described in "Materials and Methods" and a representative image is presented. Arrow indicates the position of the band corresponding to the protein.

between grey dotted lines). HPCA shows a single, distinct peak, starting at fraction 7. The fractions were analyzed by SDS-PAGE (Fig. 4.2-2A; fraction numbers correspond to Fig. 4.2-1A). It is noted that HPCA is expressed at high levels (Fig. 2.2-2B;

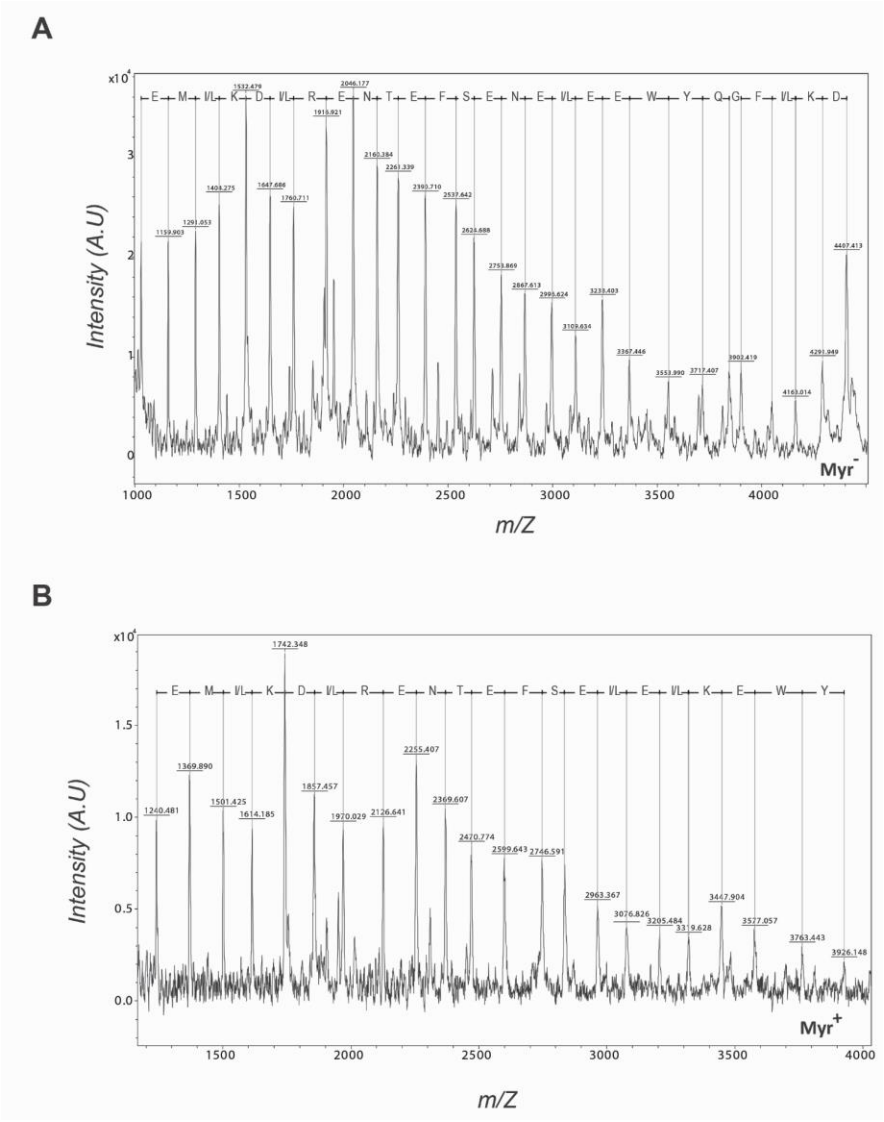

Figure 4.2-3: In-source decay analysis of purified recombinant HPCA. ISD spectrum of N- terminal peptide fragments of expected molecular masses confirming the presence of intact protein. The sequence of the protein was determined using the mass differences between the fragments. It is noted that some residues may be misidentified due to inability to distinguish between very close mass numbers. ISD spectrum of both myristoylated (A) and non-myristoylated (B) recombinant HPCA are presented.

Lysate, indicated by an arrow) and binds almost exclusively to the column under the described conditions (Compare "Lysate" and "1" in Fig. 4.2-2B). In fractions 7 through 11, the protein is obtained in near-homogeneity. In this single column purification step, little to no contamination was observable. Following the HIC purification, HPCA was concentrated as described in the Materials and Methods section. Similar results were obtained whether the protein was in its myristoylated or non-myristoylated form. Typically, when the cells are grown at 37°C, the yield is 4-5 mg protein/L, with the inclusion bodies yielding 3 – 4 mg/L and the soluble fraction, 1 mg/L. Almost all the protein was obtained from the soluble fraction if the cells were grown at lower temperature (22 °C).

To verify that the protein purified was HPCA, western blot analysis was

Fragment	Molecular Weight		
	Myr^-	Myr^+	Difference
GKQNSKLR***P***	1030.0	1240.5	210.5
GKQNSKLRP***E***	1159.9	1369.9	210.0
GKQNSKLRPE***M***	1291.1	1501.4	210.3
GKQNSKLRPEM***L***	1404.3	1614.2	209.9
GKQNSKLRPEML***Q***	1533.5	1742.3	208.8
GKQNSKLRPEMLQ***D***	1647.7	1857.5	209.8
GKQNSKLRPEMLQD***L***	1760.7	1970.0	209.3
GKQNSKLRPEMLQDL***R***	1916.9	2126.6	209.7

Table 4.2-1: N-terminal fragments generated from myristoylated and non-myristoylated HPCA. Purified HPCA was analyzed through mass spectrometry. MOLDI-TOF ISD analyses were independently carried out with the myristoylated and non-myristoylated forms of HPCA. Table 1 displays the sequence of the first 8 fragments identified by ISD. The difference between non-myristoylated and myristoylated forms, as expected, is 210 Da.

performed (Fig. 4.2-2B). Both the myristoylated (Myr^+) and non-myristoylated (Myr^-) forms of HPCA were analyzed. The blot shows a single, strong band at 22kDa for both forms of the protein (indicated by an arrow). There is no observable difference in the reactivity of the antibody to HPCA whether it is in its myristoylated or non-myristoylated form.

4.2.1 Analysis of purified HPCA by Mass Spectrometry:

Purified HPCA was analyzed by mass spectrometry/ISD. Sequencing results from the N-terminus are presented in figure 3. Analysis of both non-myristoylated (Fig. 4.2-3A) and myristoylated (Fig. 4.2-3B) forms of HPCA were carried out independently. The results confirm the N-terminal sequence of the expressed protein. Furthermore, analyses shown in Table 4.2-1 and Figure 4.2-4 also demonstrate that it lacks the N-terminal methionine and is myristoylated at the Gly residue. Thus, the expression conditions permit efficient and accurate myristoylation of HPCA.

4.2.2 Functional analyses of purified HPCA:

HPCA, like other NCS proteins, contains 2 tryptophans, one at position 30, located in the non-calcium binding EF-1 hand and the other at position 103, located in EF-3, which binds calcium [45, 147].

```
    M  G  K  Q  N  S  K  L  R  P  E  M  L  Q  D  L  R  E  N  T
1   atgggcaagcagaatagcaagctgcggccagagatgctgcaggacctgcgagagaacacc 60

    E  F  S  E  L  E  L  Q  E  W  Y  K  G  F  L  K  D  C  P  T
61  gagttctctgagctggagcttcaggagtggtacaagggcttcctgaaggactgcccgact 120

    G  I  L  N  V  D  E  F  K  K  I  Y  A  N  F  F  P  Y  G  D
121 ggcatcctcaacgtggatgagttcaagaagatctacgccaacttcttcccctacggcgat 180

    A  S  K  F  A  E  H  V  F  R  T  F  D  T  N  S  D  G  T  I
181 gcctccaagttcgccgagcatgtcttccgcacttttgacaccaacagcgacggcaccatc 240

    D  F  R  E  F  I  I  A  L  S  V  T  S  R  G  R  L  E  Q  K
241 gacttccgggagttcatcatcgctctgagcgtgacctcgcgtggccgcctggagcagaag 300

    L  M  W  A  F  S  M  Y  D  L  D  G  N  G  Y  I  S  R  E  E
301 ctcatgtgggccttcagcatgtacgacctggacggcaatggctacatcagccgggaggag 360

    M  L  E  I  V  Q  A  I  Y  K  M  V  S  S  V  M  K  M  P  E
361 atgctagaaattgtgcaggccatttacaagatggtttcgtccgtgatgaagatgcctgag 420

    D  E  S  T  P  E  K  R  T  E  K  I  F  R  Q  M  D  T  N  N
421 gatgagtctaccccggaaaagaggactgagaaaatcttccgccaaatggacacaaacaat 480

    D  G  K  L  S  L  E  E  F  I  R  G  A  K  S  D  P  S  I  V
481 gacggcaagctgtcactggaggagttcatccgcggggccaaaagcgacccatcgatcgtg 540

    R  L  L  Q  C  D  P  S  S  A  S  Q  F  *
541 cgcctgctgcaatgcgatcccagcagcgcttcccagttctga 582
```

Figure 4.2-4: Sequence of expressed HPCA. Data presented confirms the identity of the expressed protein, derived from the cDNA sequence as well as through MALDI-TOF ISD (underlined sequence) as HPCA [2, 3]. Together, the data demonstrate the loss of the first methionine (in grey; Table. 4.2-1) in the purified protein.

Previously, fluorescence emission from these residues has been demonstrated to be sensitive to calcium- dependent conformational change in other members of the NCS family [68, 69, 121, 148]. We set out to determine if such a change was observable in HPCA as well. Figure 4.2-5A shows representative fluorescence emission spectra of

HPCA from 300 to 400 nm. Both myristoylated (grey lines) and non- myristoylated (black lines) were analyzed in the absence (solid lines) or presence (dotted lines) of calcium. It is observed that the non-myristoylated form has higher amplitude of the

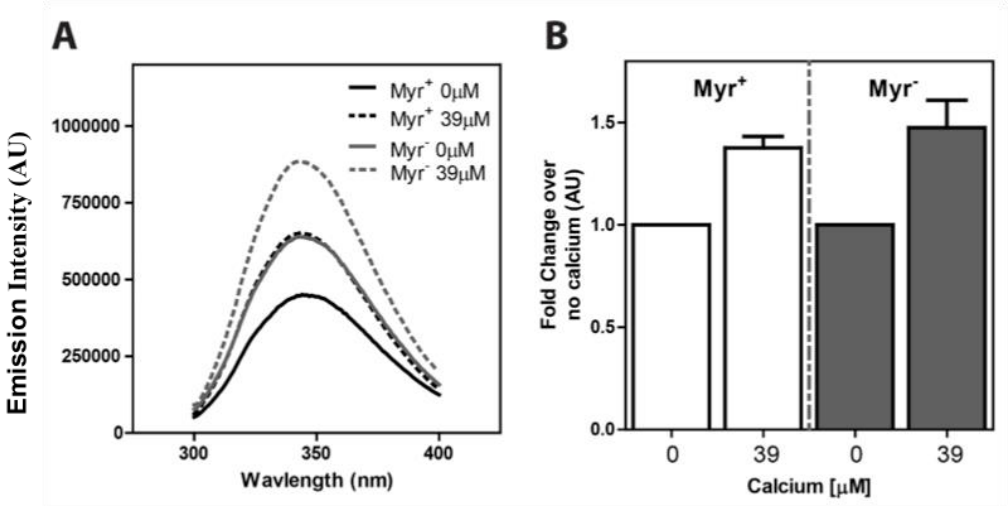

Figure 4.2-5: Response of HPCA to calcium – Tryptophan Fluorescence analyses. HPCA was purified in its myristoylated or non-myristoylated form. All fluorescence measurements were made on a spectrofluorimeter Fluoromax -3. Tryptophan emission fluorescence spectra were recorded at 22 °C from 0.1 ml samples containing 4 μM protein in 20mm Tris-HCl and varying concentrations of Ca/EGTA. The excitation wavelength was set at 290 nm (bandwidth, 4 nm), and the emission wavelength was varied from 300 to 400 nm (bandwidth, 4nm). Background fluorescence was recorded similarly in the absence of added proteins and subtracted from all the spectra. Spectra of HPCA without (solid line) and with (dotted line) calcium at 39 □M concentration. A representative curve is presented. Increase in fluorescence upon addition of calcium. Data obtained with the myristoylated (Myr^+) and non- myristoylated (Myr^-) forms of HPCA are presented. At least three independent runs were for each sample, which included at least two independent preparations and two independent clones.

peak in the absence of calcium compared to the myristoylated form. However, both forms respond with an increase in emission in the presence of calcium. To investigate if the increase was dose-dependent, experiments were repeated with incremental calcium concentrations. Data from several experiments were compiled and response to calcium was analyzed (Fig. 4.2-5B). It is observed that both the myristoylated and non-myristoylated forms respond with a dose-dependent increase

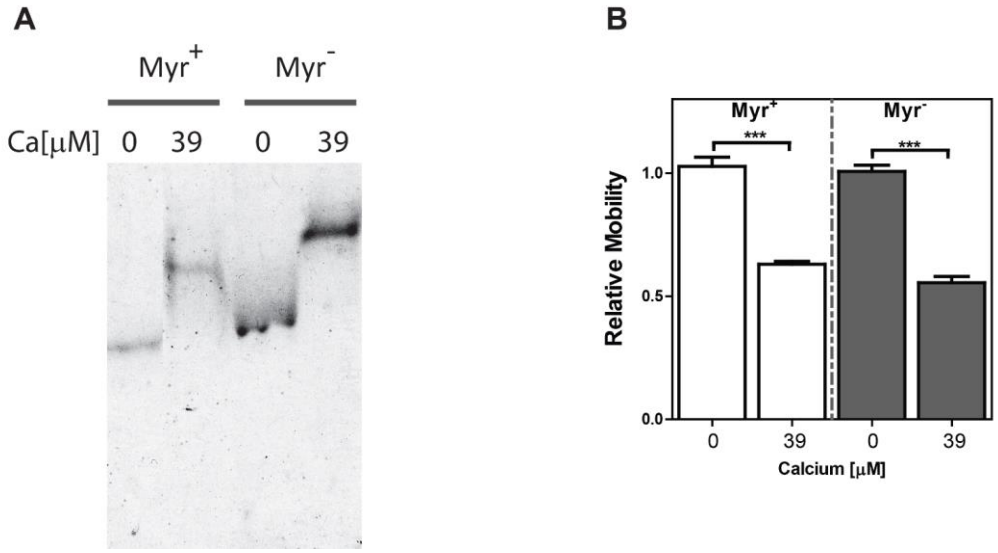

Figure 4.2-6 : Mobility of NCS proteins is retarded by calcium under native conditions. Purified HPCA –myristoylated (Myr^+) or non-myristoylated (Myr^-) -- was electrophoresed under native conditions as described in Materials and Methods. The proteins were independently incubated with either 0 μM (-) or 39μM (+) calcium. The incubation time was inconsequential (data not shown). (A) Representative gel images of mobility shift in native gels; (B) Statistical analyses of mobility data under native conditions. Relative mobility values were compiled from at least two different preparations of the proteins with two replicates each (minimum n=4) and the data is presented as mean ± SE.

in relative fluorescence intensity with increasing calcium. Again, the non-myristoylated form (grey bars) exhibits a slightly (statistically nonsignificant) higher amplitude than the myristoylated (white bars) form. It is noted that the increase corresponds with data reported for the closely related NCS protein, NCALD [121].

4.2.3 Native gel mobility shift response to calcium binding:

It has recently been demonstrated that members of the NCS protein family exhibit a retardation in mobility in native gels [149] and this response is specific to calcium, but not to magnesium, barium or strontium [149, 150]. In order to examine if myristoylation plays a critical role in this phenomenon in HPCA, mobility shift analyses were carried out with the myristoylated and non-myristoylated forms. A representative gel image is presented

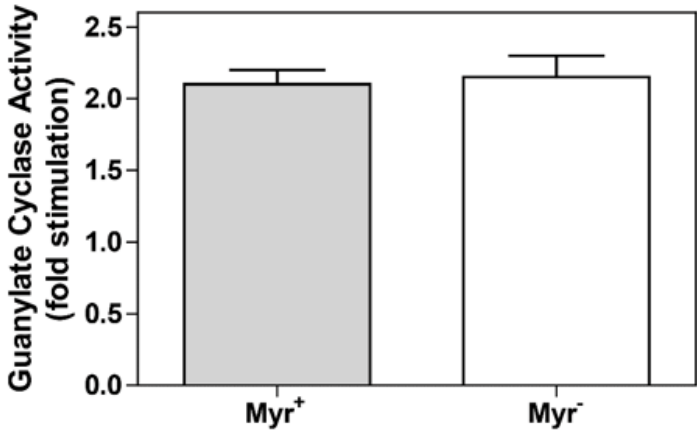

Figure 4.2-7: Stimulation of membrane guanylate cyclase activity by HPCA. ROS-GC1 activity was assayed as described in Materials and Methods. Stimulation by purified HPCA –myristoylated (Myr^+) or non- myristoylated (Myr^-) was measured in the presence of calcium and is presented as fold stimulation over control (absence of protein). Data were compiled from at least two different preparations of the proteins with two replicates each (minimum n=4). No significant difference was observed between the two forms of HPCA.

(Fig. 4.2-6A) along with statistical analyses from replicates (Fig. 4.2-6B). Both forms respond with a retarded mobility in the presence of calcium (Compare "0" Vs. "39" □M). The results are consistent with earlier observations for the myristoylated form and suggest that myristoylation does not significantly alter the response to calcium [151].

4.2.4 Stimulation of membrane guanylate cyclase activity by HPCA:

It has been previously demonstrated that myristoylated HPCA stimulates the activity of the membrane guanylate cyclase, ROS-GC1. The activity of the myristoylated and non-myristoylated forms were compared in this assay as described in Materials and Methods. The results (Fig. 4.2-7) show that both forms stimulate ROS-GC1 activity in a comparable fashion. The 2-fold stimulation observed is consistent with earlier report as is the observation that stimulation is obtained only in the presence of calcium [45].

This optimized method allows for high yield, high purity, tag less expression of HPCA. While purification of HPCA has been documented before [152, 153], the protocols involve tagged protein or multiple steps. We demonstrate in this report that the protein may be purified with good yield from a single column, and is of high purity using SDS-PAGE. Furthermore, we have demonstrated that: (1) Both the myristoylated and non- myristoylated forms can be purified, (2) near-total myristoylation is observed based on MALDI-MS analyses, and (3) the protein is active and responds to calcium as measured by three distinct assays –tryptophan fluorescence, mobility shift in native gels and biological activity. The first two assays allow investigations into structural changes in the protein upon calcium binding,

while the guanylate cyclase assay provides information on target interaction of the protein. Thus, the described procedure fills an important gap – ability to obtain a high-purity, biologically active preparation of HPCA through a single column and will enable analyses of the various functions of this important protein.

4.3 Electrophoretic mobility shift in native gels indicates calcium-dependent structural changes of neuronal calcium sensor proteins.

Portions of this work were previously published in:

Viviano J*, *Krishnan A,* ***Wu H,*** *Venkataraman V. Electrophoretic Mobility Shift in Native Gels Indicates Calcium-dependent Structural Changes of Neuronal Calcium Sensor Proteins. Analytical Biochemistry Volume 494, 1 February 2016, Pages 93–100. doi: 10.1016/j.ab.2015.11.005*

Viviano J*, *Krishnan A, Scully J, Wu H, Venkataraman V. Datasets depicting mobility retardation of NCS proteins observed upon incubation with calcium, but not with magnesium, barium or strontium. Data in Brief. 2016 April 21. doi:10.1016/j.dib.2016.04.035*

Viviano J*, *Wu H, Krishnan A, Venkataraman V, Data on the calcium-induced mobility shift of myristoylated and non-myristoylated forms of neurocalcin delta, Data in Brief. 2016 Mar; 7: 630–633. doi:10.1016/ j.dib.2016.03.021.*

Viviano J**, Wu H, Krishnan A, Ramanujachary K, Venkataraman V. (2016) Data on Final Calcium Concentration in Native Gel Reagents Determined Accurately through Inductively Coupled Plasma Measurement. Data in Brief, 2016 Jan 29. doi: 10.1016/j.dib.2016.01.030*

Change in protein function, which is at the heart of cell signaling, is governed by change in its structure. This change may be captured through the simple technique of electrophoresis. The relationship between the structure of a particle and its mobility in electrical field has been derived mathematically by several investigators beginning with von Smoulouchowski, Huckel and Henry [reviewed in: [154]] and extended to proteins [155-157]; the general agreement is that a protein's mobility is a balance between the electrostatic driving force and the hydrodynamic drag on the protein. Properties that influence these two parameters include amino acid composition, charge, shape and mass of the protein as well as the pH and viscosity of the medium. However, mobility in gels containing SDS (denaturing conditions) is

NCS protein	Molecular weight (**Da**)	Length (aa)	pI	Charge at pH	
				7.4	8.8
Calmodulin	**16837.54**	**149**	**4.22**	**−24.1**	**−25.5**
GCAP1	**22919.64**	**201**	**4.45**	**−19.4**	**−23.6**
KChIP2	30906.72	270	5.11	−12.1	−18.3
S100B	**10713.01**	**92**	**4.59**	**−13.8**	**−16.7**
GCAP2	**23419.60**	**200**	**4.83**	**−12.2**	**−16.0**
KChIP3	29231.15	256	5.41	−9.7	−15.0
KChIP4	28728.58	250	5.21	−9.1	−14.2
KChIP1	26817.33	227	5.25	−8.9	−13.5
HPCL4	22202.33	191	4.89	−9.3	−13.2
GCAP3	23822.06	209	5.10	−8.9	−12.1
Frequenin	21898.73	190	4.83	−9.3	−12.0
HPCA	**22427.34**	**193**	**4.97**	**−8.3**	**−11.4**
VSNL1	22142.27	191	5.14	−7.2	−11.3
Recoverin	23130.20	200	5.16	−7.2	−10.9
HPCAL1 (VILIP3)	22313.13	193	5.36	−6.0	−9.5
NCALD	**22245.17**	**193**	**5.36**	**−6.0**	**−9.5**
Ovalbumin	**42881.11**	**386**	**5.29**	**−11.9**	**−18.6**

Table 4.3-1: Size and charge of NCS proteins. Information on the members of the NCS family is presented together with Calmodulin, S100B, and Ovalbumin. The isoelectric point and the charges calculated at two different pH values -- both at physiological pH (7.4) and at the pH of the separating gel (8.8) -- are presented for each protein. It is noted that these numbers give only a rough estimate of the charge for folded proteins. The amino acid length and the molecular weight are also provided for each protein. The tested proteins are indicated in bold format.

mostly determined by size [126, 158] and such denaturing gels are typically used to assess addition or removal of larger groups such as phosphate, ubiquitin, thiols etc. [reviewed in: [159-161]]. Electrophoresis under non-denaturing (native) conditions allows the charge, shape and size of a protein to contribute to its mobility. Therefore, this technique can serve as a tool to investigate changes in conformation of a protein brought about by charge density modification due to its interaction with ligand(s) and/or other protein(s).

In this report, we provide answers to these questions and demonstrate, for the first time, the use of electrophoresis in native gels to assess structural changes solely due to calcium (ligand) binding in several members of the NCS protein family.

4.3.1 Calcium induces a mobility shift in NCS proteins

As a first step towards investigating the mobility of NCS proteins in native gels, information on their charge and size was compiled, along with other proteins used in this study as controls (Table 4.3-1). The molecular weights of the NCS family members range from about 22 kDa (FRQN) to 31 kDa (KChIP2).

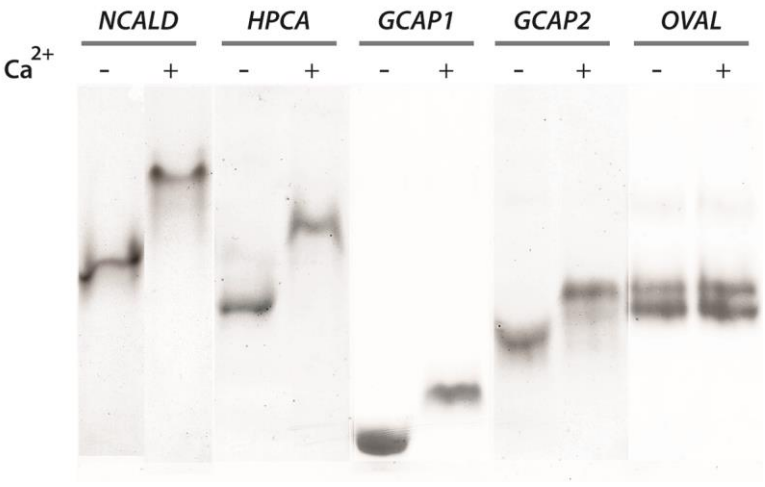

Figure 4.3-1: Mobility of NCS proteins is retarded by calcium under native conditions. Purified proteins were electrophoresed under native or denatured conditions as described in Materials and Methods. The proteins NCALD, HPCA, GCAP1, GCAP2 and OVAL were independently incubated with either 0 μM (-) or 39μM (+) calcium. The incubation time was inconsequential (data not shown). Representative gel images of mobility shift in native gels.

The proteins are presented in order of increasing charge at pH 8.8 (that of the gel matrix and the buffer used for electrophoresis). The charges at pH 8.8 range from -25.50 (CALM) to -9.50 (NCALD and HPCL1). The charges at pH 7.4 (the physiological pH) have also been provided for the proteins along with their isoelectric points for comparison. Four proteins were chosen for our study to represent the range in charges: GCAP1 and NCALD represent the extremes, while GCAP2 and HPCA represent the middle of the range. Three proteins were chosen in addition (Table 4.3-1; indicated in bold format): (a) Calmodulin, an archetypal calcium sensor protein with 4 EF hands like the NCS family, (b) S100B, that also binds calcium but contains only 2 EF hands, and (c) Ovalbumin, which is not known to bind calcium, but is similar in charge to the proteins being studied.

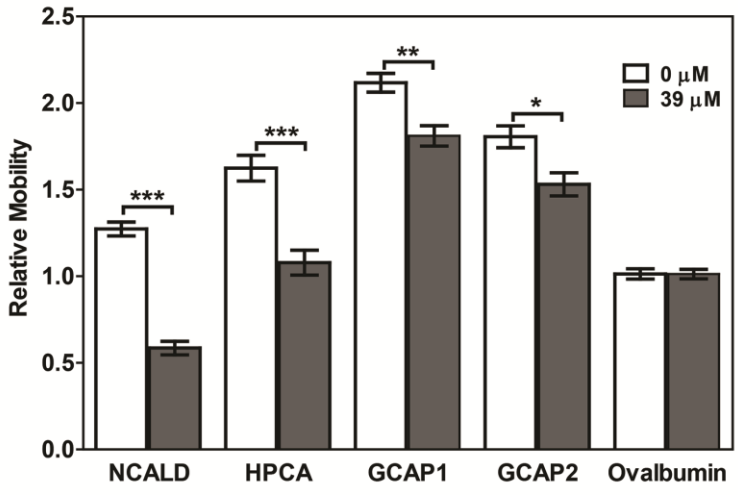

Figure 4.3-2: Statistical analyses of mobility data under native conditions. Relative mobility values were compiled from at least three different preparations of the proteins and the data is presented as mean ± SE. The results from *t*-test are indicated as follows: *, P<0.05; **, P<0.01; ***, P<0.001.

In order to investigate if the calcium-induced conformational changes in NCS proteins may be detected by electrophoresis under native conditions, proteins were incubated in the presence (39 □M) or absence (0 □M) of calcium and subjected to electrophoretic analyses as described in the Materials and Methods section. A representative result is depicted in figure 4.3-1. Each of the proteins migrated to a different position in the absence of calcium (Fig. 4.3-1, "- " lanes). Addition of calcium retards the mobility of each of the NCS proteins in a distinct fashion (Fig. 1A, compare "- " vs "+ " lanes). Ovalbumin, which does not bind calcium, did not show any change in mobility (Fig. 4.3-A; "OVAL"

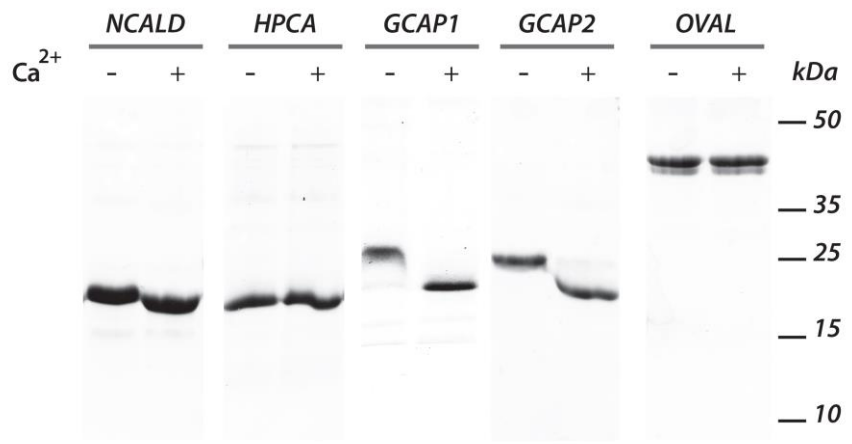

Figure 4.3-3: Representative gel images of mobility shift in denaturing (SDS-Polyacrylamide) gels. Incubation was carried out as for Figure X, only the electrophoresis was on SDS-polyacrylamide gel. Molecular size markers are indicated alongside.

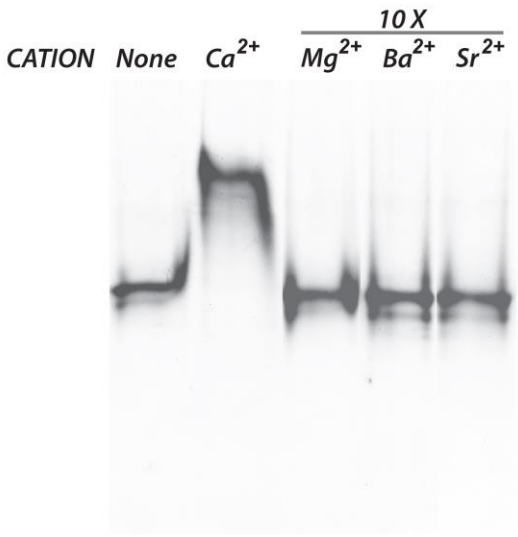

Figure 4.3-4– Calcium induces mobility shift of NCALD, but not magnesium, barium or strontium. Purified proteins were electrophoresed under native conditions as described in Materials and Methods. Representative data obtained with NCALD is presented. The protein was incubated with either 39μM calcium (Ca^{2+}) or a ten-fold excess (~400 □M) each of magnesium (Mg^{2+}), barium (Ba^{2+}) or strontium (Sr^{2+}). Incubation without divalent cations served as control (*None*).

lanes) indicating that the mobility change observed in the NCS proteins is due to the binding of calcium. The observation of multiple bands for Ovalbumin is consistent with previous studies [162]. The difference in mobility upon binding to calcium was reproducible and is significant (Fig. 4.3-2). Considering the fact that the molecular weights are comparable, the relative mobility value appears to correlate to the charge of the protein in the absence of added divalent cation: GCAP1, the most negatively charged migrates the farthest while NCALD, the least negatively charged migrates the least. Addition of calcium produces a shift in mobility that also appears to be characteristic for the protein: NCALD exhibits the greatest change while GCAP1 exhibits the least.

In order to determine if such mobility changes could be observed under denaturing conditions, the experiments were repeated as above, except that the

samples were electrophoresed on SDS-polyacrylamide (denaturing) gels. The results (Fig. 4.3-3) demonstrate that no significant difference in mobility upon addition of calcium is exhibited by NCALD or by HPCA (Fig. 1C, compare "-" vs "+" lanes). Both GCAP1 and GCAP2 exhibit a significant shift in mobility (Fig. 4.3-3, compare "-" Vs "+" lanes); however, the mobility shift is in the opposite direction to that observed in the native gels (Fig. 4.3-1). Calcium retards the mobility of GCAPs in the native gels, but increases it in denaturing gels. The results with GCAPs is consistent with earlier reports [163-165] and appears to be a unique property of GCAPs that is not shared with other NCS proteins such as NCALD and HPCA. No effect is observed on the mobility of Ovalbumin either in the presence or absence of calcium (Fig. 4.3-3, compare "-" vs. "+" lanes). Taken together, these results lead to the conclusions that calcium retards the mobility of all tested NCS proteins in native (but not denaturing) gels and that such retardation requires native conformation of the proteins.

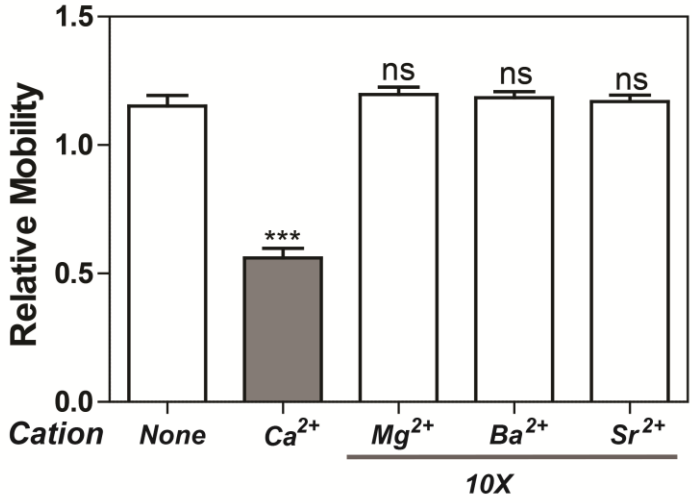

Figure 4.3-:5 Statistical analyses of the mobility data of NCALD under native conditions. Relative mobility values were compiled from at least three different preparations of NCALD. The data is presented as mean ± SE. The results from *t*-test are indicated as follows: *, P<0.05; **, P<0.01; ***, P<0.001

4.3.2 Do other cations cause a mobility shift in NCS proteins?

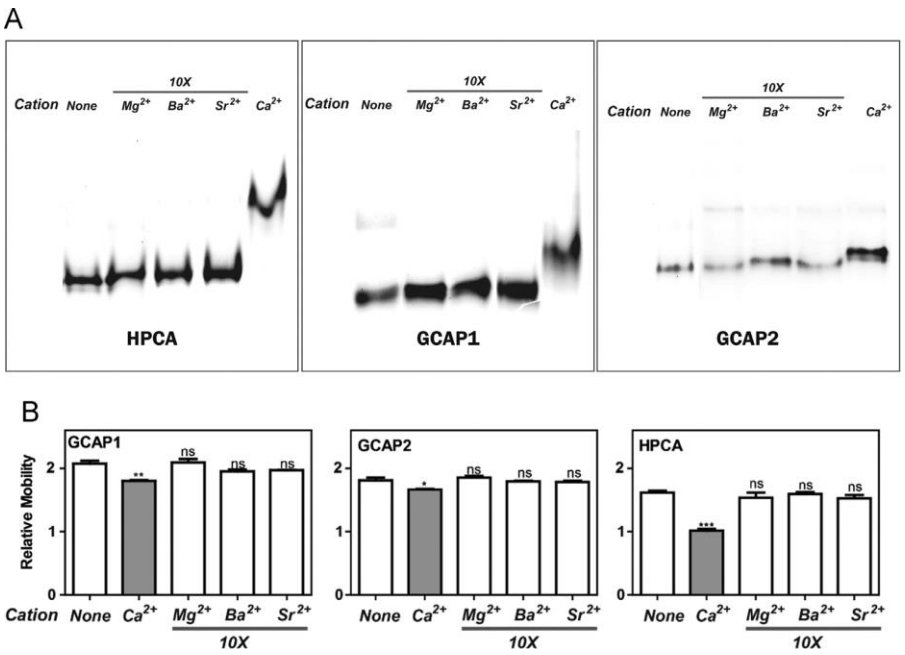

Fig. 4.3-6. Effects of divalent cations on mobility of HPCA, GCAP1 and GCAP2 in native gels. Bacterially expressed proteins - Hippocalcin (HPCA), Guanylate Cyclase Activating Proteins 1 and 2 (GCAP1 and GCAP2) -- were purified in their myristoylated forms. The proteins were incubated with the divalent cation (Ca^{2+}, Mg^{2+}, Ba^{2+}, or Sr^{2+}) and were subjected to electrophoresis in native gels. Representative images are provided in figure 1A. Data was compiled from at least two independent preparations of the proteins with three independent replicates from each preparation. The mobility values were determined. The data (mean + SEM) is presented as a bar graph (Fig. 1B). Results from Student t-tests are also presented for each group against the control group (**, $P<0.05$; **, $P<0.01$; ***, $P<0.001$; ns – not significant). Mobility retardation is observed with the addition of calcium but not with any of the other divalent cations, even at concentrations ten times that of calcium.

The next step was to determine the specificity of the effect for calcium. It is noted that NCALD, HPCA, GCAP1 and GCAP2 are all demonstrated to bind calcium specifically and respond through increased binding to membranes and stimulate membrane guanylate cyclase activity [45, 105, 121]. The ability of other divalent cations from the same main group of the periodic table as calcium – magnesium, strontium or barium – to influence the mobility of the proteins was tested. As a first step, two different concentrations – same as calcium or ten-fold excess – were used for each divalent cation. Representative results from NCALD incubated with ten-fold excess of the individual divalent cations or with calcium are presented as an image (Fig. 4.3-4) and as a graph of data compiled from multiple experiments (Fig. 4.3-5). No significant change in mobility was observed for any of the divalent cations except calcium, even at concentrations ten-fold higher (~400 □M) than that of calcium (Fig. 4.3-4 and 4.3-5:

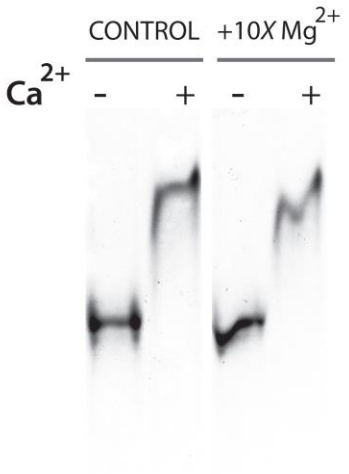

Figure 4.3-7: Competition experiments with magnesium: NCALD was incubated with 0 μM calcium (-) or 39 μM calcium (+) in the presence of ten-fold excess of magnesium (+10*X* Mg^{2+}) or its absence (CONTROL). A representative gel image of mobility shift in native gels is presented.

Compare "None" with "Mg^{2+}", "Ba^{2+}" or "Sr^{2+}"). Similar results were obtained with HPCA, GCAP1 and GCAP2 (Fig 4.3-6) [166]. As the next step, the ability of each divalent cation to influence the calcium-dependent mobility shift was tested. A representative result with NCALD analyzing the effect of magnesium and barium/strontium is presented (Fig. 2C and 2D respectively). To test the effect of magnesium, incubations were carried out in the absence ("CONTROL") or presence of 10-fold excess of magnesium ("+10*X* Mg^{2+}"). Addition of magnesium by itself, even at 10-fold excess, does not cause a change in mobility of the protein (Fig. 24.3-7: Compare "-" lanes in CONTROL Vs. +10*X* Mg^{2+}). Addition of calcium causes retardation of the mobility and the change is not influenced by the presence of magnesium (Fig. 4.3-7: Compare "+" lanes in CONTROL Vs. +10*X* Mg^{2+}). Thus, it is concluded that the observed mobility shift is specific for calcium and is not competed by a ten-fold excess of magnesium. Identical conclusion could be reached with barium and strontium (Fig. 4.3-8): neither cation caused a mobility shift by itself, nor did it influence the calcium-dependent mobility shift (Fig. 4.3-8: compare corresponding lanes in "CONTROL" Vs. "+10*X* Ba^{2+}" or "+10*X* Sr^{2+}"). Experiments were repeated at least

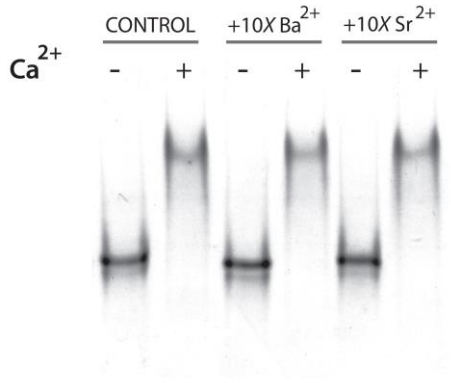

Figure 4.3-8: Competition experiments with barium and strontium: Experiments were carried out as above except that a ten-fold excess of barium (+10*X* Ba^{2+}) or strontium (+10*X* Sr^{2+}) was used.

three times and the relative mobility values were calculated. No significant difference was observed by the addition of any cation other than calcium; nor could they affect the calcium-dependent mobility change (Figure 4.3--6). With ovalbumin, none of the cations could bring about any shift in mobility. Thus, the results lead to the conclusion that the mobility shift in native gels under the tested conditions is calcium-dependent and is not induced by magnesium, barium or strontium.

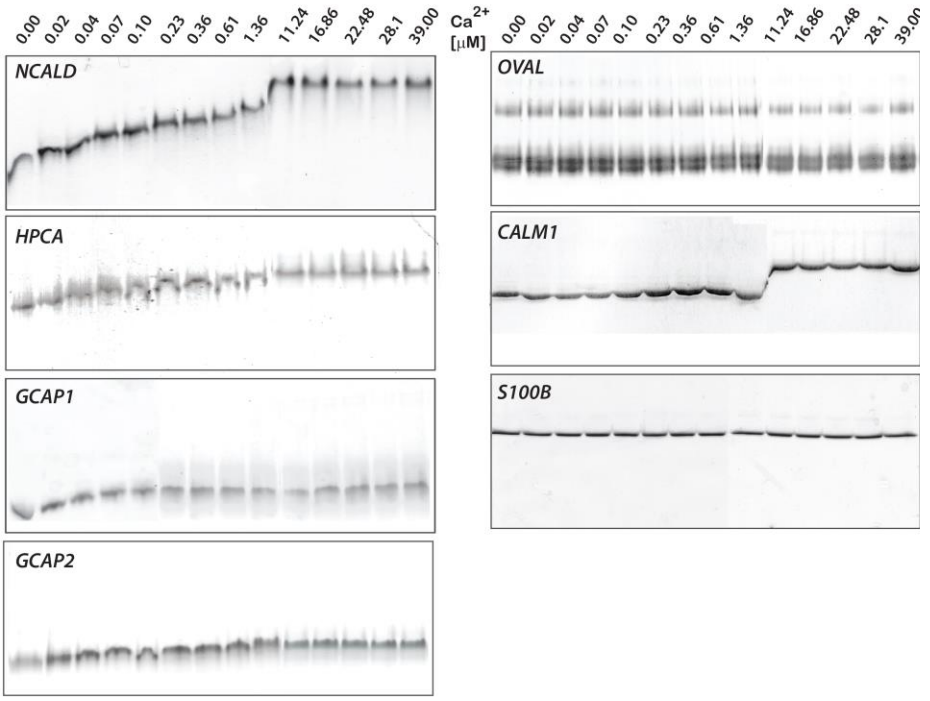

Figure 4.3-9: Mobility of NCS proteins is retarded in a dose-dependent fashion in response to calcium. Purified proteins were run on native gels under conditions described in Materials and Methods. Representative images are presented for NCALD, HPCA, GCAP1, GCAP2, ovalbumin (OVAL), calmodulin (CALM1), and S100B.

4.3.3 Dose dependent calcium shift

Having established a difference in mobility for NCS proteins when they are bound to calcium, we sought to determine if this response is dose-dependent. Analyses were carried out with proteins that were incubated with incremental concentrations of calcium. Representative results for each tested protein (indicated within the panel) are presented in figure 4.3-9. Addition of increasing amount of calcium decreased the mobility of the NCS proteins through the gel in a gradual, dose-dependent manner (Fig. 4.3-9; Panels NCALD, HPCA, GCAP1 and GCAP2). Each of the NCS proteins demonstrated a distinct pattern of response to calcium binding despite their similar size. It is evident that even small changes in calcium can elicit detectable changes in the mobility of all the NCS proteins. NCALD (Fig. 4.3-9; Panel NCALD) shows the greatest decrease in mobility due to calcium binding, especially at lower calcium concentrations. When compared to NCALD, HPCA shows a more tempered response (Fig. 4.3-9; Panel HPCA) despite the fact that the two proteins share 88% sequence identity. The other two highly similar proteins, GCAP1 and GCAP2, show less marked difference in mobility with increasing calcium concentrations.

Of the other calcium-binding proteins tested, Calmodulin also exhibited mobility retardation in the presence of calcium (Fig. 4.3-9; Panel CALM1). However, unlike the NCS proteins, there is a significant change in mobility at 11.24 □M calcium concentration. Based on molar ratios, at this concentration of free calcium, all binding sites in Calmodulin would be occupied. In order to investigate this transition further, additional calcium concentrations (between 1.36 □M and 11.24

□M) were tested with NCALD and Calmodulin. The results are presented in figure 4.3-10. Both NCALD and CALM1 show a decrease in mobility over the tested range. Taken together, NCALD (and other NCS proteins) respond to calcium concentrations over a broad range (Fig. 4.3-10), while Calmodulin response is detected only in micromolar calcium concentrations. Under identical conditions, calcium has little effect on the mobility of S100B, which has been demonstrated to be a calcium-binding protein [167]. Ovalbumin, which does not bind calcium did not show any change in mobility under these conditions (Fig. 4.3-9; Panel OVAL).

Sample	% Total Volume in Sample	$[Ca^{2+}]$ In µM
Chelex-water	0	BLANK
20 mM Tris pH 7.5 (Chelex-treated)	17	-
Running Buffer	17	1.464 ± 0.174
Loading Dye	17	-
Total per Lane	100	0.244 ±0.029

Table 4.3-2: Concentration of calcium in native gel reagents. The calcium-dependent mobility shift of NCS proteins were determined by loading the proteins in native gels and subjecting them to electrophoresis. Apart from the protein and calcium calibration buffer, the loaded sample contained additional components that were tested in this report. They are; 20mm Tris pH 7.5 (Chelex100-treated), loading dye and running buffer, and distilled water treated with Chelex-100 (Chelex-water). Samples and standards were diluted in 5% nitric acid in ICP grade water rated at 18.2 MΩ·cm. Data was compiled from at least three independent replicates for each reagent.

It is noted that the calcium concentration was increased by 240 nM (based on inductively coupled plasma measurements), due to the addition of the running buffer, except those at 0 mM calcium (Table 4.3-2). In order to determine if divalent cations such as calcium were still carried over in solutions, ICP analyses were carried out. Components other than the protein and calcium calibration buffer in the sample loaded for electrophoresis are: 20mM Tris pH 7.5 (Chelex-treated), loading dye (63mM Tris HCl, 0.1% , betamercaptoethanol, 0.0005% bromophenol blue, 10% Glycerol) and running buffer (25 mM Tris, 192 mM glycine). The concentration of calcium in these components was determined by ICP. Chelex-treated water served as a blank. Briefly, samples were diluted into 10mL of 5% nitric acid in ICP grade water rated at 18.2 MΩ·cm. The quantity of calcium present was estimated as parts per billion (ppb) and converted into molarity. The data is presented in table 4.3-2. It is noted that 20mM Tris pH 7.5

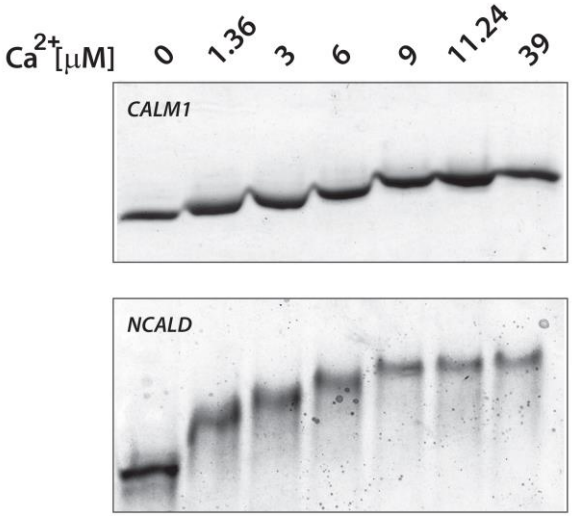

Figure 4.3-10: CALM Responds in a dose dependent manor. Representative images are presented for NCALD and CALM1. The calcium concentration, increasing from left to right, is indicated above each lane. To accommodate size and charge, electrophoresis of calmodulin was for 60 min, and electrophoresis of NCALD was for 150 min.

(Chelex-treated) and the loading dye were comparable to Chelex-water, which served

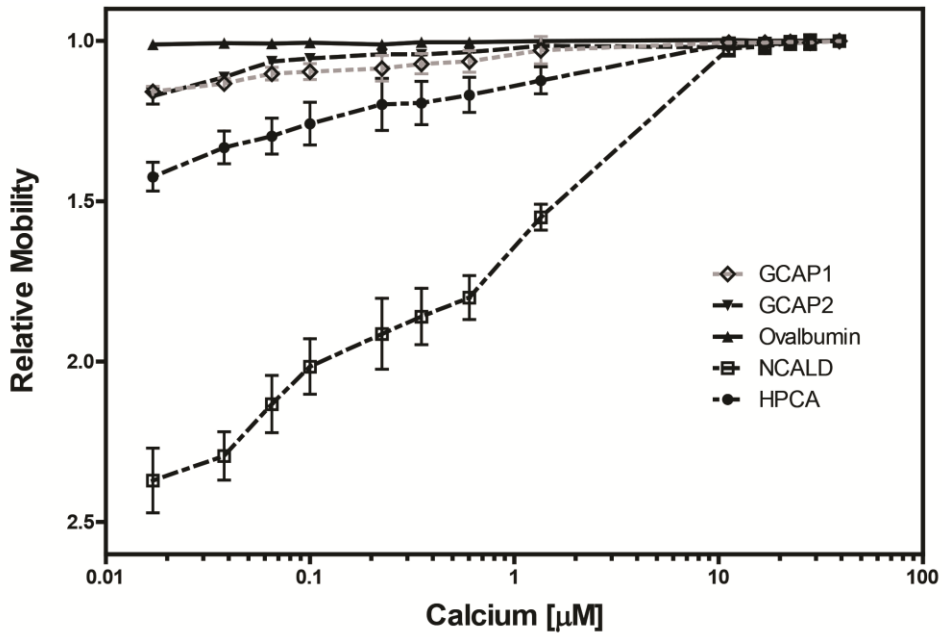

Figure 4.3-11: Mobility of NCS proteins is retarded in a dose-dependent fashion in response to calcium statistical analysis. Data from several independent experiments (typically at least three replicates with three different preparations of the proteins) were collected. Relative mobility values at indicated calcium concentrations were determined and normalized to that at 39 mM calcium. The means ± standard errors are presented.

as the reference. Only the running buffer contained measurable calcium above the reference.

The experiments were repeated with different protein preparations and the results are summarized in figure 4.3-11 as a plot of the relative mobility values to better compare the varied responses of these proteins to calcium. To facilitate direct comparison, the relative mobility values at different calcium concentrations were normalized to that at the highest calcium concentration (39 □M) for each protein.

The dose-response curve of mobility shift is distinct for each of the proteins (Fig. 4.3-11). Of all the tested proteins, NCALD shows the greatest decrease in electrophoretic mobility over the calcium range, especially between 0 and 0.5 □M, suggesting it is the most sensitive to calcium, followed by HPCA (which shares an 88% identity with NCALD), GCAP1 and GCAP2.

Taken together, these results lead to the conclusions that (i) binding of calcium, but not magnesium, barium or strontium, causes altered mobility of NCS proteins in electrophoresis under native conditions; (ii) the NCS proteins exhibit a gradual decrease in mobility with increasing calcium concentrations; (iii) the decrease in mobility is not solely due to a change in charge upon calcium-binding, since

Description	**Myr$^-$ Neurocalcin**	**Myr$^+$ Neurocalcin**
Molar Mass (g.mol-1 ±SD) (MALDI-MS)	22107.1 ± 0 .8	22325.8 ± 1.4
Previously Reported Molar Mass (g.mol-1 ±SD) (ESI-MS)	22110 ± 2	22325 ± 2

Table 4.3-3: Mass Spectrometric Analyses of NCALD. NCALD was expressed in *E. coli* ER2566 as described in the mateals and methods section. For myristoylation, cells with yeast *N*-Myristoyl Transferase were used and myristic acid was supplemented. Cells without the transferase were used to generate the non-myristoylated form; the supplementation was also skipped. Protein samples were co-crystallized with a 1:1 mixture of sinapinic acid and matrix solution (50% acetonitrile/0.05% trifluoroacetic acid in water). Mass spectrometric analyses were carried out in linear, negative modes on a Bruker LRF MALDI-TOF instrument. The mass values were in good agreement with those reported earlier for the respective forms [4]. There was no peak corresponding to the non-myristoylated form in the myristoylated preparation.

S100B, a calcium-binding protein, shows no detectable change in mobility; and (iv) the change in mobility is an inherent characteristic of the protein.

4.3.4 Contribution of Myr group

Interestingly, out of the two other calcium-binding proteins tested, Calmodulin exhibits a response over a narrow, micromolar range of calcium, while S100B exhibits no change. A lower affinity for calcium [168] may explain the result with S100B. However, the overall affinity of Calmodulin for calcium is about 1 □M,

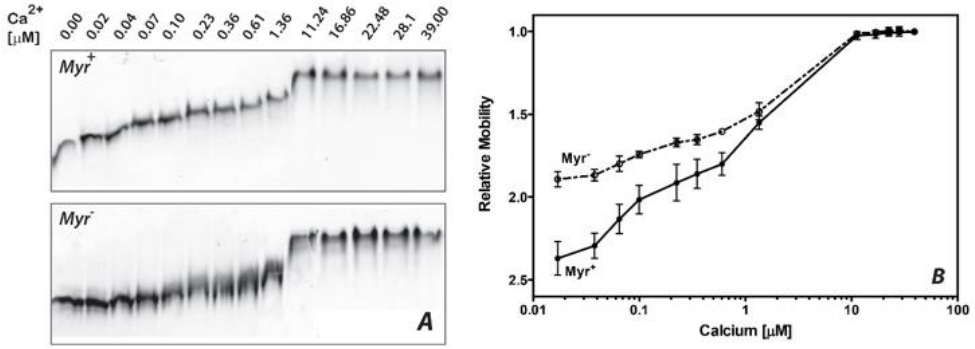

Figure 4.3-12. Mobility Retardation of NCALD (and other NCS proteins) in native gels has been documented. The retardation was directly dependent on the concentration of calcium. It has been suggested that the calcium-myristoyl switch may be responsible for the observed phenomenon [4]. In order to determine if myristoylation of NCALD was essential for the calcium-dependent mobility shift, analyses were carried out with the non-myristoylated (Myr^-) or myristoylated (Myr^+) NCALD. Protein was incubated in the presence of indicated concentration of calcium and electrophoresed in native gels as described [4]. A representative image of the gel is presented in Panel A. Relative mobility values were determined from at least three experiments and plotted as a function of calcium concentration (Panel B). To facilitate direct comparison, the data for the myristoylated NCALD has been reproduced from [4].

which is comparable to that of 0.6 □M documented for NCALD [121, 169-171] [; reviewed in:] [172, 173]. What is unique about the NCS proteins' graded response to calcium over a broad range? All NCS proteins are characterized by the calcium myristoyl switch [reviewed in: [5, 42, 174], which is absent in both Calmodulin and S100B. This switch, upon calcium binding to EF hands, causes a rearrangement of the protein conformation, allowing for the protrusion of the myristoylated *N*-terminus [40, 43, 121, 175]. It is possible that this unique property was detected in the native gel. We then sought to determine if the presence of the myristoyl group is critical for these changes using NCALD, which exhibits the greatest difference in mobility between the Ca^{2+}-bound and Ca^{2+}-free states. The myristoylated (myr^{+}) and non-myristoylated (myr^{-}) forms of NCALD were purified. Mass spectrometric analyses demonstrate that the observed mass values are in good agreement with previously reported values and indicate the presence of the myristoyl side chain. Furthermore, in the myristoylated form, no peak corresponding to the non-myristoylated form was observed. These observations lead to the conclusion that the myristoylation was almost 100% efficient, as reported generally for NCS proteins. The results are presented in Viviano *et al.* (Table 4.3-3) [176]. The two forms of NCALD were subjected to electrophoresis on native gels with incremental calcium as before. The results show that the presence of the myristoyl group does, indeed, contribute to the mobility difference. The non-myristoylated form of NCALD still displayed a response to calcium binding in a dose dependent manner; however, it is less sensitive to this change (1.89 ± 0.017 fold decrease over the calcium range tested) compared to the myristoylated form (2.37 ± 0.017 fold decrease) ([176]Viviano *et al.* Fig. 4.3-11:

Compare Myr^+ vs Myr^-). The result suggests that the presence of the myristoyl side chain is not a critical component of the calcium myristoyl switch.

4.3.5 Ferguson Plot

The mobility of protein in a native gel can be modified due to multiple factors, which would not be detectable on an SDS-PAGE. Changes like phosphorylation state or even structure are easily detectable. In addition changes mass due to dimerization or oligomerization, can have a profound effect on the migration

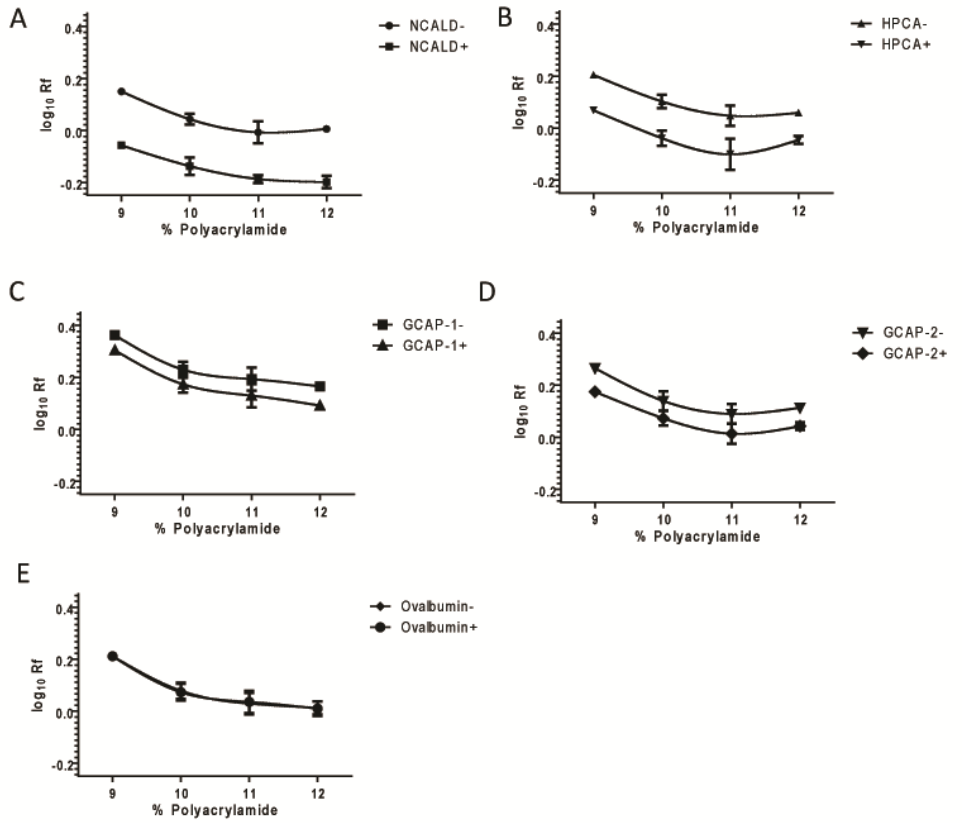

Figure 4.3-13- Ferguson response of NCS proteins. Purified proteins were run on increasing % polyacrylamide gels in triplicate, in the presence of 0μM calcium (-) or 39μM (+) calcium as described in the materials and methods. All of the NCS proteins (A. NCALD, B. HPCA, C. GCAP-1, D GCAP-2) show a parallel response, suggesting that the differences in migration between the calcium bound and calcium free forms is primarily due change in charge. Ovalbumin shows no difference between calcium and non-calcium forms.

of a band though a native gel. In order to better understand the changes that are observed in native gels a Ferguson plot was constructed.

A Ferguson plot was developed by first published by Kenneth Ferguson analyzing hormones in starch gels [177]. The Ferguson plot allows for the extrapolation of the mass, charge or both. By plotting the Ferguson graph, conclusions can be made biased on the line pattern. If the lines intersect, the change in mobility is due to a change in mass. If the lines of the plot do not intersect and remain parallel, than it can be concluded that differences in mobility are due to changes in charge.

We previously demonstrated that upon Ca binding changes in structure leads to retardation in mobility. To better understand the contribution of charge and mass, a Ferguson plot was constructed (4.3-13). Calcium and non-calcium bound forms of each of the proteins were run on native gels of varying acrylamide concentrations, as described in the Materials and Methods section. The slopes of the calcium free (-) and calcium bound (+) form for each of the proteins show a parallel response, indicating the difference in mobility is not due to a change in mass, such as a dimerization event. Rather, the parallel slopes indicate a distinct change in charge. Ovalbumin shows no difference between the calcium bound and calcium free forms.

The change is charge is likely caused by the structural rearrangements brought on by calcium binding. This causes differences in the exposed surface charges of the protein, which are observed on the gel as a band shift. This result also suggests that the migration is independent of the ability to dimerize, since NCALD is a calcium induced dimer. Further analysis and mathematical extrapolation of the slopes of the

Ferguson plot will help better dissect the contributions of change on the mobility of the NCS proteins through a native gel.

Chapter 4.4 Three amino acids in the dimer interface of the neuronal calcium sensor protein neurocalcin delta also govern its response to calcium

In order to investigate if NCALD and HPCA exhibited similar properties, three different aspects of calcium responsiveness were examined: (1) ability to form dimers and the effect of calcium, if any (2) local conformational changes in response to calcium binding, and (3) mobility shift on native gels in response to calcium (Calcium-Induced Mobility Shift Assay or CIMSA).

4.4.1 Ability to form dimers and the effect of calcium:

NCALD is known to be a dimer in its calcium-bound form based on the crystal structure. At present no information is available on its apo-form. No information is available on HPCA for either its apo or calcium-bound form. Size exclusion chromatography was used to assess the dimerization state of the two proteins as described in Materials and Methods (Fig. 4.4-1). For this experiment, the cytosolically expressed soluble fraction of the protein was used. Hence, purification did not include a denaturation and refolding step, prior to HIC on phenyl sepharose column. It is noted that the soluble form is comparable in properties (mobility shift, Tro fluorescence, mGC stimulation) to the one purified from inclusion bodies. Both proteins—NCALD and HPCA -- are around 22kDa as monomers and would be ~44kDa as dimers. Bacterially expressed and purified proteins were separated on Superdex75 column, pre-calibrated with standards of known sizes. The same protein preparation was analyzed under two different conditions: in the presence (+ Calcium) or absence (- Calcium) of calcium. The respective elution profiles under the two

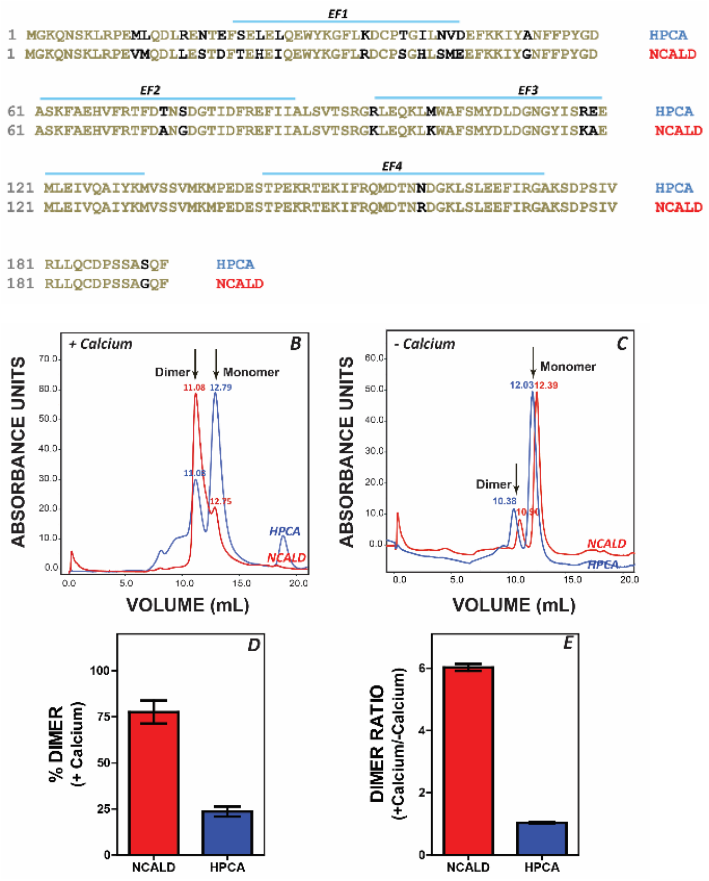

Figure 4.4-1. NCALD dimerizes in the presence of calcium, but HPCA is primarily monomeric. (A) Sequence alignment of HPCA and NCALD. Identical residues are colored grey and dissimilar residues, in black. Representative elution profiles of NCALD and HPCA from size exclusion chromatography are presented (B) with calcium (+ calcium) or (C) with EGTA (- calcium). The arrows indicate the dimer and monomer peaks corresponding to molecular weights 44kDa and 22kDa, calibrated with standards. (D) The percentage of dimer was calculated from the percentage of the area under the peak corresponding to dimer in the presence of calcium. Data from multiple runs (n=4) were averaged and presented as mean± SE. (E) The area under the dimer peaks with or without calcium was averaged from several experiments. The ratio was calculated to determine the effect of calcium on dimerization. Addition of calcium causes a 6-fold increase in dimerization of NCALD, but has no significant effect on HPCA. Data from multiple runs (n=4) were averaged and presented as mean± SE.

conditions are presented for both NCALD and HPCA in figure 4.4-1B and 4.4-1C. In the presence of calcium, consistent with the crystal structure, NCALD is predominantly a dimer (eluting at 11.08 mL), with some monomeric fraction (12.75 mL). In contrast, HPCA is predominantly a monomer (12.79 mL). However, in the absence of calcium, both proteins are predominantly monomeric (12.03 mL and 12.39 mL respectively). These results demonstrate that only NCALD forms dimers and the process is calcium-dependent.

The data was analyzed further through two parameters: the ability to dimerize and the influence of calcium on the process. The percentage of dimers that were detectable in the presence of calcium was determined from multiple experiments (n=4) for the two proteins (Fig. 4.4-1D). It is observed that ~75% of the calcium-bound NCALD is in dimeric state, while only ~ 25% of HPCA exists as a dimer in the presence of calcium. To analyze the influence of calcium, the ratio of dimer populations in the presence and absence of calcium was calculated (Fig. 4.4-11E). The addition of calcium causes a 6-fold increase in the proportion of dimers in NCALD, but it has no significant effect on HPCA. Based on size exclusion chromatography analyses, the following conclusions are derived: (1) both NCALD and HPCA are predominantly monomeric in the absence of calcium, and (2) addition of calcium promotes dimerization in NCALD, but not in HPCA.

4.4.2 Response to calcium through tryptophan fluorescence:

It is well-established that the structural rearrangements in NCS proteins upon binding calcium are observable as changes in tryptophan fluorescence [121]. Both NCALD and HPCA contain two conserved tryptophans at positions 30 (within the

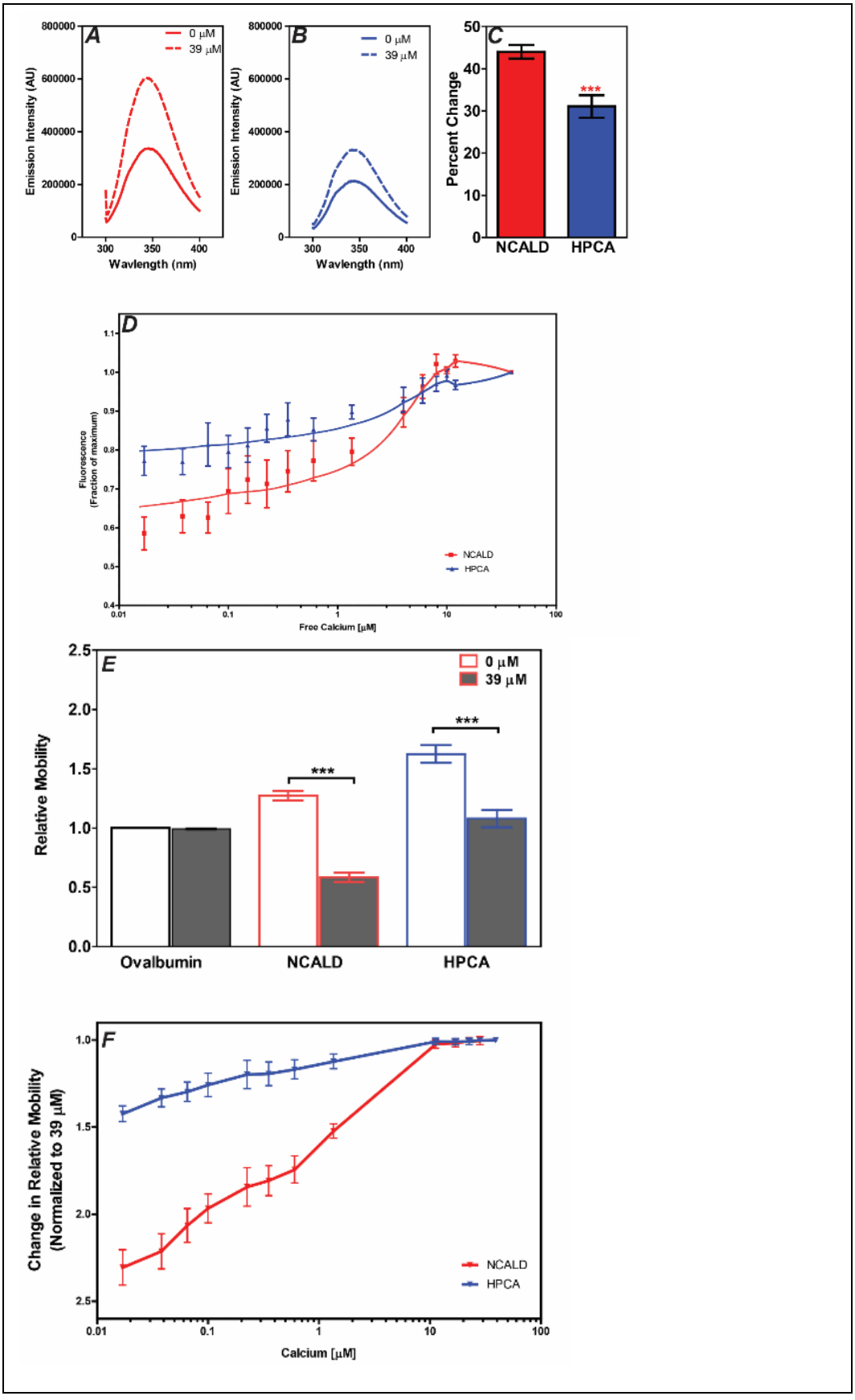
A
0 μM
39 μM
Emission Intensity (AU)
Wavlength (nm)
B
0 μM
39 μM
Emission Intensity (AU)
Wavlength (nm)
C
Percent Change
***
NCALD
HPCA
D
Fluorescence
(Fraction of maximum)
NCALD
HPCA
Free Calcium [μM]
E
0 μM
39 μM
Relative Mobility
***
***
Ovalbumin
NCALD
HPCA
F
Change in Relative Mobility
(Normalized to 39 μM)
NCALD
HPCA
Calcium [μM]

Figure 4.4-2. NCALD and HCPA exhibit different calcium-driven responses in tryptophan fluorescence and mobility shift on native gels. Representative tryptophan fluorescence spectra in free calcium at concentrations of 0 μM, and 39 μM are presented for (A) NCALD and (B) HPCA. (C) The average (n=8) percentage increase in peak fluorescence intensities (344 nm) from 0 μM to 39 μM calcium (D) The peak fluorescence intensities at incremental free calcium concentrations were obtained and normalized to the maximum (at 39 μM free calcium). Data for selected calcium concentrations are presented as mean ± SEM (n=8). (E) Mobility shift of NCALD and HPCA was determined as described previously [1-4]. Relative mobility of NCALD and HPCA in the presence (39 μM) and absence (0 μM) of calcium. Ovalbumin served as a negative control. (F) Dose-dependent response of mobility shift to calcium is displayed for NCALD and HPCA. The values are normalized to that obtained at maximal calcium concentration (39 μM). Data is presented as mean ± SEM (n=8).

EF1 region) and 103 (within the EF3 region). In order to monitor local conformational changes around these residues due to calcium binding, changes in tryptophan fluorescence as a function of calcium were determined as described in Materials and Methods. Proteins were individually incubated with indicated concentrations of calcium and emission

was monitored between 300 and 400 nm. Representative spectra for NCALD (Fig. 4.4-2A) and HPCA (Fig. 4.4-2B) are presented in the presence of 0 or 39 □M calcium. Both proteins show an increase in fluorescence intensity upon the addition of calcium, suggesting that the environment around the Trp residues become more hydrophobic. For both of the proteins the peak wavelength is 344nm and no significant red/blue shift between the calcium free and calcium bound forms was

observed. However, the increase in fluorescence intensity is more striking with NCALD (44%) than with HPCA (31%) (Fig.4.4-2C).

The experiments were repeated with incremental calcium concentrations between 0 and 39 μM. In order to better compare the responses of the two proteins at different calcium concentrations, they were calculated as a fraction of response at the highest calcium concentration tested (39 μM). Data from multiple runs of at least 2 biological replicates were averaged (Fig 4.4-2D). This was done to facilitate a direct comparison of the calcium response of the proteins. It is evident that both NCALD and HPCA respond in a dose-dependent fashion over two orders of magnitude of calcium concentrations. However, the magnitude of change is higher in NCALD over the tested range. The results suggest that, in terms of local conformational changes around the tryptophans, NCALD is more hydrophobic as a result of the response to calcium when compared to HPCA.

4.4.3 Response to calcium through mobility shift on native gels:

We have recently described mobility shift on native gels that enables examination of response of proteins to calcium [1-4]. The calcium dependent response is specific for each NCS protein and appears to correlate to global conformational changes induced by the calcium-myristoyl switch [5, 6, 18]. Purified HPCA and NCALD were analyzed by this method as described (Materials and Methods). Ovalbumin served as a negative control. Addition of calcium causes retardation in mobility as reflected in the relative mobility values for NCALD and HPCA, but not on ovalbumin (Fig. 4.4-2D). The response of the two proteins over a

A

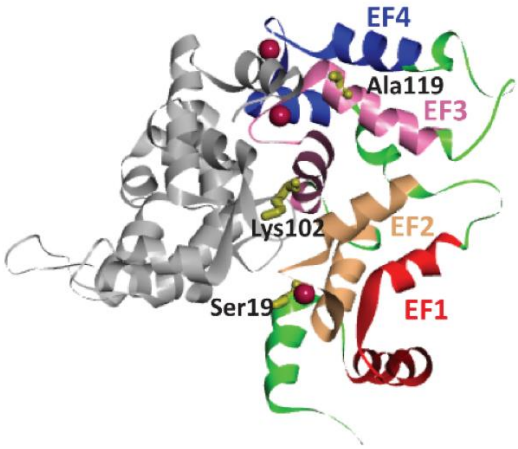

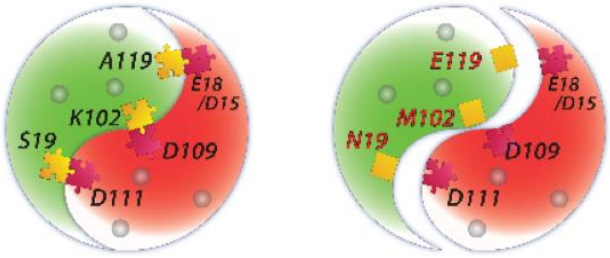

B.

Figure 4.4-3: Three residues of the dimer interface in NCALD may be critical for dimerization. (A) Crystal structure of NCALD (1BJF) with one monomer in grey and the other in color: The four EF hands are colored differently and labeled. Calcium atoms are indicated as red spheres. The side chains of the residues S19 (in EF1), K102 and A119 (in EF3) are displayed in yellow and labeled. (B) A schematic diagram of the dimer interface residues of interest in NCALD is provided. The S19, K102 and A119 residues on one monomer and their potential interacting residues on the other monomer (E18, E15, D109 and D111) are indicated. Presence of N19, M102 and E119 in HPCA is proposed to destabilize dimer formation.

range of calcium concentrations was determined and the relative mobility was normalized to that at 39 µM (Fig. 4.4-2E). NCALD exhibits a greater magnitude of response over the calcium concentrations tested. The conclusion is consistent with data obtained through analyses of tryptophan fluorescence.

Taken together, the results establish that despite a high degree of conservation of primary sequence, NCALD and HPCA exhibit distinct and different responses to changing free calcium concentrations. The most striking difference is that NCALD exhibits calcium-dependent dimerization, while HPCA does not. Does dimerization define the difference between the two proteins?

4.4.4 Three amino acids at the dimer interface of NCALD may define the difference between the proteins

The crystal structure of NCALD (1BJF) was resolved in a dimeric, calcium bound form [178]. Careful examination of the crystal structure for aa residues on the two monomeric units of NCALD that may promote formation of salt bridges to stabilize the dimeric form and the following residues were identified as contributing to either hydrogen bonding, electrostatic interactions or both: S19, E98, Q99, K102, D109, D111, N113, Y115, and A119. When the conservation of these residues between NCALD and HPCA was examined, three aa residues were unique for NCALD: S19, K102 and A119 (Fig. 4.4-1A). The positions of these residues are indicated in the three-dimensional model of NCALD (Fig. 4.4-3B). The model (ribbon structure) depicts one monomer in grey and the other in color, with different EF hands distinguished by color and labeled.

S19 is located close to the EF-1 region of NCALD that does not bind calcium. The EF-1 region is the least conserved through the family [32, 42].. K102 and A119 on NCALD are located in the calcium binding EF-3 hand, which was previously shown to the highest affinity site for calcium on NCALD [121]. A schematic diagram outlines potential polar interactions involving these residues in a dimer of NCALD

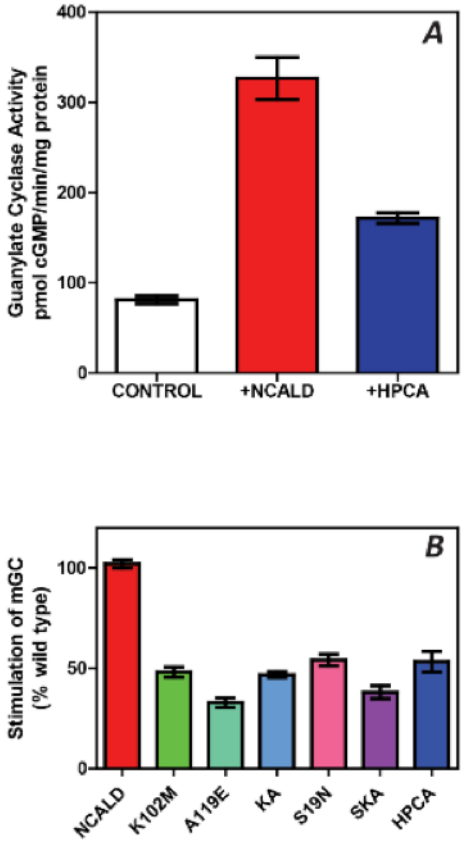

Figure 4.4-4: The protein can stimulate of membrane guanylate cyclase activity after mutations, but with reduced ability. Stimulation of membrane guanylate cyclase activity was measured using 4 μM each of the proteins at 10 μM calcium concentration. Cos cell membranes transfected with ROS-GC1 served as the source of the membrane guanylate cyclase. The assay was carried out and the cGMP produced was measured using competitive ELISA as described in the materials and methods section. (A) Stimulation of membrane guanylate cyclase activity by NCALD and HPCA. Data (n=4) is presented as specific activity. Specific activities were determined for wild type as well as mutant proteins and normalized to that of NCALD as 100%. The data is presented in (B).

(Fig. 4.4-3B). Such interactions are absent in HPCA (Fig. 4.4-3C). Ser19 can form an intermolecular H+ bond with Asp111 in the EF-3 region on the other monomeric unit. In HPCA the position is occupied by an Asn residue. N19 could possibly hinder D111 binding, preventing it from interacting with K102 (Fig. 4.4-3C), however it is also possible that this change might actually increase dimer stability, due to the decreased bond length. In NCALD, K102 appears to form a salt bridge with D111 and D109. This position is occupied by a methionine in HPCA. M102 cannot form a

salt bridge with D111 and D109. A119 is not charged and will not form an ionic bond; however, in HPCA this site is E119. The residues Glu18 and Asp15 on the other monomer would likely repel the Glu residue at 119 and would be predicted to prevent dimerization (Fig. 4.4-3C). Having an Ala residue at 119 in NCALD would avoid this repulsion and promote dimerization. If these three residues on NCALD were mutated to those on HPCA, would it lead to disruption of dimerization and convert the calcium-driven responses to be HPCA-like?

In order to answer this question, we created NCALD mutants as described in the methods section. The single mutations K102M, and A119E and the double mutation K102MA119E (hereafter referred to as KA) were created and focus on the role of the high affinity, calcium-binding EF hand EF-3. The S19N mutant would help delineate any role of the non-calcium binding EF-1 region. Finally the S19NK102MA119E (hereafter referred to as SKA) mutant would have converted all three residues to be HPCA-like and would help analyze the combined roles of the EF-1 and EF-3.

4.4.5 Effect of mutations on the dimerization of NCALD:

The mutant forms of NCALD were bacterially expressed and purified. All mutants were biologically active (albeit diminished compared to the wild type) based on their ability to stimulate membrane guanylate cyclase (Fig 4.4-4). The purified proteins were analyzed on Superdex75 columns and the results were analyzed using the criteria established before to examine the percentage of dimers and the effect of calcium on dimerization. Total purified protein was loaded to resolve aggregation, if any, and reliably estimate the dimer and monomer percentage in different

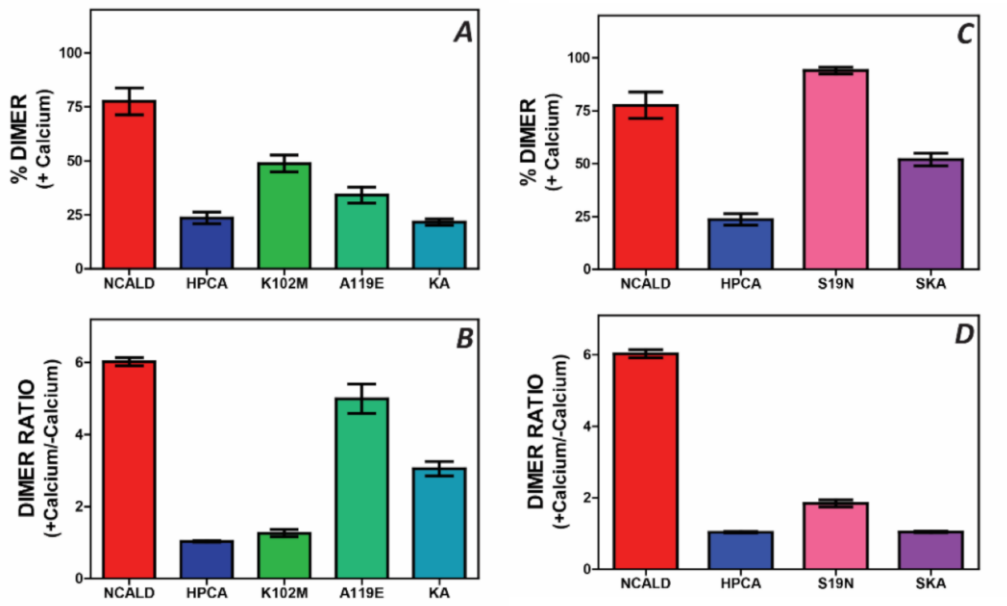

Figure 4.4-5. **Effects of mutations on dimer formation in NCALD**. The three predicted dimer interface residues, S19, K102 and A119, were mutated individually or together and the proteins were purified as described. Analyses were carried out through size exclusion chromatography in the presence or absence of calcium. Percentages of dimers were calculated as described earlier. Data for K102M, A119E and the double mutant K102MA119E (KA) is provided as (A) Percentage of dimers in the presence of calcium as well as (B) The ratio between dimer percentages in the presence and absence of calcium. Data for S19N and S19NK102MA119E (SKA) is provided as (C) Percentage of dimers in the presence of calcium, and (D) The ratio between dimer percentages in the presence and absence of calcium. Data presented is mean ± SE from multiple runs (n = 4).

preparations. Proteins that eluted as a dimer, several times, were concentrated and analyzed again on the column to ensure that they were indeed dimeric. Fractions were concentrated, electrophoresed and stained to ensure the identity of the protein.

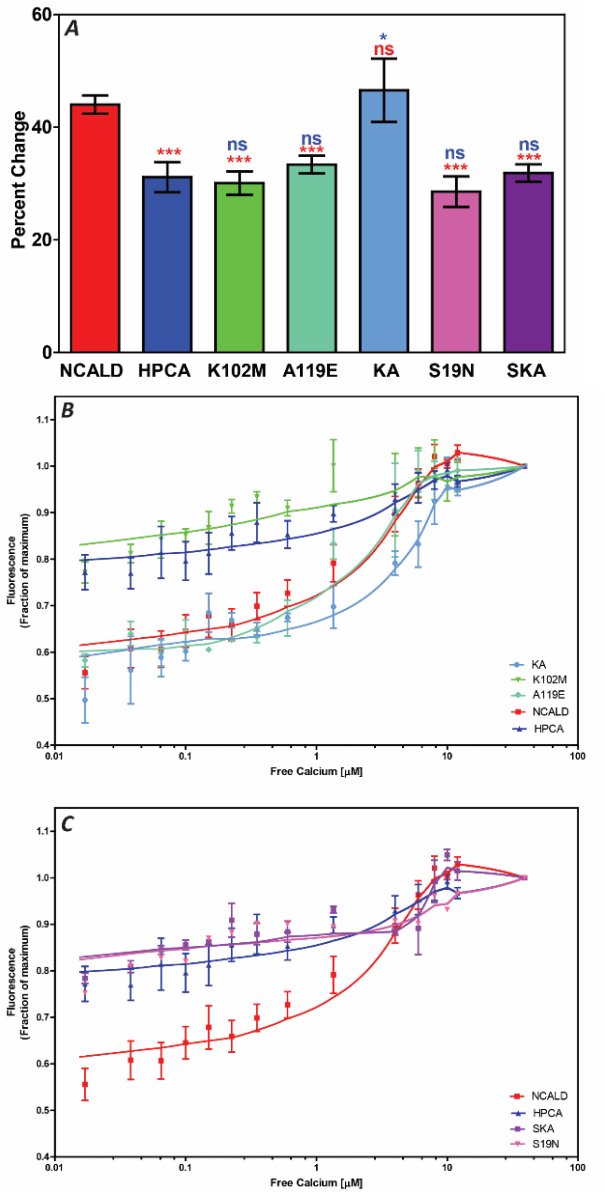

Figure 4.4-7. Effect of mutations on response to calcium as assayed by tryptophan fluorescence. Fluorescence Spectra for the wild type and mutants were obtained as described in "Materials and Methods". The average (n=8) percentage increase in peak fluorescence intensities at 344 nm from 0 μM to 39 μM calcium for NCALD, HPCA and the five mutants of NCALD are presented (A).The peak fluorescence intensities for varying free calcium concentrations from 0 μM to 39 μM were averaged from several measurements (n=8) and normalized to that at saturating calcium (39 μM) concentration. Data is presented as mean ± SE for (B) K102M, A119E and KA, and (C) S19N and SKA along with wild type NCALD and HPCA for comparison.

Results presented in figure 4.4-5A show that K102M, A119E and KA mutations decrease dimer formation in NCALD. The double mutant has the most significant effect, with the dimer levels comparable to HPCA (~ 25%). Both K102M (49%) as well as A119E (34%) also show decreased dimer fraction compared to wild type NCALD (75%). The results validate the predicted roles for these residues in stabilizing the dimer through formation of salt bridges.

Analyses of calcium effect on dimerization reveal additional roles for these residues (Fig. 4.4-5B). There is nearly a 6 fold change in dimer percentage between the calcium bound and calcium free forms of NCALD. The K102M mutation nearly abolishes this conversion by calcium and the ratio is HPCA like. The A119E mutation still leaves a 5-fold conversion to dimer upon addition of calcium, even though it reduces dimerization, despite its reduced ability to form a dimer. The KA mutant shows a calcium-dependent conversion intermediate between K102M and A119E. Thus the residues appear to have two distinct effects: on dimer formation and calcium-dependent dimer conversion.

Results from the S19N and SKA mutants are presented in figure 4.4-5C and 4.4-54D. The former mutation causes a striking increase in the percentage of dimer, nearly 95%. When combined with the KA mutation, SKA dimers are diminished to about 50% of wt, still notably more than KA (~25%). The S19N mutation also affects the calcium-dependent dimerization significantly (1.8 fold compared to 6 fold for NCALD). It also abolishes the calcium induced dimerization effect on KA, with the SKA mutant resembling HPCA. Taken together, the results underscore the importance of the three residues not only in dimer formation, but also mediating calcium responses in

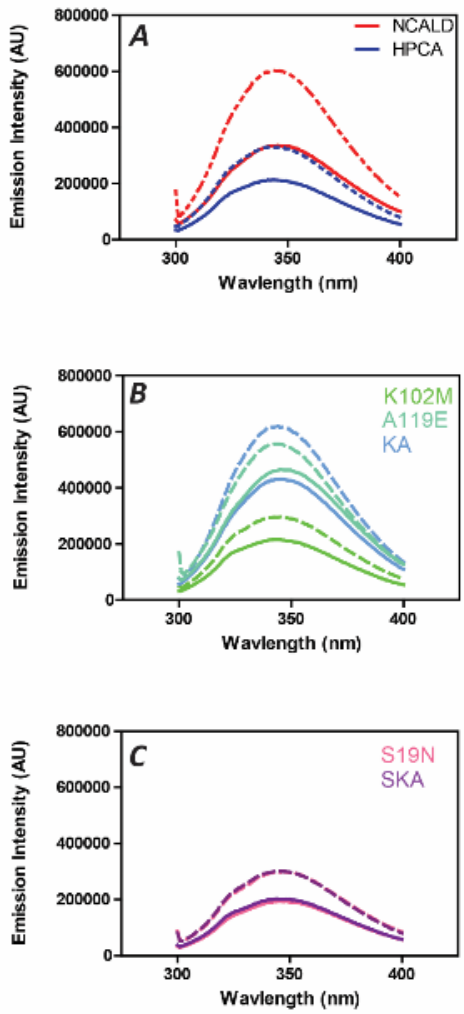

4.4-6. Effect of mutations on response to calcium as assayed by tryptophan fluorescence. Fluorescence spectra for the mutants were obtained as described in "Materials and Methods." Representative spectra at 0 (solid lines) and 39 μM (dotted lines) are presented for (A) NCALD and HPCA (B) K102M, A119E and K102MA119E (KA), and (C) S19N and S19NK102MA119E (SKA).

NCALD.

4.4.6 Effect of mutations on calcium-dependent changes in tryptophan fluorescence of NCALD:

Tryptophan fluorescence spectra were obtained for NCALD, HPCA and the five mutants of NCALD. Representative spectra obtained at 0 (solid lines) and 39 μM (dotted lines) calcium concentrations are presented for NCALD and HPCA (Figure 4.4-6A), K102M, A119E and KA (Supplemental Figure 4.4-6B) and S19N and SKA (Supplemental Figure 2C). Each of the mutants responds to calcium with an increase in fluorescence intensity (Supplemental Figure 2). Figure 4.4-7A highlights the average percentage change in fluorescence intensity from 0 to 39 μM calcium. The K102M and A119E mutations reduce the total amplitude of response compared to the wild type NCALD (44% vs 30 and 33% respectively). On the other hand, the double mutant KA is closest to the wild type (46%) in magnitude of the response. The calcium induced change in fluorescence intensity spectra for S19N (29%) and SKA (32%) show no significant difference compared to HPCA (31%), indicating the importance of the S19 residue.

Changes over a range of calcium concentrations were then determined for each construct and plotted as a fraction of the maximum fluorescence intensity (at 39 μM). Multiple runs of at least 2 biological replicates were averaged. Further analyses of these response curves (Fig. 4.4-7B and 4.4-7C) largely reinforce the earlier observations. K102M response is more like HPCA. Interestingly the A119E mutant is, overall, more like NCALD, as is the double mutant, KA (Fig. 5B). The S19N mutant is able to convert the response to HPCA-like, both individually and in the KA

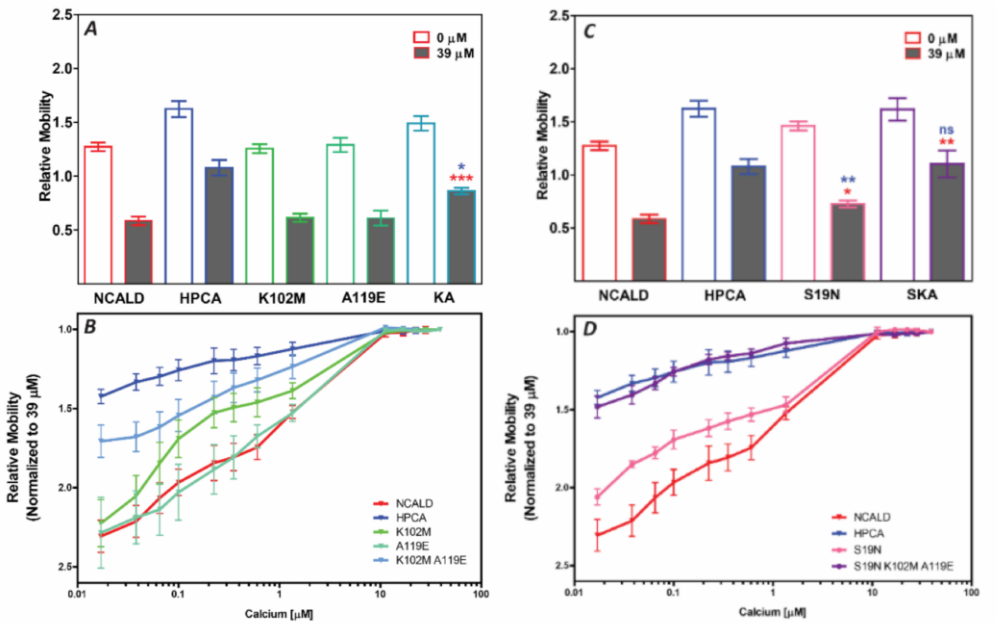

Figure 4.4-8. Effect of mutations on calcium-induced mobility shift on native gels. CIMSA was carried out as described in "Materials and Methods" and relative mobility values were determined. The relative mobility in the presence of 0 or 39 μM of free calcium from several gels (n=6) was calculated. Data is presented as mean ± SE for (A) K102M, A119E and KA mutants, and (B) S19N and SKA mutants. The relative mobility values determined for each mutant over a range of incremental calcium concentrations were normalized to that obtained at 39 μM (maximal concentration tested). Data is presented as mean ± SE for (C) K102M, A119E and KA mutants, and (D) S19N and SKA mutants. Student's t-test were performed on pairs. The following mutants that exhibited significant difference are indicated: When compared to wild-type NCALD or HPCA, KA exhibited a significant difference from NCALD ($p < 0.001$), but less significant from HPCA ($p<0.05$). SKA was not significantly different from HPCA. (* - $p<0.05$; ** - $p<0.02$; *** - $p<0.001$).

background (SKA mutant) (Fig. 4.4-7C). Together with the observation that both these mutants (S19N, SKA) are more dimeric than HPCA, response to calcium as

measured by tryptophan fluorescence appears to be independent of dimerization. Furthermore, S19N mutation (near the calcium non-binding EF1 hand) has the strongest effect and is dominant over the other two (in the calcium-binding EF3 hand).

4.4.7 Effect of Mutations on CIMSA:

The CIMSA serves as a measure of overall conformational changes in NCS proteins, driven by the calcium-myristoyl switch [1-4]. Therefore, it was of interest to assess the effect of the mutations through CIMSA. The relative mobility values of K102M, A119E and KA mutants at 0 and 39 μM calcium are presented in figure 4.4-8A, along with those for NCALD and HPCA for comparison. The single mutations do not alter the mobility shift significantly when compared to the wild type. The double mutant KA, however, is significantly different from NCALD in its response and approaches HPCA. The response of each construct over a range of calcium concentrations were tested, the results (Figure 4.4-8) were normalized to that obtained at 39 μM to facilitate more direct comparison and are presented in figure 6B. In addition to reinforcing the conclusions above, the data shows that K102M is more effective than A119E in altering the wild type response.

The S19N mutation also affects the response and the effect is statistically more significant than that of the other single mutations (Fig 4.4-8C). This response is in between NCALD and HPCA. When combined with the K102M and A119E mutations (SKA), the CIMSA response of the protein at 0 and 39 μM calcium is not significantly different then HPCA and is significantly different than NCALD. Over the calcium range, SKA overlaps with that of HPCA. These results suggest that the

global calcium response of NCALD is dictated by a combination of the EF-1 and EF-3 regions, since all three mutations were required to completely convert NCALD to be HPCA like.

In summary, we have demonstrated, for the first time, NCALD exhibits a greater magnitude of response to changing calcium concentrations over two logarithmic units when compared to HPCA, despite 95% similarity (88% identity) at the primary amino acid level. We have identified three amino acid residues – S19, K102 and A119 – in the dimer interface of NCALD and conversion of these residues to N19, M102 and E119 (present in HPCA) significantly affects the ability of NCALD to dimerize. Mutation of all three residues is sufficient to convert the calcium-dependent response of NCALD to be HPCA-like in functional dimerization, tryptophan fluorescence and CIMSA assays. Analyses of the effect of individual mutations reveals a significant role for the non-calcium binding EF1 hand and its interaction with the EF3 hand in shaping the response of these two NCS proteins.

4.5 The EF-1 helps determine the calcium-induced response of NCLAD and HPCA

NCALD and HPCA share an 88% identity and are co-expressed in the same tissues. The majority of the differences between the two proteins are localized to the non-calcium binding EF-1 region. This region is highly dissimilar, not only between the two VILIPS, but amongst the entire NCS family. Several residues in this region have been highlighted as important for the calcium myristoyl switch mechanism [36,

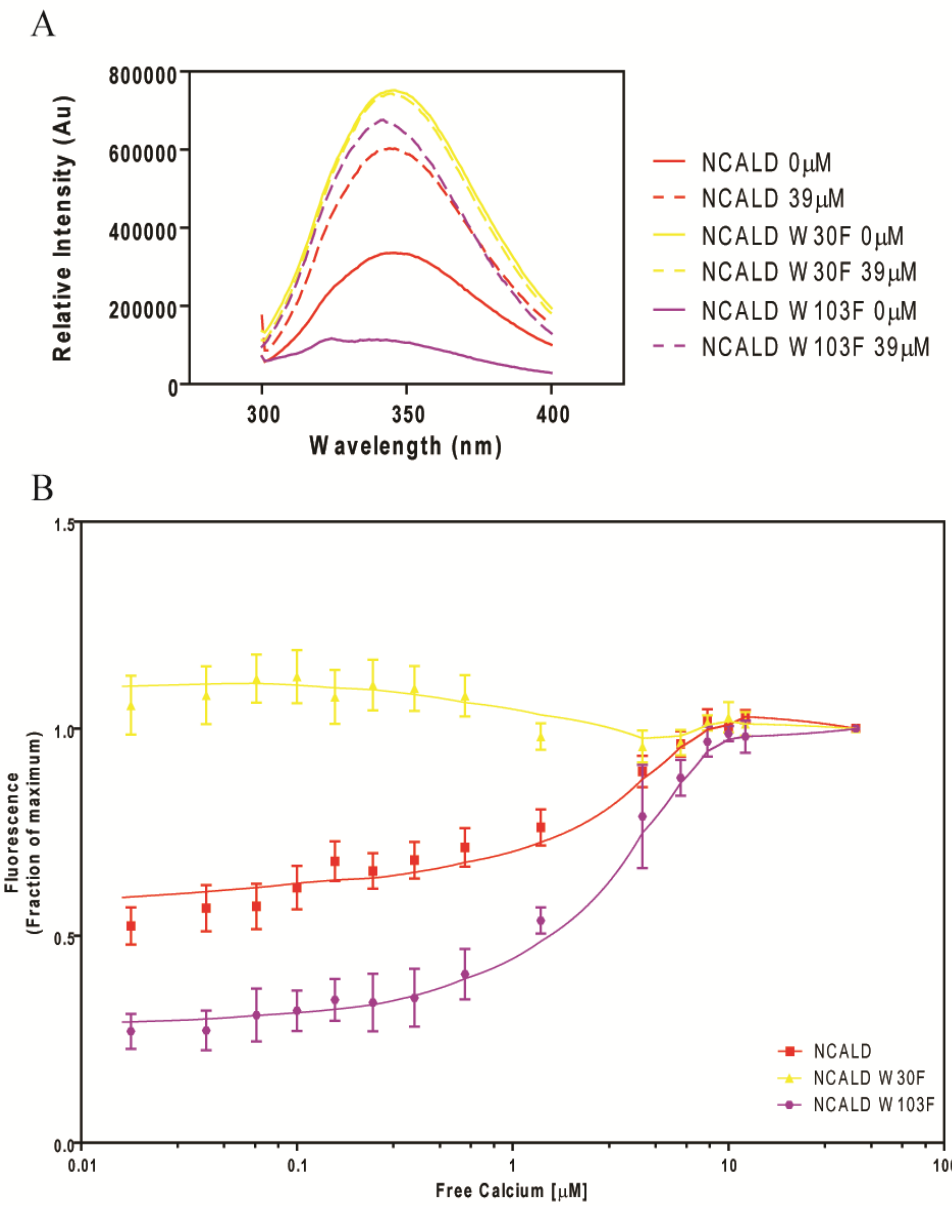

Figure 4.5-1: Tryptophan Florescence response of NCALD Try to Phe mutants. (A) The fluorescence spectra of NCALD, NCALD W30F and NCALD W103F. Solid line indicates no calcium (0μM), dotted line indicated saturating calcium (39μM). (B) The peak fluorescence intensities for increasing free calcium concentrations were normalized to saturating calcium (39μM). Results are presented as mean ± SEM (N=8).

41]. In this study we highlight the role of the EF-1 region and how the non-calcium binding region helps to determine the type of response initiated by calcium binding.

4.5.1 Role of tryptophans in NCALD and HPCA

To first identify the roles of the EF-1 and the EF-3 regions, two mutants were created. These mutants were specifically designed to help understand what is being observed in tryptophan fluorescence. This is critical to help understand the calcium induced structural changes, as well as the relationship between NCALD and HPCA. NCALD and HPCA share two conserved Trp, one at position 30, and one at a position 103. Tryptophan florescence spectra are combinations of the fluorescence from both the Trp residues of the protein. To better understand the role of the EF-1 and the EF-3 regions, and their relationship to calcium response, mutations were created to knock down the fluorescence from W30 (EF-1) or W103 (EF-3) and look at the responses of the residues individually, while still retaining the ability to respond to calcium.

First the W30F mutations were created individually in NCALD and HPCA. This mutation is located in the non-calcium binding EF-1 hand and should allow for the study of the Trp at 103. The second mutation was W103F, which allows for the study of the W30. These two mutations allow for the clearer understanding of the movement observed in tryptophan fluorescence experiments.

First, the NCALD tryptophan mutants were studied (Fig. 4.5-1). The fluorescence spectra of NCALD, NCALD W30F and NCALD W103F are presented. In NCALD, there is an observable increase in fluorescence intensity (red solid to dotted lines) brought on by the addition of calcium. This increase is amplified in the W103F mutant, which examines the contribution of fluorescence from the EF-1 W30.

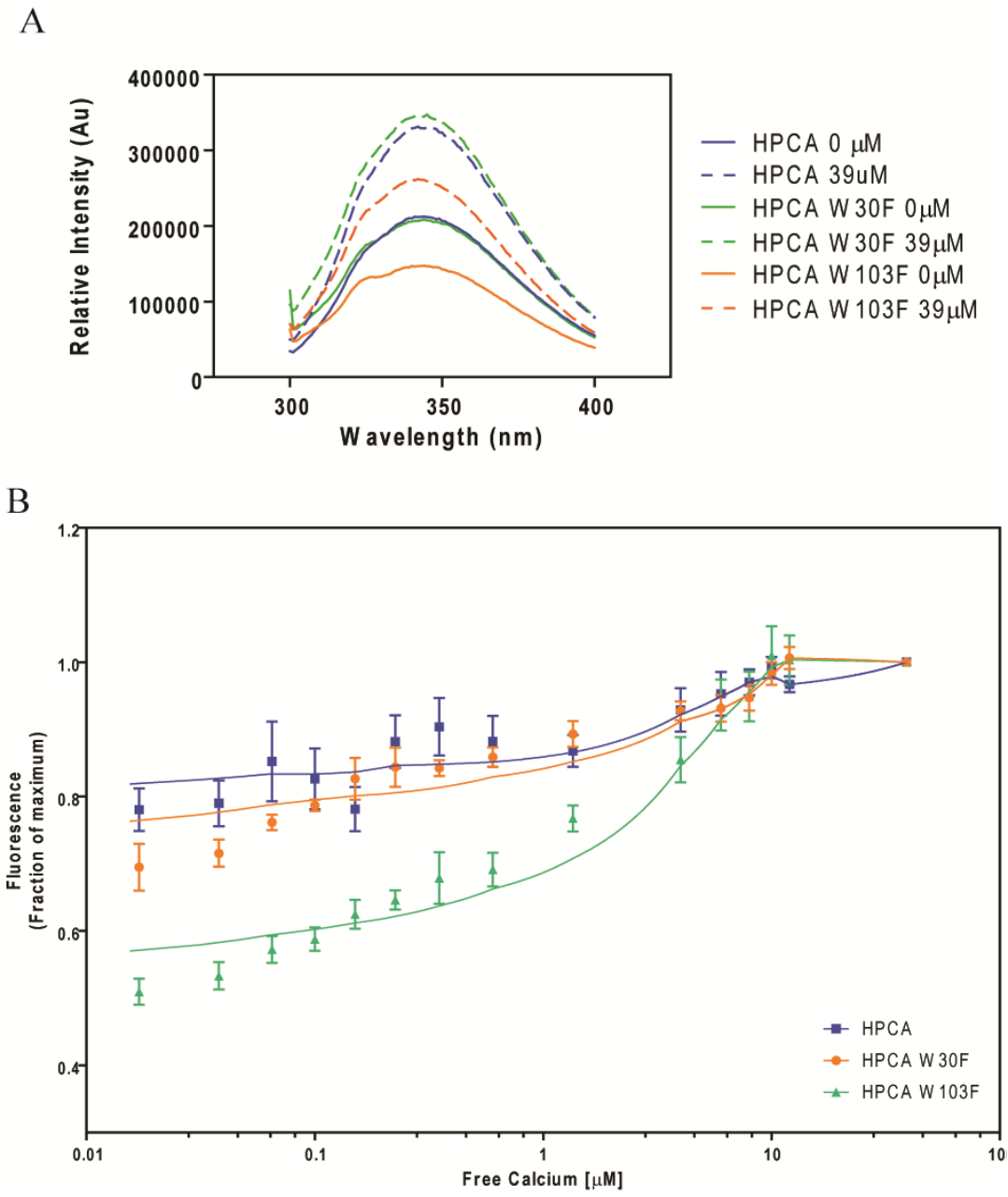

Figure 4.5-2: Calcium induced Tryptophan Florescence response of HPCA Try mutants. (A) The fluorescence spectra of HPCA, HPCA W30F and HOCA W103F at 0µM calcium (solid line) and 39µM (dotted line). (B) Peak fluorescence intensities for increasing free calcium concentrations were normalized to saturating calcium (39µM). Results are presented as mean ± SEM (N=8)

However, in the W30F mutations, which examine W103, shows no detectable

increase in fluorescence intensity upon the addition of calcium. This mutation has a different basal fluorescence than the wild type, demonstrating that this mutation has altered the conformation of the protein, demonstrating that W30 is critical for the proper folding and/or response to calcium of the protein. However, the protein is still functional in translocation and mobility shift assays (data not shown) confirming that the mutation retains biologically relevant responses to calcium.

To further examine the calcium induced response as measured by tryptophan fluorescence, the maximal fluorescence intensities for experiments at 344nm were normalized at saturating calcium for the wild type and the mutant proteins after incubation with increasing calcium contractions. Fig. 4.5-2B shows the response of these proteins over the range of calcium. Again, we observed a dose dependent increase in fluorescence intensity corresponding to an increase in free calcium in the wild type NCALD. The NCALD W103F mutation shows an even larger increase in fluorescence intensities than NCALD. Again, the NCALD W30F shows no change in fluorescence intensity, in either direction, over the calcium range. These results show that the major structural rearrangement brought upon by calcium binding are primarily the result of conformational rearrangements in the EF-1 region.

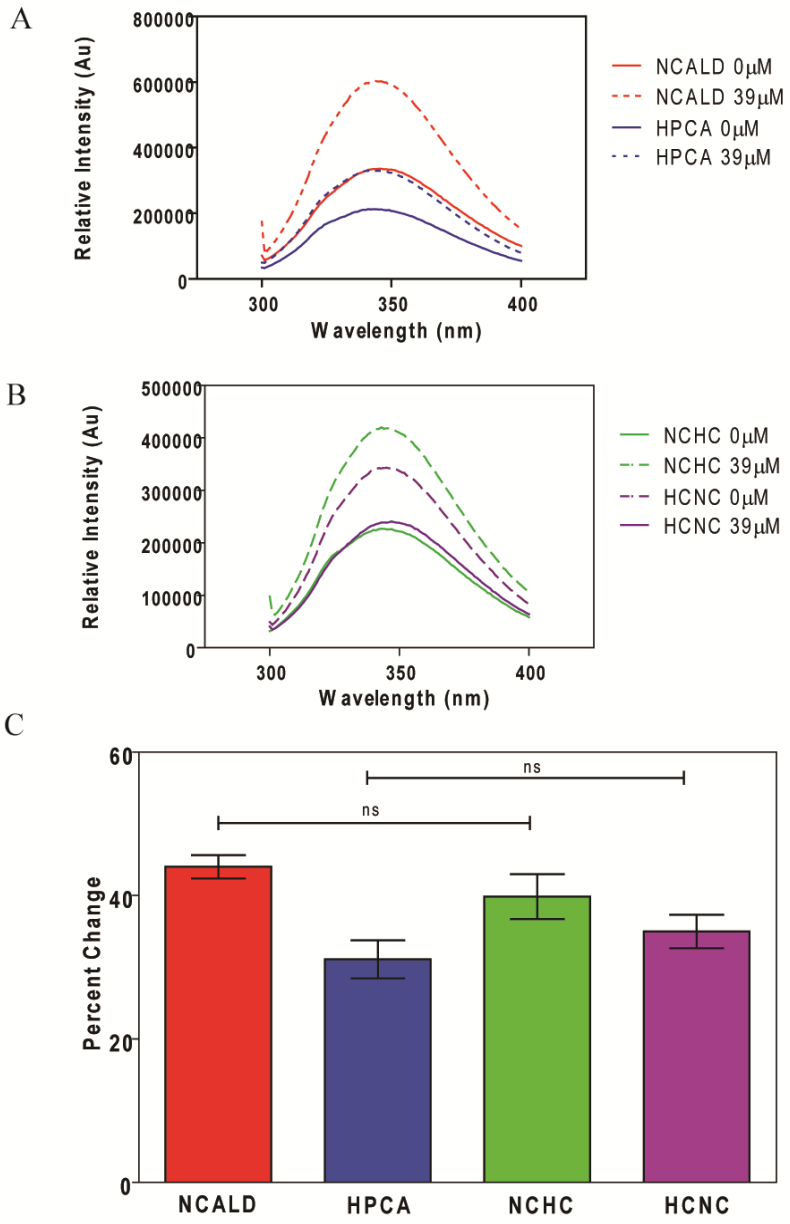

Figure 4.5-4: Calcium induced fluorescence response of the chimeric proteins. (A) The fluorescence spectra of NCALD, HPCA (A) and NCHC<, HCNC at 0μM calcium (solid line) and 39μM (dotted line). (C) The percentage increase in fluorescence intensity from 0μM to 39μM free calcium. Results are presented as mean ± SEM (N=8).

The tryptophan mutants of HPCA were then examined. Figure 4.5-2 (A), highlights the fluorescence spectra of these mutants. HPCA demonstrated an increase in fluorescence intensity upon the addition of calcium. Both the HPCA W30F and the HPCA W103F mutations demonstrate this increase in fluorescence intensity. When

multiple free calcium concentrations were normalized to 39μM calcium, we see, like NCALD W103F, HPCA W103F shows an increased fluorescence response over the range. In contrast, HPCA W30F, on the shows a wild type like-response.

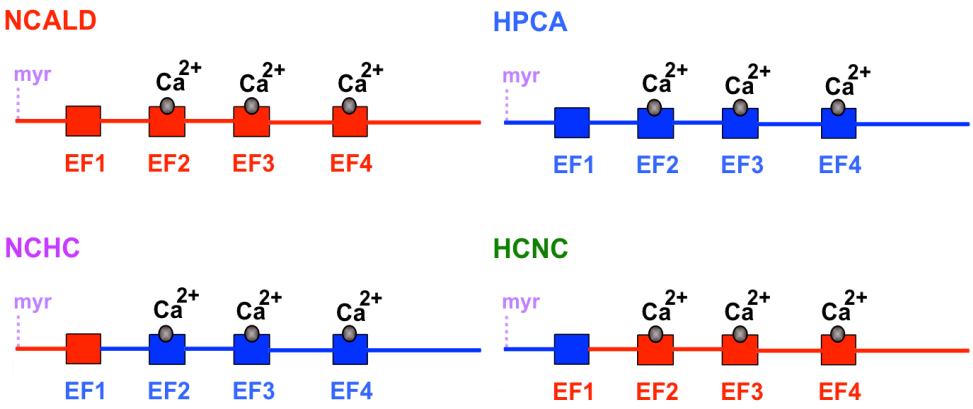

Figure 4.5-3: Construction of Chimeric proteins. Chimeric proteins were created by swapping the EF-1 hands of the wild type proteins. NCHC contains the EF-1 of NCALD and EF2-4 of HPCA. HCNC contains the EF-1 of HPCA and EF2-4 of NCALD.

4.5.2 Creation of Chimeric EF-1 proteins

The two proteins showed unique responses to calcium binding which allow for a clearer understanding of the calcium response observed in the tryptophan fluorescence experiments. In NCALD, the results show that the major structural rearrangement brought upon by calcium binding is the result of the EF-1 region. This is because the W30F mutant (which looks at W103 response) showed no increase or decrease in fluorescence intensity, likely due to the mutation altering the structure and/or the response of the protein. On the other hand, both of the HPCA mutants show an increase in fluorescence intensity upon the addition of calcium. This critical

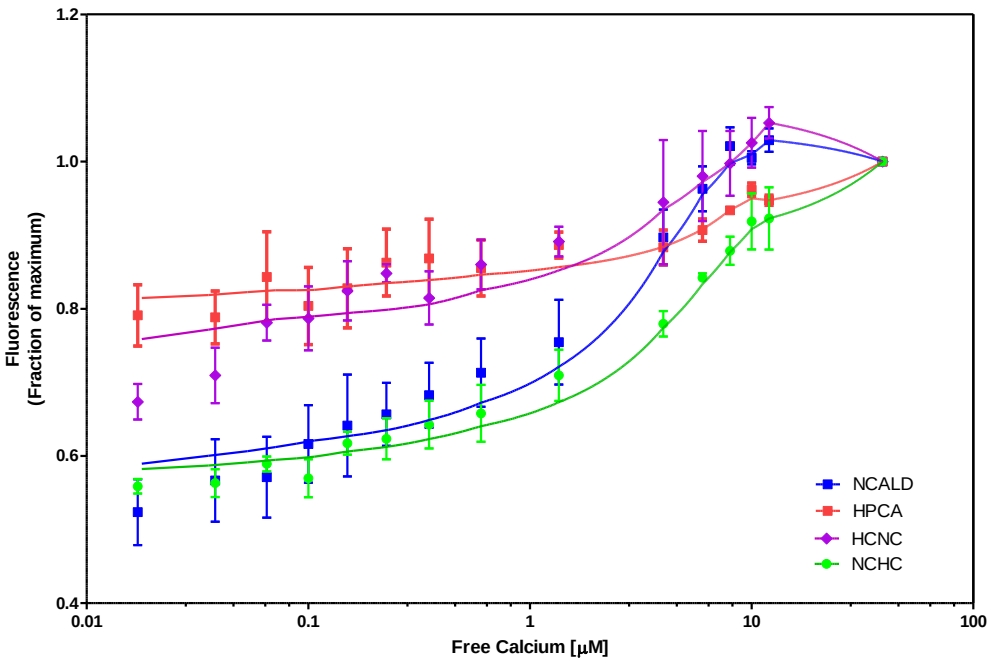

Figure 4.5-5: Effect of EF1 swap on response to calcium as assayed by tryptophan fluorescence. Fluorescence spectra for the wild type and chimeric proteins were obtained as described in "Materials and Methods". The average (n=8) percentage increase in peak fluorescence intensities at 344 nm from 0 μM to 39 μM calcium for NCALD, HPCA NCHC, and HCNC and are presented (A). The peak fluorescence intensities for varying free calcium concentrations from 0 μM to 39 μM were averaged from several measurements (n=8) and normalized to that at saturating calcium (39 μM) concentration.

result demonstrated that the rearrangement in NCALD is different than the rearrangement in HPCA.

The tryptophan mutants revealed a key finding; the W30 response to calcium binding between the two proteins is unique. W30 is located in the non-calcium binding EF-1 hand. This would suggest that the EF-1 region helps to determine the type of calcium response of the proteins. To help understand the role of the EF-1 region, chimeric

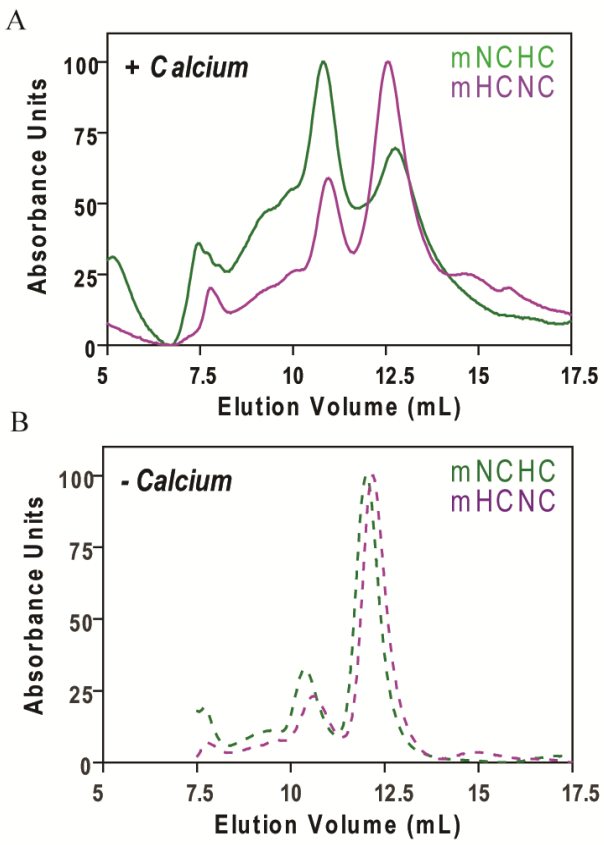

Figure 4.5-6: Size Exclusion Chromatography Results of chimeric proteins. Representative elution profiles of NCHC and HCNC from size exclusion chromatography are presented. (A) With calcium (+ calcium) or (B) with EGTA (- calcium). The dimer and monomer peaks corresponding to molecular weights 44kDa and 22kDa, calibrated with standards.

proteins were devised. Chimeric constructs that retain EF hands 2-4, but are swapped for the EF1 hand were created. The first of these chimeras was labeled NCHC, which contains the EF1 hand of NCALD, but the remaining three EF hands of HPCA. The second, HCNC, contains the EF1 hand of HPCA, but the remaining three EF hands of NCALD (Fig. 4.5-3).

4.5.3 The role of the EF-1 in calcium response of NCALD and HPCA

The chimeric proteins were constructed to better understand the

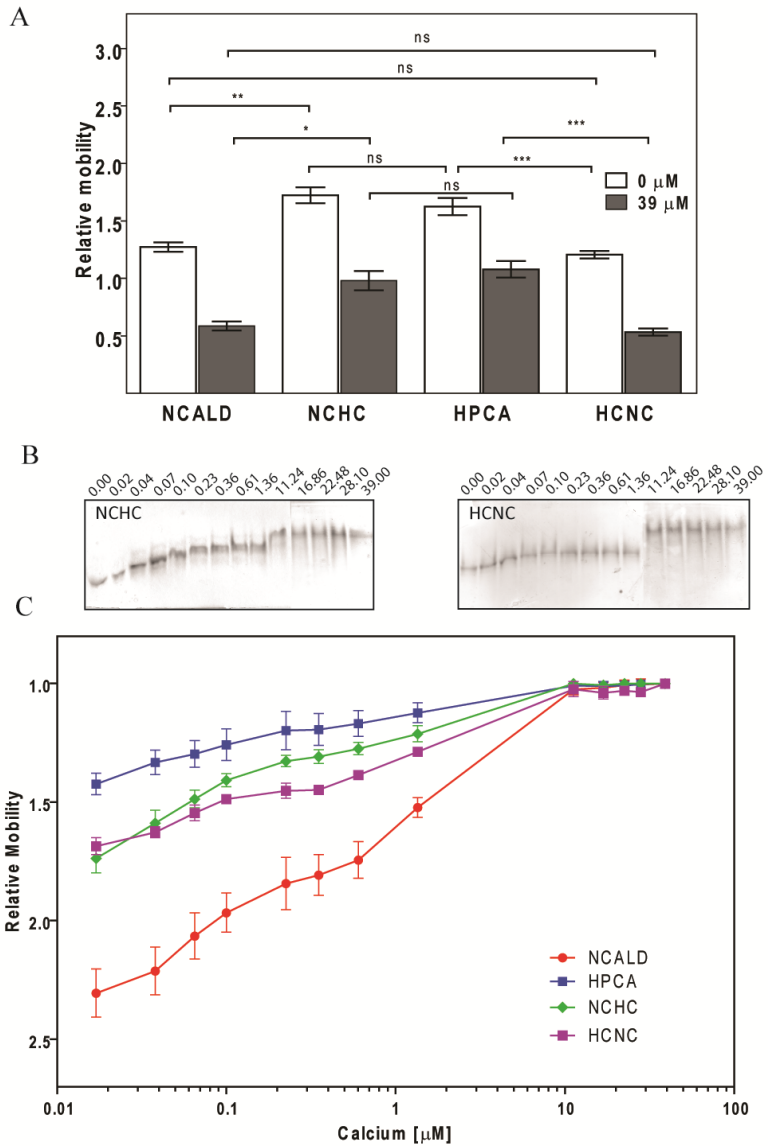

Figure 4.5-7: Effect of EF1 chimeras on calcium-induced mobility shift on native gels. CIMSA was carried out as described in "Materials and Methods" and relative mobility values were determined. The relative mobility in the presence of 0 or 39 μM of free calcium from several gels (n=6) was calculated. Data is presented as mean ± SE (A). Student's t-test were performed on pairs (* - $p<0.05$; ** - $p<0.02$; *** - $p<0.001$). (B) The relative mobility over a range of incremental calcium concentrations for NCHC and HCNC. (C) The relative mobility values determined for each mutant over a range of incremental calcium concentrations were normalized to that obtained at 39 μM (maximal concentration tested).

role of the EF1 hand with respect to calcium binding. NCHC, which contains the EF1 hand of NCALD, but the remaining three EF hands of HPCA, responds much like NCALD, showing a similar change to NCALD. Figure 4.5-4 B vs 4.5-4 A. HCNC responds more like HPCA with a clustered, mitigated response (Fig. 4.5-4). It contains the EF1 hand of HPCA, but the remaining three EF hands of NCALD.

To better compare the mutants, the percentage change obtained over multiple runs were averaged and compared (Fig 4.5-4 C). NCHC showed no significant difference in calcium induced change compared to NCALD. The same results were observed with HCNC vs. HPCA. The proteins were then examined over a range of free calcium (Fig. 4.5-5). Here, NCHC showed a response over a range of calcium in a similar manner as NCALD, whereas HCNC responded like HPCA. These results suggest that the EF1 region of the protein is responsible for the type of response the protein has to calcium as measured by tryptophan fluorescence. This idea is novel in the field.

Size exclusion chromatography was then used to identify if the EF1 region also contributed to the dimerization state of NCALD. Previously, we demonstrated that NCALD forms a dimer in the presence of calcium and is monomeric in its non-calcium loaded form. HPCA on the other hand is always monomeric. Previous results with the dimer mutants suggested a role in the EF-1to EF-3 interaction in helping to determine the calcium induced dimerization event in NCALD. Figure 4.5-6 displays representative chromatograms for the chimeras. NCHC, represented in green, shows a prominent peak corresponding to the dimer in the presence of calcium. In total, there was an average of 52% dimerization in the presence of calcium in NCHC. When you

move the protein to EGTA, the peak shifts to be predominantly monomeric. HCNC, has like a HPCA like presence, with a average of 33% dimer in the presence of calcium. It is noted that NCHC has less dimer then NCALD and HCNC has more than HPCA. This again supports the conclusion that the EF-1 region is a major contributor to the calcium induced dimerization seen in NCALD. Both the dimer mutants, and the chimeras support the conclusion that the there is an important interrelationship between the EF-1 and the EF-3.

Recently our group has detailed the mobility of in NCS proteins through a native gel. This technique measures the calcium induced structural changes and at the tertiary level. The native gel experiment was carried out as described in the Materials and Methods section with the chimeric proteins. Figure 4.5-7 B displays the gels for in NCHC and HCNC. To better compare the chimeric proteins to NCALD and HPCA, the migration of the bands through the gels were measured as described in the Materials and Methods section and the results were plotted in figure 4.5-7A. The calcium loaded (39 μM) and calcium free (0 μM) forms of the proteins are displayed. Here we observe interesting results; NCHC has a HPCA-like response with respect to the location of migration, and a total difference in migration through the gel. HCNC shows a NCALD-like response through the gel. These results would indicate that the migration location through the gel as seen by CIMSA is dependent on the calcium binding hands.

To test if this was the true response, each of the chimeras was then tested over a range of calcium concentrations. The results are plotted in Figure 4.5-7C and were

normalized to the migration obtained at 39 μM. Interestingly, both NCHC and HCNC show an intermediate response; one which is in between NCALD and HPCA.

This result shows several critical observations about, not only the CIMSA experiment, but also the role of the EF-1. The CIMSA experiment examines a combination of events within the total protein; binding of calcium at the EF2-4 hands and the resultant structural rearrangement within the EF-1 region, which may then result in global changes in the protein structure. It is, therefore, suggested that both the calcium binding and the non- calcium binding EF hands govern the total response of the protein to calcium.

4.6 Dystonia and HPCA

The neuromuscular movement disorder Dystonia is characterized by repetitive movements and tremors. Charlersworth *et al*l [10] identified two critical mutations in HPCA which caused the autosomal recessive primary isolated dystonia, or type two dystonia. The authors first identified a family that had inherited Dystonia in an autosomal recessive manner. The family's genes were sequenced and a single mutation was identified. The gene that was affected was HPCA and the mutation - an N75K point mutation. The authors then searched a database of people suffering with dystonia and found another patient who also had a different mutation in HPCA, specifically T71N.

Both of these mutations are located in the EF-2 calcium binding hand in HPCA. Based on the positions and location of the mutation, the authors concluded that the HPCA in the dystonia patients would be rendered non-functional. The authors came to this conclusion because the EF-2 is one of the critical calcium binding EF hands.

Based on my understanding of HPCA, I do not agree with the conclusion that these two mutations would render the proteins non-functional. Both of the mutant forms of HPCA expressed in these patients would still contain 2 functional EF hands, which should still bind calcium even if the EF-2 hand was rendered inoperable. I propose that the HPCA proteins still function, however, at a reduced capacity.

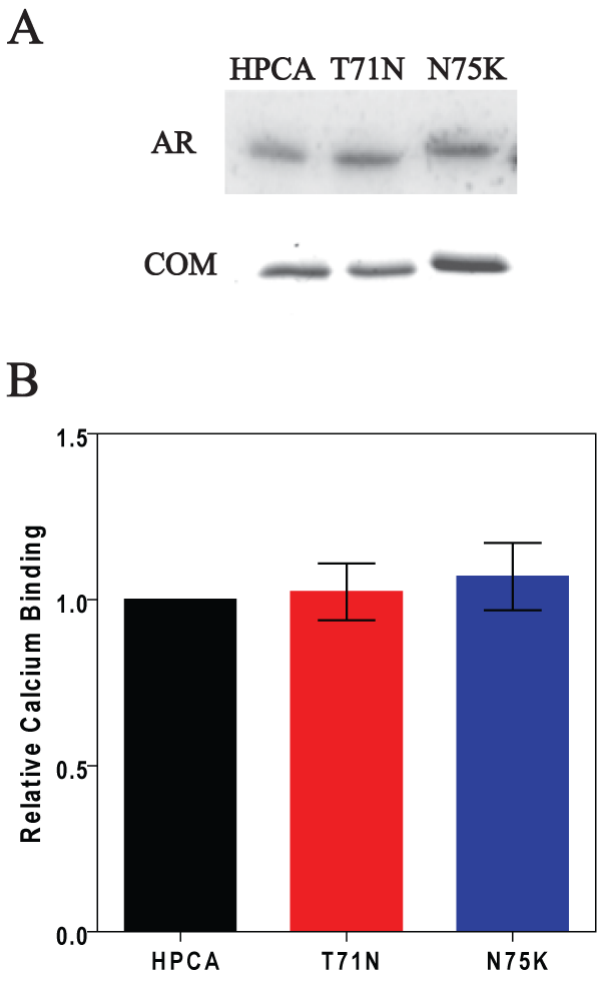

Figure 4.6-1: Direct calcium binding of the dystonia mutants. Purified proteins were incubated Calcium 45 with as described in the materials and methods. (A) Autoradiogram (AR) of calcium bound to purified HPCA, T71N and N75K, as well as the corresponding SDS-PAGE gel stained with coomassie (COM). (B) The mean intensity of each band from multiple experiment (N=4) was averaged and plotted relative to wild type calcium binding.

The two mutations are likely to cause different effects on HPCA. Both mutations are in the EF-2 binding hand. Thr at 71 is not directly involved in calcium binding. The mutation to Asn, another polar, uncharged residue is not a great change. The Asn at 75, on the other hand, is directly involved in the coordination of calcium binding in the EF-2. Furthermore, the mutation to the positively charged Lys could potentially interfere with calcium binding, possibly knocking out the calcium binding in the EF-2 hand.

In order to test the hypothesis that the HPCA in the dystonia patients causes a dysfunctional protein, mutations of HPCA were created using site directed

mutagenesis. The T71N and N75K HPCA proteins were then expressed in *E. coli* and purified as described in the Materials and Methods section.

To first test if the proteins were simply non-functional with respect to binding calcium, direct binding experiment was performed as described in the Materials and Methods section. Briefly, purified proteins were separated on an 8.8% SDS-PAGE and then transferred to nitrocellulose. The blot was then incubated with Ca^{45}, washed, and imaged using the phosphoimager. Figure 4.6-1A, shows the result of the direct binding assay. T71N and N75K mutants do bind calcium, and they appear to bind to the same amount of calcium as the wild type (top bands labeled AR). Below, the Coomassie stained loading controls (COM) are displayed. To better compare the intensities of the bands, the mean intensity was averaged for each band from multiple experiments and plotted as relative calcium binding compared to wild type HPCA. The intensity of calcium binding for the HPCA mutants and the wild type are comparable over multiple experiments. This result demonstrated that the dystonia mutations, despite being in the EF-2 calcium binding hand, do bind calcium and furthermore, the binding is comparable to wild type levels. Therefore, these results demonstrate that the proteins seem unaffected in their ability to bind calcium.

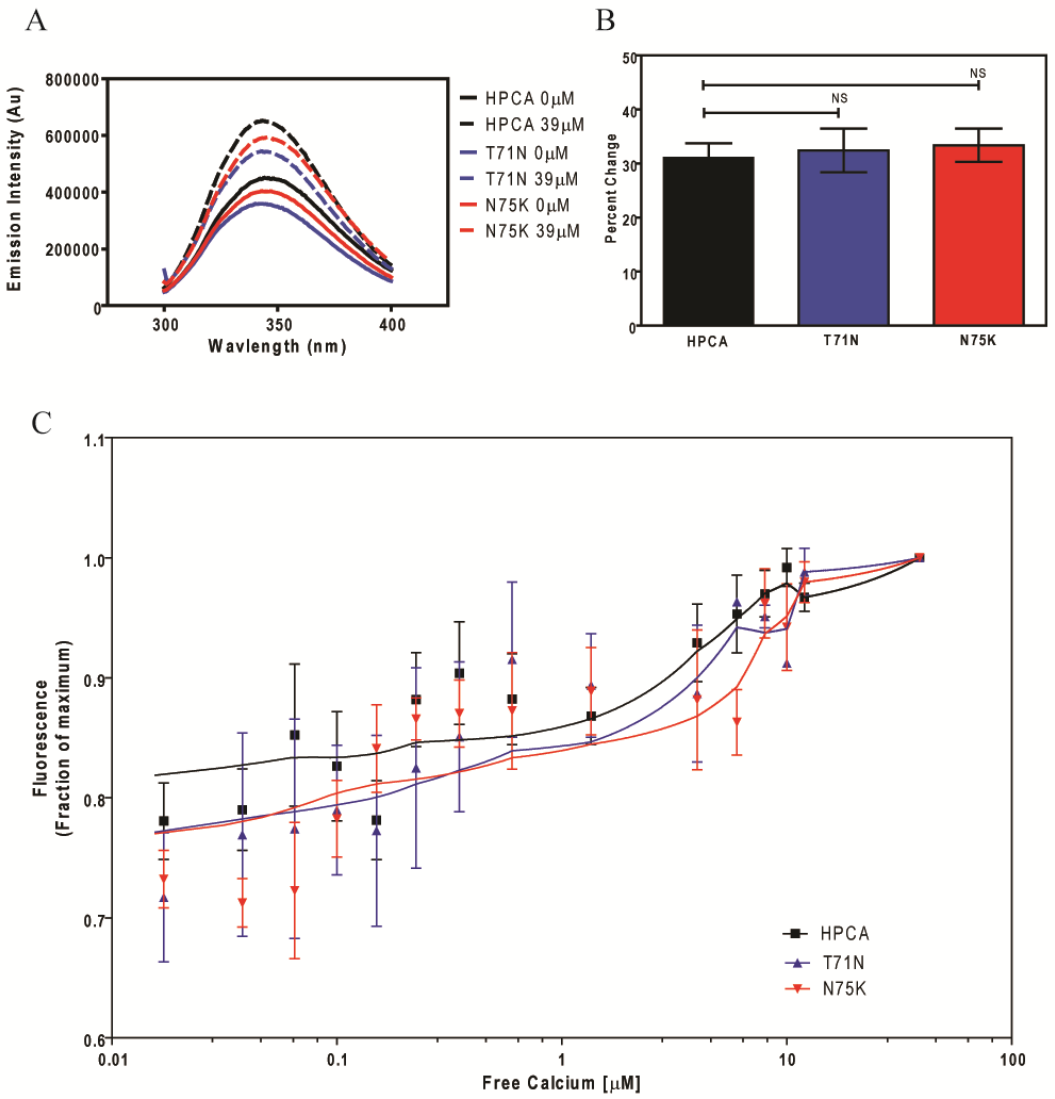

Figure 4.6-2: **Tryptophan fluorescence response of dystonia mutants to calcium binding**. (A) Represented spectra of HPCA and the dystonia mutants T71N and N75K at 0 µM and 39 µM free calcium. (B) The average (n=7) percentage increase in peak fluorescence intensities (344 nm) from 0µM, to 39µM calcium. (C) The peak fluorescence intensities at incremental free calcium concentrations were obtained and normalized to the maximum (at 39µM free calcium). Data for selected calcium concentrations are presented as mean ± SEM

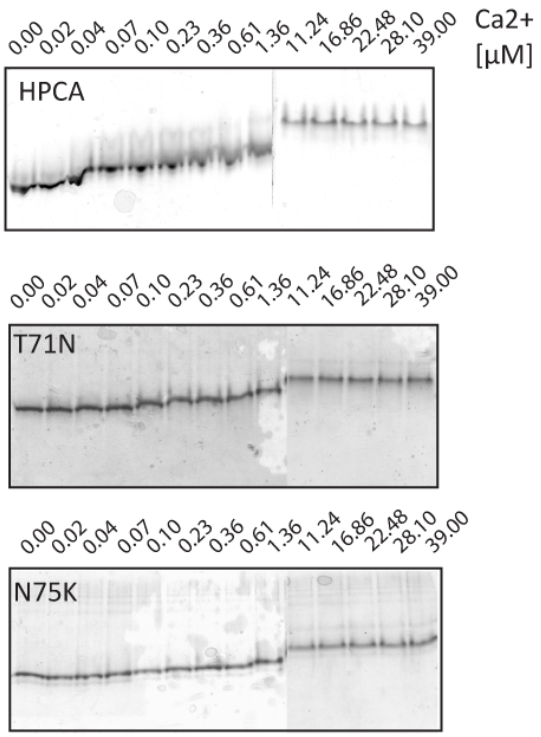

Figure 4.6-3: Effect of Dystonia mutations on calcium-induced mobility shift on native gels. Purified HPCA, T71N and N75K were incubated with increasing free calcium concentrations and run under native conditions as described in the Materials and Methods section.

The possibility still remained that the proteins could bind calcium, but not respond to the binding of calcium. To investigate this possibility, tryptophan fluorescence assays were performed. The spectra of the dystonia mutant proteins were compared to HPCA (Fig. 4.6-2A). No detectable red/blue shift was observed in either of the mutants in either the presence or absence of calcium. Upon the addition of calcium the fluorescence intensity of both wild type HPCA and the two mutants increased.

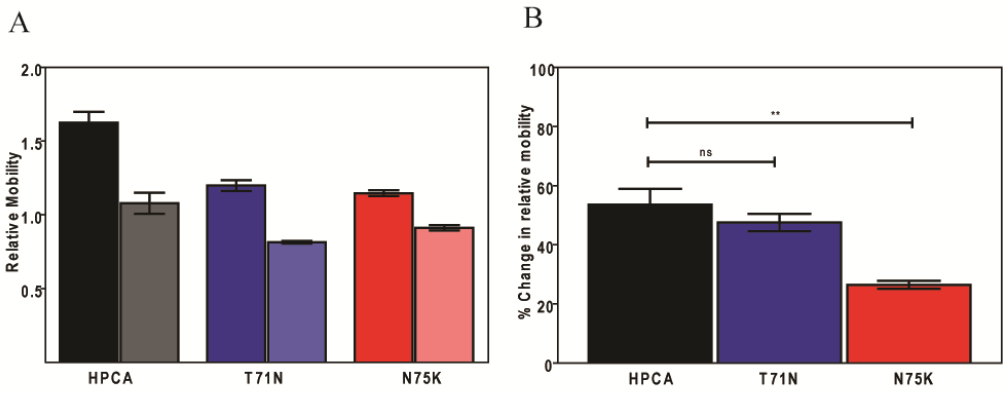

Figure 4.6-4: Effect of Dystonia mutations on calcium-induced mobility shift on native gels. CIMSA was carried out as described in "Materials and Methods" and relative mobility values were determined. (A) The relative mobility in the presence of 0 or 39 μM of free calcium from several gels (n=6) was calculated. Data is presented as mean □ SE (B) Data is presented as mean SE for the percentage change in relative mobility. Student's t-test were performed on pairs. T71N showed no significant difference compared to HPCA in the percentage change in relative mobility. N75K exhibited a significant difference from HPCA (*p=0.05; **p=0.02; *** p=0.001).

In order to better observe the influence of calcium on the structure, the amount of change was calculated (Fig 4.6-2B) by averaging the percentage of change in peak fluorescence intensity from 0μM to 39μM free calcium for HPCA and the two mutants. T71N showed a 32% increase in fluorescence intensity upon calcium binding, while N75K demonstrated a 33% change, compared to the 31% change observed by the wild type HPCA. There was no significant difference in total percentage change between HPCA and the two mutants.

The Dystonia mutants' calcium response over a large calcium range was then tested. The peak wavelength (344nM) for each calcium concentration was normalized to saturating calcium at 39μM calcium (Fig 4.6-2C). Both mutants respond to calcium in a dose dependent manner as observed in the wild type and the overall response was, very much like wild type HPCA. The tryptophan fluorescence showed that the proteins are able to both bind to, and respond to calcium and in a similar manner as the wild type protein.

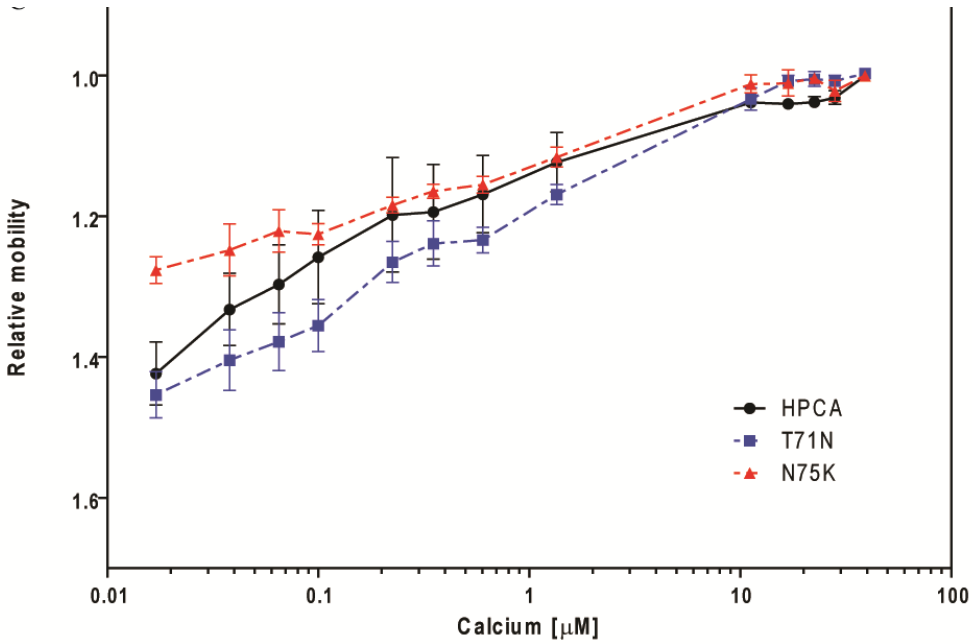

Figure 4.6-5: The response of the dystonia mutants to a range of calcium binding. The relative mobility values determined for each mutant over a range of incremental calcium concentrations were normalized to that obtained at 39μM (maximal concentration tested).

Next, the dystonia mutants' calcium response was examined by CIMSA. Multiple gels were run across the entire calcium range (Fig. 4.6-3). The band positions for 0μM or 39μM calcium were measured (Fig 4.6-4A). Both the T71N and

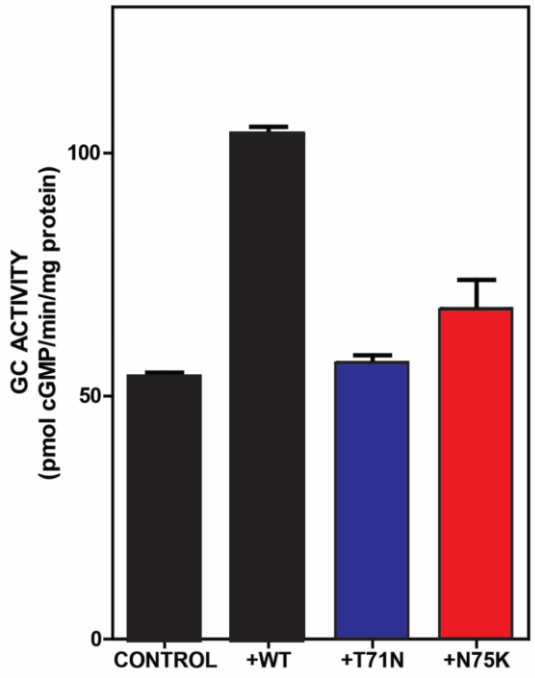

Figure 4.6-6: The ability of the Dystonia mutants to stimulate ROSGC-1. ROS-GC1 activity was assayed as described in Materials and Methods. Stimulation by purified HPCA, T71N and N75K was measured in the presence of calcium. Results are presented as pmol cGMP/min/mg protein. Control is innate ROS-GC1 activity. Data were compiled from at least two different preparations of the proteins with two replicates each (*n*=4).

the N71K HPCA proteins showed a calcium induced shift, again demonstrating that the proteins, despite their mutations, can respond to calcium. However, the initial migration position is different in both of the mutants compared to HPCA, suggesting that there is a structural difference, which is reflected in a difference in surface charge compared to wild type HPCA. Then, the percentage change in the relative mobility (Fig 4.6-4B) was calculated. Here, the N75K response is significantly different then the HPCA, while the T71N mutant is HPCA-like. Finally, the band positions of multiple gels run across the entire calcium range were normalized to that obtained at 39μM (maximal concentration tested) (Figure 4.6-5). Overall, the T71N responds like the wild type protein over the entire range. The N75K mutation response overall is very HPCA like, however, it is less responsive to calcium at lower

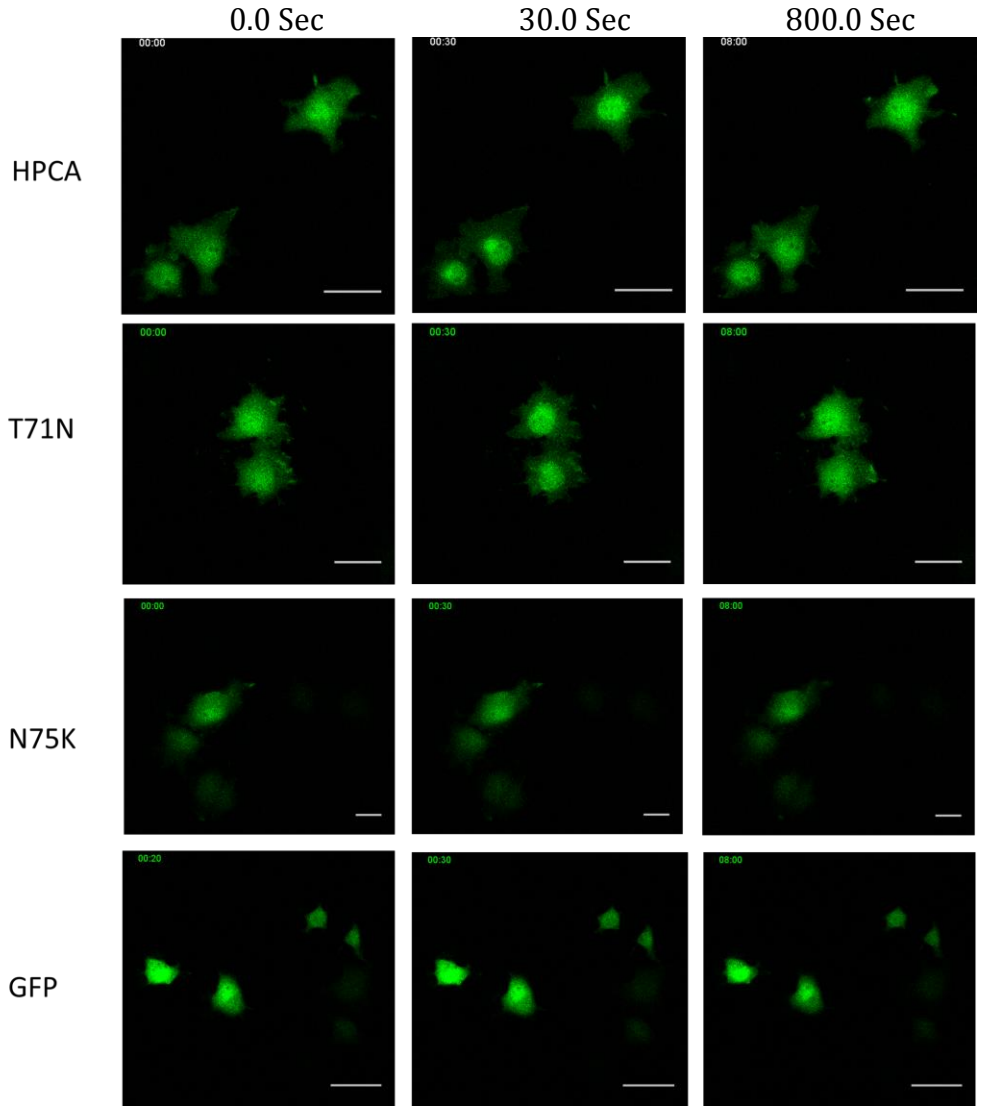

Figure 4.6-7: Calcium Induced Translocation of HPCA and the dystonia mutants. COS7 cells were transfected with wild type or mutant pCDNA3 - GFP constructs and experiments were carried out after 24 h. The cells were treated with 6 mM Histamine to increase intracellular calcium levels and live imaging was performed on a Nikon C1 laser confocal microscope equipped with a TokaiHit on-stage incubator.

concentrations, CIMSA analysis demonstrated that the dystonia mutants can respond

to calcium, however, there are detectible differences in the structural responses of the

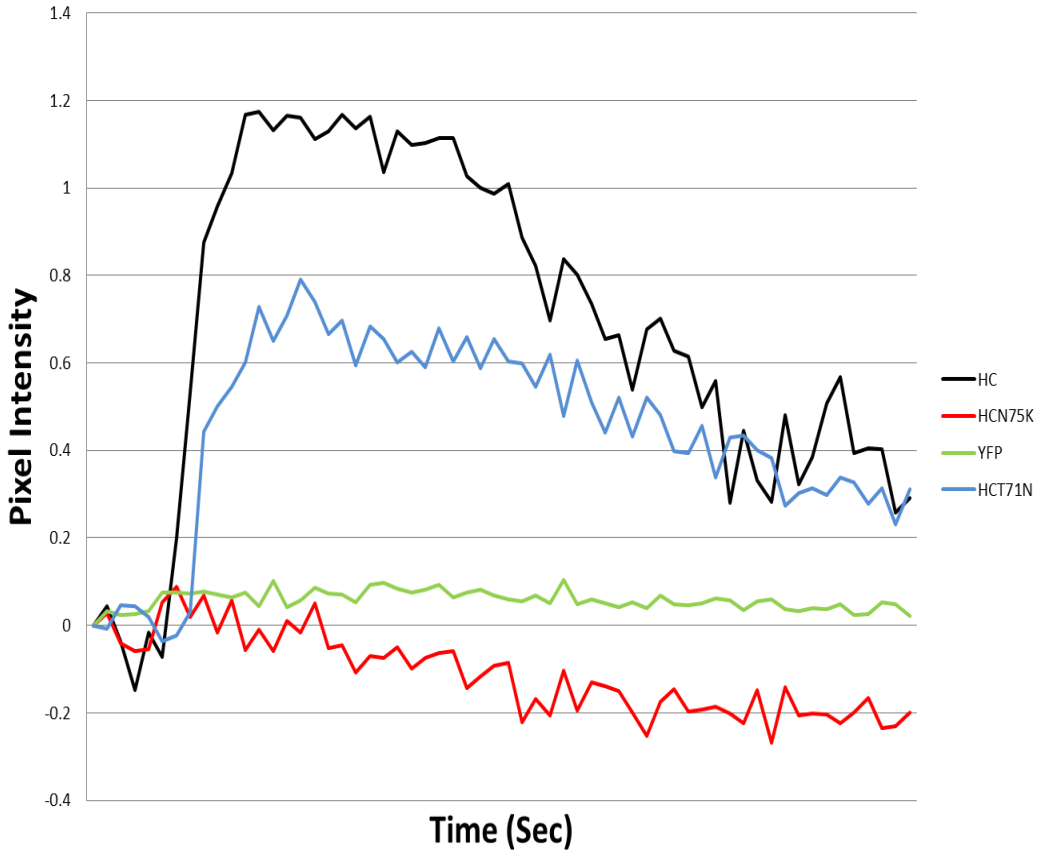

Figure 4.6-8: Quantitation of Translocation of the Dystonia Mutants. Images from multiple experiments were compiled. The distribution of pixel intensities along a line of interest was quantitated and the results were plotted. HPCA and T71N show translocation ability, whereas N75K shows none, like YFP.

mutant proteins compared to HPCA.

The ability to stimulate Guanylate cyclase has been demonstrated to be a critical signaling function of NCS proteins [6, 45, 47-53]. This ability was tested with the Dystonia mutants (Fig. 4.6-6). In the presence of calcium, HPCA stimulates ROSGC-1, with an increase in cGMP produced of about 50 pmol/cGMP/min/mg over

basal activity. Both of the mutations showed a significant decrease in their ability to stimulate the membrane Guanylate cyclase ROS-GC1. T71N shows no ability to stimulate ROS-GC-1. N75K shows some ability, though at a diminished rate compared to the wild type HPCA. This loss of ability to stimulate ROS-GC1 might be one of the critical functions compromised in the dystonia mutations, leading to the disease state.

HPCA has been demonstrated to cycle between the cytosol to the membrane upon the binding of calcium [179, 180]. In this manner, HPCA acts as a calcium sensor. To investigate the dystonia mutations effect on this cycling ability, GFP conjugated constructs were created. The constructs were then transformed into Cos-7 cells as described in the Materials and Methods section. Histamine was used to increase the intracellular calcium levels. In figure 4.6-7, the addition of histamine causes HPCA to translocate form the cytosol to the perinuclear region, where Guanylate cyclase is located. In order to better observe the translocation event over time the distribution of pixel intensities along a line of interest was quantitated and the results were plotted in figure 4.6-8. Compared to HPCA, cells transfected with just YFP show no translocation ability. T71N shows the ability to translate in a manner similar to HPCA. However, the N75K mutation shows no ability to translocate, demonstrating a critical difference between the disease protein and the wild type, as well as a distinction between the two disease states.

Chapter 5: Discussion

5.1 Evolutionary Interrelationships and Insights into Molecular Mechanisms of Functional Divergence: An Analysis of Neuronal Calcium Sensor Proteins

This study was designed to examine if analyses of phylogenetic relationships among closely related proteins would yield insights into molecular mechanism of functional divergence. We used the NCS protein family for this purpose. Sequence alignment led to the formation of three distinct groups. While GCAPs and VILIPs share a common function – modulation of mGC activity – they cause opposing effects in their calcium-loaded states. For KChIPs, their ability to bind DRE sequences was used as the function. Experimental data on residues important for each of these specific interactions provided the platform to evaluate relative roles of these residues in each interaction. Based on sequence divergence during evolution, predictions could be made whether a given residue could contribute to the specificity of the interaction, is more likely to play a role in general molecular integrity or least likely to contribute at all. Where experimental data was available, they did indeed validate the predictions. Thus, this approach is likely to enhance experimental design in analyzing functional divergence as well as molecular interactions that mediate target interactions of proteins, especially given the abundance of sequence information across genomes.

5.2 Single-column purification of the tag-free, recombinant form of the neuronal calcium sensor protein, hippocalcin expressed in Escherichia coli

This optimized method allows for high yield, high purity, tag less expression of HPCA. While purification of HPCA has been documented before [152, 153], the protocols involve tagged protein or multiple steps. We demonstrate in this report that the protein may be purified with good yield from a single column, and is of high purity using SDS-PAGE. Furthermore, we have demonstrated that: (1) Both the myristoylated and non- myristoylated forms can be purified, (2) near-total myristoylation is observed based on MALDI-MS analyses, and (3) the protein is active and responds to calcium as measured by three distinct assays –tryptophan fluorescence, mobility shift in native gels and biological activity. The first two assays allow investigations into structural changes in the protein upon calcium binding, while the guanylate cyclase assay provides information on target interaction of the protein. Thus, the described procedure fills an important gap – ability to obtain a high-purity, biologically active preparation of HPCA through a single column and will enable analyses of the various functions of this important protein.

5.3. Electrophoretic mobility shift in native gels indicates calcium-dependent structural changes of neuronal calcium sensor proteins

NCS proteins are thought to have evolved to detect small changes in intracellular calcium levels. Upon binding calcium, these proteins undergo changes in conformation that mediate the cellular response to calcium levels. Our results show that this conformational change can be detected as retardation in mobility in the presence of calcium in a native gel. All NCS proteins tested exhibited this feature. Furthermore, the results suggest that the calcium-myristoyl switch, which involves the reordering of the EF1 hand, may be an integral part of the mechanism that underlies the conformational change. As the calcium level increases, the reordering likely alters the surface charges exposed to the gel matrix causing it to migrate slower through the gel matrix. The presence of the myristoyl group itself contributes to, but does not appear to be essential for, the conformational change detectable in native gels.

These observations can be tied in physiologically. Since the proteins are highly conserved across vertebrate species and are co-expressed, it is reasonable to propose that they may be different in their response ranges and/or sensitivity to calcium. Our results support the theory that multiple NCS proteins are needed to direct cellular responses to different calcium ranges [32, 42]. In our study, the NCS proteins show more conformational intermediates in their response to calcium, making additional conformational intermediates available to potentially interact with different target proteins across a broad range of calcium. In contrast, Calmodulin

appears to respond over a narrower range (1 – 11.24 □M) of calcium. Importantly, Calmodulin does not have a calcium-myristoyl switch. Nor does S100B; however, no difference in mobility of S100B is detected at any calcium concentration. It is possible that S100B does not bind calcium under conditions tested (lower affinity) or the structural changes brought about by calcium in S100B are beyond detection under conditions used in this study. However, differences in affinity cannot explain the difference in patterns of mobility shift among Calmodulin and NCS proteins, all of which have comparable affinities (reviewed in: [173]). What could be a potential mechanism to explain the observed differences? The results lead to the conclusion that the NCS proteins and Calmodulin are able to bind calcium tightly and the binding is stable under conditions of electrophoresis – otherwise, we would expect a "smear" rather than discrete bands upon electrophoresis. Upon binding, a conformational change is introduced in the protein. This conformational change is most likely initiated by the EF hand with the highest affinity, which then recruits other EF hands as the protein transitions from an "unbound" to a "bound" conformation. In Calmodulin, this transition begins only 1.36 □M of calcium, while in the NCS proteins, it begins at the lowest tested concentration. Notably, the NCS proteins possess an EF hand that does not bind calcium, unlike Calmodulin. We propose that this EF hand is critical in mediating the conformational shift in the NCS proteins. It is noteworthy that myristoylation is also localized to this EF hand. Furthermore, this is also the most diverse region among the NCS proteins and may explain the diversity of the mobility shift responses among the NCS proteins. Thus, in addition to binding,

global structural changes seem to be necessary for detectable mobility shift in the native gel.

The results obtained with magnesium in our study are also consistent with this conclusion. At least in the case of CALM1, GCAP1 and GCAP2, binding of magnesium to the protein has been clearly demonstrated [68, 181, 182] and it appears that the binding site for magnesium is nested within those for calcium, albeit defined by different amino acids [68, 183]. Yet no mobility shift is observed in these or any of the other NCS proteins tested. The explanation resides in two key earlier observations made with CALM1: (a) magnesium causes only local conformational changes around the binding site [181]; and (b) the apo-conformation (calcium-free) is stabilized by magnesium [182]. It is noteworthy that the magnesium action on GCAP1 and GCAP2 is also in their calcium-free state [68, 184, 185]. Thus, binding of magnesium serves to preserve the calcium-free conformational state of the protein and, therefore, would not elicit a detectable mobility shift. The local conformational changes brought about by magnesium, however, may be detected by assays such as tryptophan fluorescence and has been described for GCAP1 [69]. The results from this study suggest that these local changes do not culminate in global changes detected in the native gel assay.

Calcium can induce a mobility shift even under denaturing conditions, but only in the case of GCAPs and the proteins move faster with calcium, unlike in native gel where the mobility is retarded (Fig. 4.3-3). The results are consistent with earlier observations by Koch's laboratory [163, 164] and suggest that the proteins (GCAP1 and GCAP2) are capable of interacting with calcium even in the presence of SDS. It

is noteworthy that a similar mobility shift under denaturing conditions has been reported for Calmodulin and analyzed as early as 1980 [186]. However, NCALD and HPCA do not show a significant calcium-induced mobility difference under denaturing conditions (Fig. 4.3-3). The mechanism remains to be elucidated.

In summary, we have demonstrated that: (i) NCS proteins undergo calcium-dependent conformational changes that are detected in native gels; (ii) these changes are specifically induced by calcium; (iii) different proteins behave differently in the same matrix under identical conditions, suggesting that the behavior is protein-specific; (iv) in the NCS family members, characterized by the calcium-myristoyl switch, a gradual decrease in mobility is observed with incremental increases in calcium, and (v) the presence of a myristoyl group is not essential for this behavior, but needed for maximal response. Thus, distinct global structural responses to calcium binding have been documented in NCS proteins through mobility in native gels. In NCS proteins, this simple technique is able to assess overall changes in protein conformations. The correlation of these results to those obtained from established methods to analyze structure (NMR or crystallographic analyses) or activity (such as enzyme assays or target-protein interactions) remains to be determined. We believe that such analyses will provide further structural insights regarding calcium-driven conformational changes in the NCS proteins, especially in terms of the electrostatic drive and the hydrodynamic drag. It is not inconceivable that similar analyses may be possible in other proteins that bind small ligands.

5.4 Three amino acids in the dimer interface of the neuronal calcium sensor protein neurocalcin delta also govern its response to calcium

NCS proteins function as efficient calcium sensors and mediate cellular responses to the divalent cation. All of them bind to calcium, undergo intramolecular rearrangements (such as the calcium-myristoyl switch or the myristoyl tug) that facilitate intermolecular interactions that may lead to oligomerization and/or binding to target molecules. Thus, the cellular response to the calcium signal is orchestrated. In lower organisms, typically only one (or a few) NCS proteins exist and mediate calcium-regulated responses. As organisms become more complex, there is a rise in the number of NCS proteins, which mirrors an increase in the diversity and complexity of cellular responses that they mediate.

In this report, we have investigated two of the most closely related NCS proteins; NCALD and HPCA, which are independently conserved through all vertebrates even though they exhibit 88% identity at the primary sequence level. Based on experimental approaches that examine both intramolecular rearrangments (such as tryptophan fluorescence and CIMSA) as well as intermolecular interactions (such as size exclusion chromatography and membrane guanylate cyclase stimulation), the two proteins were found to differ in the magnitude of their response. Furthermore, mutation of three amino acids: S19N, K102M, A119E, at the dimer interface of NCALD to those found in HPCA appear to be sufficient to convert the response to be HPCA-like.

Intramolecular Rearrangements:

The way that calcium influences the intramolecular rearrangement of the NCS proteins was assayed by tryptophan fluorescence and native gels. The S19N mutation is sufficient to convert the tryptophan fluorescence response of NCALD to HPCA-like, but not the CIMSA response. This result suggests that the calcium-dependent response observed with tryptophan florescence is likely due to local intramolecular rearrangement around the W30 position and that it is sensitive to the residue at position 19. However, it is not sufficient to translate this response into a more global intramolecular rearrangement detected by the CIMSA assay. Similarly, the K102M mutation makes the protein respond like HPCA in tryptophan fluorescence, but not in CIMSA. However, the A119E mutation alters neither the tryptophan fluorescence response nor in CIMSA. It cannot be ruled out that the effect of K102M may be due its proximity to W103.

The results with the S19N mutation suggest a greater role for the EF1 region in shaping the intramolecular rearrangements in response to calcium. This is further supported by the effect of S19N K102M A119E, which causes a HPCA like response in both tryptophan fluorescence and native gels. The observation that tryptophan fluorescence is HPCA-like following the S19N mutation, suggests the dominance of this mutation over the others in determining the local conformational response around W30. It is noted that the EF1 hand is also pivotal for the calcium-myristoyl switch; the conformational rearrangement by which the buried myristoyl group is extruded when the protein binds calcium. We have already demonstrated, however, that the myristoyl group is somewhat secondary to the process; its presence affects only the

magnitude of the response [2, 28]. In GCAPs, the myristoyl tug (an interaction between EF1 and EF4 domains) has been suggested to act in place of the calcium-myristoyl switch.

Intermolecular Interactions:

Ability of two or more molecules of a protein to interact with one another is a theme that is observed frequently in the NCS family. VILIP1, GCAP1, GCAP2 are all known to dimerize. When the ability to dimerize is influenced by extrinsic factors such as presence of calcium or the oxidation state, it may be termed as functional dimerization. Results presented here suggest that this is a key process in determining protein-specific functions. Despite a high degree of conservation, NCALD exhibits functional dimerization, but HPCA does not. Consistent with the idea that NCALD forms a head-to-tail dimer, a critical interplay between the EF-1 and EF-3 domains in the dimerization of NCALD is also observed. Based on size exclusion experiments, each of the three residues contributed to the overall dimerization state of NCALD. K102 in NCALD is critical for calcium-induced oligomerization, as observed by the amount of protein converted to dimer. The other EF-3 mutant A119E showed a large decrease in the total percentage of dimer, but not in the ability for calcium to influence dimerization. S19 is critical for dimer stability, with the S19N mutation increasing the total dimer over wild type, but with decreased calcium responsiveness. The double and triple mutations, K102M A119E and S19N K102M A119E support this idea, with both of these point mutants causing both decrease in overall dimerization of NCALD and decreased ability for calcium to influence dimerization

compared to wild type. Of interest is the observation that about 25% of HPCA remains a dimer regardless of the presence of calcium. It remains to be determined whether this is due to stabilization offered by N19 or the conserved Cys residues as suggested for VILIP1.

The complexity of the intermolecular interactions is further underscored by the ability of the proteins, wild type and mutants, to stimulate membrane guanylate cyclase activity. Both NCALD and HPCA stimulate Rod Outer Segment membrane Guanylate Cyclase type 1 (ROSGC1; gene symbol GUCY2D). Under identical conditions, the magnitude of stimulation by NCALD is about twice of that of HPCA. Any of the mutations, individually or together, cause a significant decrease in activity when compared to the wild type. These results suggest that the dimer interface may be necessary for maximal stimulation of ROSGC1 activity but not for the interaction itself. The mere presence of a dimer is not sufficient for stimulation; as the S19N and SKA mutants, which are dimeric even in the absence of calcium, failed to stimulate ROSGC1 in the absence of calcium (data not shown). Thus, interaction of NCALD with ROSGC1 appears to be a two-step process: calcium binding is an essential first step that brings about intramolecular rearrangements in different domains of the protein, which, in turn, facilitate optimal interaction with ROSGC1. The results are consistent with earlier reports emphasizing the role of different domains on GCAP2-ROSGC1 interactions. Further investigations into binding affinities of the wild type and mutant NCALD along with HPCA will help delineate the relative role of these residues (and the domains) in the target interaction.

Generally, different NCS sub-family members have evolved to carry out similar, but not identical, functions. For example, all GCAPs appear to be linked to activation of ROSGCs, although differences exist in their relative affinities and efficiencies, some of which may be traced back to their intramolecular rearrangements [54]. Mutations in GCAP1 and GCAP2 affect phototransduction and lead to retinal degeneration (44, 67). Most members of the KChIP family interact with potassium channels [77, 78, 81, 83, 139, 187]. In contrast, the VILIP subfamily appears to be functionally the most diverse group. Knockout mice exist only for HPCA and have established a role for this protein in long term potentiation of

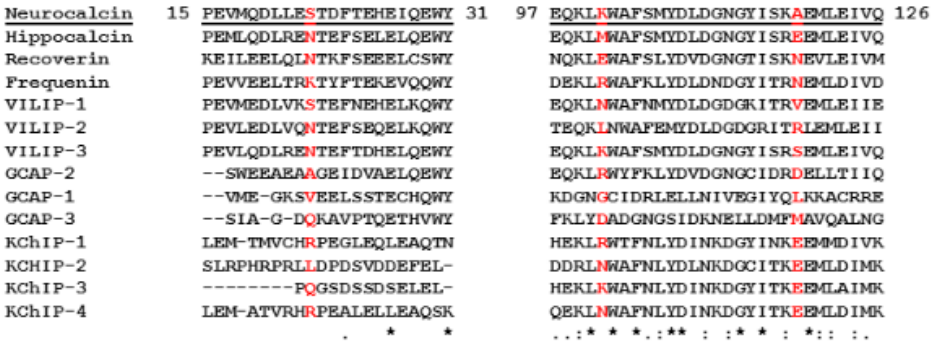

Figure 5.4-1: Conservation of the 19, 102 and 119 sites through the NCS Family. Sequences for the 14 gene coding members of the NCS family were aligned using Clustal Omega as described in the materials and methods section. The left panel highlights highly variable N-terminal region around S19 in NCALD. The right panel shows the EF-3 calcium binding regions around K102 and A119. The EF-3 region is highly conserved among the NCS family, however 102 and 119 positions are hypervariable.

memory [20]. Mutations have linked some of these proteins to diverse disorders affecting intellectual abilities and musculoskeletal system [10, 59, 108].

Biochemically, VILIP1 and NCALD form dimers, while VILIP3, NCS1 and HPCA

do not [29, 120, 178]. A large variety of non-overlapping targets have been identified for these proteins – even the very closely related NCALD and HPCA. Results from this study enable insights into the evolution of intra- and intermolecular rearrangements that distinguish the responses of these proteins to calcium.

Comparison of NCALD and HPCA suggest that the two proteins share common mechanisms yet generate distinct responses to calcium. Both proteins respond over the same range of calcium; however, the magnitude is lower with HPCA when compared to NCALD. The proteins are likely to have comparable affinities for calcium since the EF2 through EF4 regions are highly conserved. The crystal structure of NCALD falls into the general picture of an N-terminal lobe and C-terminal lobe, each comprising two EF hands. In the archetypal NCS protein, calmodulin, relative rotation of the two lobes mediates the response to calcium. However, this linker region between EF2 and EF3 is completely conserved between NCALD and HPCA and, therefore, is unlikely to be the pivotal difference. Nor is the shared calcium-myristoyl switch likely to be the distinguishing factor.

This study, for the first time, has identified three amino acid residues that are sufficient to influence both dimerization and calcium responses in NCALD and convert them to HPCA-like ones. Could these residues also contribute to the responses in other NCS proteins? Figure 5.4-1 explores this idea. Sequences of NCS proteins around S19, K102 and A119 of NCALD have been aligned. The left panel presents the alignment from the S19 region, which is less well conserved. A few residues are conserved and the position 19 is highlighted. The right panel, comprising the EF3 hand, is well conserved among the proteins. Interestingly, positions 102 and

119 are seen to be hypervariable. It is possible that these residues contribute to NCS protein specific calcium dependent responses.

This idea is supported by the results with the R102Q mutant of NCS1. The R102Q mutation was originally identified to be linked to a type of autism [60]. Further analyses of the mutant protein showed that the R102Q mutation did not affect calcium binding, but rather the duration of translocation in NCS1 [61].

In conclusion, we have demonstrated that three amino acid residues in the dimer interface of NCALD are critical for dimerization in addition to determining the calcium-induced response. A novel EF1-EF3 interaction may underlie the intramolecular rearrangement facilitating the protein-specific response. The position 19 resides in a region that is already diverse among NCS proteins; within the more conserved EF3 region, hypervariability of positions 102 and 119 suggest that the mechanism may be more general in NCS proteins.

5.5 The EF-1 helps determine the calcium-induced response of NCALD and HPCA

Analysis of the EF-1 regions of NCALD and HPCA yielded critical results that underscore how these two proteins differ, despite being 88% identical. Between NCALD and HPCA the EF-1 region is the least conserved [6, 67]. The EF-1 region is the least conserved throughout the NCS family. Therefore, analysis of the EF-1 was critical to understand the role of the non-calcium binding EF hand.

First, the analysis of each tryptophan revealed that the majority of the changes observed in the experiment are primarily from the tryptophan 30 in the EF-1 hand as revealed by the W30F, W103F mutations. This is because the W103F responses in both HPCA and NCALD have an increased change in fluorescence intensity compared to the wild type. Fundamentally there is a clear difference between the roles of the tryptophans between the two proteins. In NCALD, the W30F mutation causes a complete loss of fluorescence response (change in fluorescence intensity), suggesting that the internal rearrangement around this residue is a critical part of NCALD response, whereas the HPCA W30F can still respond like the wild type. This gives us some insight into the differences in the structures of the two proteins. In HPCA, NCALD and the other NCS proteins these two positions are involved in the critical calcium-myristoyl switch mechanism [6, 102, 178]. These positions are part of a hydrophobic core that the protein structure reorients around, upon binding calcium. In NCALD, this position is critical for the protein to function properly, however, in HPCA it is not. This would suggest that the two positions differ between

the proteins. The tryptophan fluorescence experiments primarily examine changes in the local environment around the tryptophan in the EF-1 brought about by calcium structural rearrangement. Because of this result, it makes sense that the chimeras responded like the corresponding EF-1 region, with NCHC responding like NCALD, and HCNC responding like HPCA. This result suggests that the calcium-binding region drives the response observed by the rearrangement of the EF-1 region. The possibility still remains that the increased dimerization observed in HCNC could be due to aggregation. To rule out this possibility, a gel filtration step be added to the purification procedure in future experiments.

The calcium response as measured by CIMSA experiments on the chimeric proteins revealed not only an excellent insight into the structure of NCALD and HPCA, but a glimpse into what is actually being observed under native gel electrophoresis. First, the overall response appears to be driven by both the calcium binding hands and the EF-1. The innate positions of the calcium and the non-calcium bound forms of NCHC looked like HPCA, and HCNC looked like NCALD. This reveals that the calcium binding EF hand motifs primarily govern CIMSA migration, with respect to position migration and total response. However, the EF-1 does play a role in the dose dependent response of the proteins. Neither NCHC nor HCNC looked like either wild type when observed over a range of calcium, rather, each demonstrated an intermediate response between the two. Together, these two observations demonstrate that the total CIMSA response is a global contribution of the charges derived by calcium binding, as well as the structural rearrangement

brought upon by the re-orientation of the EF-1 region as a result of the calcium myristoyl switch.

The EF-1 region contributed to the dimerization state of the proteins as another calcium-induced response. The size exclusion chromatography results demonstrate that the EF-1 plays a critical role in the dimerization state of the proteins. NCHC gained some calcium-induced dimerization over HPCA, while HCNC had a loss of dimerization. This result is consistent with observations of the dimer mutants, where S19N caused a loss of the calcium inducible dimerization, again suggesting that there is a critical EF-1-EF-3 interaction.

The work done with the chimeric proteins gives new insight into the roles of the EF hands, and more specifically, the non- calcium binding EF-1. Taken together, the results demonstrate that the EF-1 region is responsible for the type of calcium response the NCS protein exhibits once it is bound to calcium. The calcium binding EF-2-4 drive this response. From an evolutionary perspective this idea makes sense. The calcium binding regions are left largely intact throughout the family, while the non-calcium binding regions differentiate their response to calcium.

5.6 HPCA and Dystonia.

Dystonia is a disease that affects 250,000 people in the United States [188, 189]. The recent discovery of the genetic cause of primary isolated type 2 dystonia allows for an opportunity to better understanding of the underlying causes of the disease. The original conclusion made by the discoverers of the HPCA mutations that resulted in dystonia was that the mutations in HPCA would render the protein inoperable. The authors made this claim because of the location of the mutations, which are in the calcium binding EF-2 hand. N75, in particular, is thought to coordinate calcium. The authors went on to conclude that a loss of HPCA causes dystonia, because HPCA knocked out neuronal cells, did not function properly [10]. Our work has demonstrated that this conclusion in fact erroneous.

First, we demonstrated that the mutant HPCA could bind calcium and that the binding was comparable to the wild type protein. While the experiment did not rule out the possibility of a lowered affinity for calcium, it did reveal that calcium could still bind to the EF-2 hand in both of the N75K and T71N mutants in a comparable manner to the wild type protein. Additional experiment tested over a range of lower free calcium concentrations would reveal this possibility.

Because the mutant proteins could effectively bind to calcium, it was important to understand how the proteins responded to calcium. Tryptophan fluorescence and CIMSA experiments were used to observe the calcium-induced response to calcium binding. Tryptophan fluorescence revealed that the proteins responded to calcium binding by inducing a structural shift, which was observed as an increase in fluorescence intensity. Both the T71N and N75K responded like HPCA.

CIMSA analyses revealed the T71N mutation had a wild-type like response to calcium binding, while N75K had a slightly reduced response to calcium binding. This result, along with the observation that the mutations altered the initial migration of the protein in the native system, reveals that there are structural differences in the dystonia mutant proteins. These structural differences are observable when compared to HPCA, but the data shows that the dystonia proteins are still able to re-orient their structure and respond to calcium binding.

After it was established that the dystonia mutations still retain the ability to bind and then respond to calcium, it was pertinent to look at one of the downstream effectors of HPCA. Stimulation of ROS-GC1 activityhas been a demonstrated ability of HPCA. Wild type HPCA can stimulate cGMP production nearly two fold. Both the N75K andT71N proteins failed to stimulate ROS-GC1. Since the proteins are binding to, and responding to calcium, it is possible that these sites in the EF-2 hands are involved in interactions with ROS-GC1. Here, we demonstrate the first clear problem with the mutant proteins. Since cGMP regulates intracellular calcium levels, it seems likely that the dystonia mutations lead to calcium dysregulation inside the cells.

Finally the translocation of the VILIP class of proteins has been demonstrated as a critical step in the calcium signaling process. HPCA translocates from the cytosol to the vesicle-rich, perinuclear region upon an increase in intracellular calcium levels (Fig 4.6-7). T71N showed translocation ability, and the translocation event was comparable to wild type HPCA. N75K demonstrated no ability to migrate under the same conditions. This is the first experiment where there was a distinction between the two dystonia mutations.

These experiments highlighted several conclusions overlooked by the original authors. First, the proteins retain the ability to bind calcium. They can bind to and respond to calcium in a manner similar to HPCA wild type, with respect to the calcium induced structural reorientation. The mutant proteins cannot stimulate ROS-GC1, showing a critical defect in their functions. Finally, we identified a difference between the two mutations, T71N and N75K, with respect to their ability to translocate. All of these results point to a calcium dysregulation issue rather than a total loss of function.

The malfunctioning dystonia proteins T71N and N75K differed in the severity of the effects of the mutations. The Charlesworth group went on to describe the patient's symptoms with the different dystonia mutations. People with the T71N mutation were described as having a mild form of dystonia. T71N still retains the ability to translocate upon the addition of histamine, inside of COS-7 cells, despite its inability to stimulate ROS-CG1.The N75K patients had a more severe form of the disease. N75K was not able to stimulate ROS-CG1 and lacked the ability to translocate. This distinction is critical in understanding dystonia and how mutations correlate to physiological symptoms.

5.7 Summary: What differentiates the Neuronal calcium sensor family?

The Neuronal calcium family is a highly conserved family of proteins responsible for the calcium-mediated response in cells, particularly neurons. Because calcium is a universal signaling molecule, it is critical for a cell to properly detect and respond to specific levels of calcium. The NCS proteins facilitate this response by binding calcium, translocating to regions inside the cell, and then interacting with specific partners, or with common partners in a distinct manner [5, 6, 18, 29, 73, 86, 121]. Due to their high similarity, NCS proteins have evolved functions, which differentiated this calcium response.

NCS proteins employ several mechanisms to differentiate themselves. The three sub-families (Fig 4.1-1) utilize different methods to differentiate members. The KChIPS use tissue expression, or sub cellular location, to differentiate their functions [81, 82]. GCAPs, by comparison, are co-expressed. To differentiate themselves, they differ in their affinities to calcium [6, 49, 71]. VILIPs can be expressed together, but it is not clear how they differentiate their functions.

This work has detailed several new discoveries; which demonstrate how the NCS family differentiates their individual members, despite their high similarity. By comparing NCALD and HPCA, two VILIPs, this work has highlighted new amino acid residues and domains of interest in the NCS proteins. A summary of these discoveries is highlighted in Fig. 5.7-1. By better understanding how the NCS family differentiate themselves, we can gather a better understanding of how evolution has increased the complexity and specificity of calcium signaling.

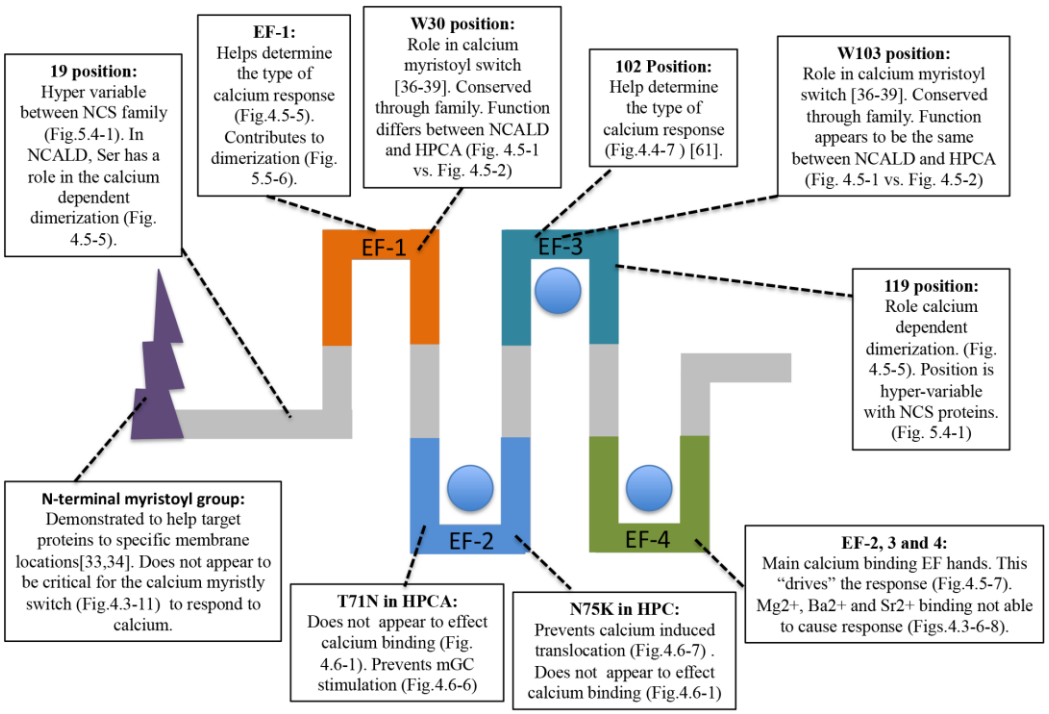

Figure 5.7-1. What differentiates the Neuronal calcium sensor family? Diagram of regions of differentiation in the NCS family. EF-1 is labeled in orange, EF-2 in Blue, EF-3 in aqua and EF-4 in green. Blue spheres represent calcium.

First a global, phylogenetic approach was taken by examining the relationships among closely related NCS proteins. The two NCS subfamily's GCAPs and VILIPs both modulate of mGC activity, but in opposite calcium states. They were shown to each have unique binding regions (Figs. 4.1-2 vs. 4.1-3). The ability for KChIPs to bind DRE sequences is a unique feature of the subfamily because the binding regions of the KChIPs are unique to that sub-group (Fig. 4.1-4).

Next, the mobility of the proteins through a native gel in an electrical field was detailed. Here it was highlighted that NCS proteins undergo calcium-dependent conformational changes that are detectable in native gels in a protein-specific manner

under identical conditions (Fig. 4.3-1). The changes in migration are specific to calcium (Figs. 4.3-3-8). It was also demonstrated that the presence of a myristoyl group is not essential for this translocation behavior (Fig. 4.3-12). This new method allows for the direct comparison in the total global charge of the protein.

The subsequent study highlighted residues for dimerization of NCALD. The first areas of interest are the 102 and 119 positions, which are hypervariable throughout the family (Fig. 5.4-1). It appears that particular residue positions have been favored by evolution to alter the functions of the NCS family in a manner, which does not directly affect binding, but rather alters the calcium induced response (Figs. 4.4-5, 4.4-7). This is because NCALD and HPCA seem to respond over the same calcium range. Mutations at the 102 positions in NCS have been shown to be one of the causes of autism [60]. This mutation led only to changes in the calcium response.

The drastic effects of the S19N mutation in NCALD, demonstrated that there could be a functional role of the non-calcium binding regions of NCALD, and the NCS family as a whole. The chimeric proteins revealed that the EF-1 region determines the type of response. This region contributes to dimerization, as well as the overall calcium response (Figs. 4.5-5-7). This conclusion is a departure from what is typically described in the field, as this region has mostly been considered non-functional. Here, it is demonstrated for the first time that this region does indeed play a role in the calcium-induced response of the NCS proteins.

This work demonstrates that the two VILIPs, NCALD and HPCA respond over the same range of calcium, and that they both can interact with ROS-GC1. What

makes them differ is their total calcium response. NCALD appears to be more responsive compared to HPCA. NCALD changes its' structure more than any other NCS protein in the CIMSA experiments (Fig 4.3-11). It has a greater change in tryptophan fluorescence response compared to HPCA (Fig 4.4-2), and stimulates ROS-GC1 two fold more than HPCA (Fig. 4.4-4). Some of these abilities are independent of its ability to dimerize.

Diseases can result from an improper response to calcium binding, not just calcium binding. This is observed with the dystonia mutations, which do not affect calcium binding, but rather the ability to stimulate ROS-GC1. In addition, the N75K mutation affects the ability of the proteins to translocate. Changes in the ability of the NCS proteins to translocate have been demonstrated with Autism as well. The R102K mutation affected the NCS1's ability to remain in contact with the intracellular membrane [11]. In this way a mutation here shows that the duration of interaction may be another way the NCS proteins differentiate themselves from each other.

In conclusion, this work has shown that the NCS family, and more specifically NCALD and HPCA, differentiate their functions in several ways. The location of expression, tissue or subcellular, calcium range, interacting partners and type of response all contribute to this differentiation. Many of these differences can be mapped to specific regions which my help us better understand how evolution has increased the complexity and specificity of calcium signaling.

Chapter 7: References

1. Viviano, J., *et al*., *Datasets depicting mobility retardation of NCS proteins observed upon incubation with calcium, but not with magnesium, barium or strontium.* Data Brief, 2016. **7**: p. 1606-8.

2. Viviano, J., *et al*., *Data on the calcium-induced mobility shift of myristoylated and non-myristoylated forms of neurocalcin delta.* Data Brief, 2016. **7**: p. 630-3.

3. Viviano, J., *et al*., *Electrophoretic mobility shift in native gels indicates calcium-dependent structural changes of neuronal calcium sensor proteins.* Anal Biochem, 2016. **494**: p. 93-100.

4. Viviano, J., *et al*., *Data on final calcium concentration in native gel reagents determined accurately through inductively coupled plasma measurements.* Data Brief, 2016. **6**: p. 820-2.

5. Burgoyne, R.D. and L.P. Haynes, *Understanding the physiological roles of the neuronal calcium sensor proteins.* Mol Brain, 2012. **5**(1): p. 2.

6. Burgoyne, R.D., *Neuronal calcium sensor proteins: generating diversity in neuronal Ca2+ signalling.* Nat Rev Neurosci, 2007. **8**(3): p. 182-93.

7. Zamponi, G.W. and K.P. Currie, *Regulation of Ca(V)2 calcium channels by G protein coupled receptors.* Biochim Biophys Acta, 2012.

8. Seaton, G., *et al*., *Sensing change: the emerging role of calcium sensors in neuronal disease.* Semin Cell Dev Biol, 2011. **22**(5): p. 530-5.

9. Ban, H.J., *et al*., *Genetic and metabolic characterization of insomnia.* PLoS One, 2011. **6**(4): p. e18455.

10. Charlesworth, G., *et al*., *Mutations in HPCA cause autosomal-recessive primary isolated dystonia.* Am J Hum Genet, 2015. **96**(4): p. 657-65.

11. Handley, M.T., *et al*., *Structural and functional deficits in a neuronal calcium sensor-1 mutant identified in a case of autistic spectrum disorder.* PLoS One, 2010. **5**(5): p. e10534.

12. Barclay, J.W., A. Morgan, and R.D. Burgoyne, *Calcium-dependent regulation of exocytosis.* Cell Calcium, 2005. **38**(3-4): p. 343-53.

13. Marenholz, I., C.W. Heizmann, and G. Fritz, *S100 proteins in mouse and man: from evolution to function and pathology (including an update of the nomenclature).* Biochem Biophys Res Commun, 2004. **322**(4): p. 1111-22.

14. Zimmer, D.B., *et al*., *Evolution of the S100 family of calcium sensor proteins.* Cell Calcium, 2013. **53**(3): p. 170-9.

15. Weiss, J.L. and R.D. Burgoyne, *Sense and sensibility in the regulation of voltage-gated Ca(2+) channels.* Trends Neurosci, 2002. **25**(10): p. 489-91.

16. Duda, T., Venkataraman, V. and Sharma, R.K., ed. *Constitution and Operational Principles of the Retinal and Odoarant - linked Neurocalcin delta-dependent Ca^{2+}-modulated ROS-GC transduction Machinery*. Neuronal Calcium Sensor Proteins, ed. P.P.a.K. Phillippov, K-W. 2006, Nova Science Publishers: New York. 91-115.

17. Kumar, V.D., *et al*., *Crystallization and preliminary X-ray crystallographic studies of recombinant bovine neurocalcin delta.* Proteins, 1996. **25**(2): p. 261-4.

18. Burgoyne, R.D. and J.L. Weiss, *The neuronal calcium sensor family of Ca2+-binding proteins.* Biochem J, 2001. **353**(Pt 1): p. 1-12.

19. Gomez, M., *et al*., *Ca2+ signaling via the neuronal calcium sensor-1 regulates associative learning and memory in C. elegans.* Neuron, 2001. **30**(1): p. 241-8.

20. Noguchi, H., *et al*., *Lack of hippocalcin causes impairment in Ras/extracellular signal-regulated kinase cascade via a Raf-mediated activation process.* J Neurosci Res, 2007. **85**(4): p. 837-44.

21. Dizhoor, A.M., S.G. Boikov, and E.V. Olshevskaya, *Constitutive activation of photoreceptor guanylate cyclase by Y99C mutant of GCAP-1. Possible role in causing human autosomal dominant cone degeneration.* J Biol Chem, 1998. **273**(28): p. 17311-4.

22. Downes, S.M., *et al.*, *Autosomal dominant cone-rod dystrophy with mutations in the guanylate cyclase 2D gene encoding retinal guanylate cyclase-1.* Arch Ophthalmol, 2001. **119**(11): p. 1667-73.

23. Payne, A.M., *et al.*, *A mutation in guanylate cyclase activator 1A (GUCA1A) in an autosomal dominant cone dystrophy pedigree mapping to a new locus on chromosome 6p21.1.* Hum Mol Genet, 1998. **7**(2): p. 273-7.

24. Duda, T., *et al.*, *Mutations in the rod outer segment membrane guanylate cyclase in a cone-rod dystrophy cause defects in calcium signaling.* Biochemistry, 1999. **38**(42): p. 13912-9.

25. Duda, T., *et al.*, *Functional consequences of a rod outer segment membrane guanylate cyclase (ROS-GC1) gene mutation linked with Leber's congenital amaurosis.* Biochemistry, 1999. **38**(2): p. 509-15.

26. Duda, T., *et al.*, *Impairment of the rod outer segment membrane guanylate cyclase dimerization in a cone-rod dystrophy results in defective calcium signaling.* Biochemistry, 2000. **39**(41): p. 12522-33.

27. Palczewski, K., *et al.*, *Ca(2+)-binding proteins in the retina: structure, function, and the etiology of human visual diseases.* Bioessays, 2000. **22**(4): p. 337-50.

28. Ames, J.B., *et al.*, *Structure and calcium-binding properties of Frq1, a novel calcium sensor in the yeast Saccharomyces cerevisiae.* Biochemistry, 2000. **39**(40): p. 12149-61.

29. Braunewell, K.H., *et al.*, *Intracellular neuronal calcium sensor (NCS) protein VILIP1 modulates cGMP signalling pathways in transfected neural cells and cerebellar granule neurones.* J Neurochem, 2001. **78**(6): p. 1277-86.

30. Krishnan, A., *et al.*, *Structural, biochemical, and functional characterization of the calcium sensor neurocalcin delta in the inner retinal neurons and its*

linkage with the rod outer segment membrane guanylate cyclase transduction system. Biochemistry, 2004. **43**(10): p. 2708-23.

31. Spilker, C., E.D. Gundelfinger, and K.H. Braunewell, *Evidence for different functional properties of the neuronal calcium sensor proteins VILIP1 and VILIP3: from subcellular localization to cellular function.* Biochim Biophys Acta, 2002. **1600**(1-2): p. 118-27.

32. Viviano, J., Wu, H., Venkataraman, V., *Evolutionary Interrelationships and Insights into Molecular Mechanisms of Functional Divergence: An Analysis of Neuronal Calcium Sensor Proteins.* Phylogenetics & Evolutionary Biology, 2013. **1**(4): p. 117.

33. O'Callaghan, D.W. and R.D. Burgoyne, *Role of myristoylation in the intracellular targeting of neuronal calcium sensor (NCS) proteins.* Biochem Soc Trans, 2003. **31**(Pt 5): p. 963-5.

34. O'Callaghan, D.W., *et al*., *Residues within the myristoylation motif determine intracellular targeting of the neuronal Ca2+ sensor protein KChIP1 to post-ER transport vesicles and traffic of Kv4 K+ channels.* J Cell Sci, 2003. **116**(Pt 23): p. 4833-45.

35. Takimoto, K., E.K. Yang, and L. Conforti, *Palmitoylation of KChIP splicing variants is required for efficient cell surface expression of Kv4.3 channels.* J Biol Chem, 2002. **277**(30): p. 26904-11.

36. Dizhoor, A.M., *et al*., *Recoverin: a calcium sensitive activator of retinal rod guanylate cyclase.* Science, 1991. **251**(4996): p. 915-8.

37. Bourne, Y., *et al*., *Immunocytochemical localization and crystal structure of human frequenin (neuronal calcium sensor 1).* J Biol Chem, 2001. **276**(15): p. 11949-55.

38. Zhou, W., *et al*., *Structural insights into the functional interaction of KChIP1 with Shal-type K(+) channels.* Neuron, 2004. **41**(4): p. 573-86.

39. Lemire, S., A. Jeromin, and E. Boisselier, *Membrane binding of Neuronal Calcium Sensor-1 (NCS1).* Colloids Surf B Biointerfaces, 2016. **139**: p. 138-47.

40. Tanaka, T., *et al*., *Sequestration of the membrane-targeting myristoyl group of recoverin in the calcium-free state.* Nature, 1995. **376**(6539): p. 444-7.

41. Xu, X., R. Ishima, and J.B. Ames, *Conformational dynamics of recoverin's Ca2+-myristoyl switch probed by 15N NMR relaxation dispersion and chemical shift analysis.* Proteins, 2011. **79**(6): p. 1910-22.

42. Ames, J.B., S. Lim, and M. Ikura, *Molecular structure and target recognition of neuronal calcium sensor proteins.* Front Mol Neurosci, 2012. **5**: p. 10.

43. Zozulya, S. and L. Stryer, *Calcium-myristoyl protein switch.* Proc Natl Acad Sci U S A, 1992. **89**(23): p. 11569-73.

44. Gorczyca, W.A., *et al*., *Guanylyl cyclase activating protein. A calcium-sensitive regulator of phototransduction.* J Biol Chem, 1995. **270**(37): p. 22029-36.

45. Krishnan, A., *et al*., *Hippocalcin, new Ca(2+) sensor of a ROS-GC subfamily member, ONE-GC, membrane guanylate cyclase transduction system.* Mol Cell Biochem, 2009. **325**(1-2): p. 1-14.

46. Lambrecht, H.G. and K.W. Koch, *Recoverin, a novel calcium-binding protein from vertebrate photoreceptors.* Biochim Biophys Acta, 1992. **1160**(1): p. 63-6.

47. Baehr, W. and K. Palczewski, *Guanylate cyclase-activating proteins and retina disease.* Subcell Biochem, 2007. **45**: p. 71-91.

48. Howes, K.A., *et al*., *GCAP1 rescues rod photoreceptor response in GCAP1/GCAP2 knockout mice.* EMBO J, 2002. **21**(7): p. 1545-54.

49. Hwang, J.Y., *et al*., *Regulatory modes of rod outer segment membrane guanylate cyclase differ in catalytic efficiency and Ca(2+)-sensitivity.* Eur J Biochem, 2003. **270**(18): p. 3814-21.

50. Lange, C., *et al*., *Regions in vertebrate photoreceptor guanylyl cyclase ROS-GC1 involved in Ca(2+)-dependent regulation by guanylyl cyclase-activating protein GCAP-1.* FEBS Lett, 1999. **460**(1): p. 27-31.

51. Pettelkau, J., *et al*., *Structural Insights into retinal guanylylcyclase-GCAP-2 interaction determined by cross-linking and mass spectrometry.* Biochemistry, 2012. **51**(24): p. 4932-49.

52. Sakurai, K., J. Chen, and V.J. Kefalov, *Role of guanylyl cyclase modulation in mouse cone phototransduction.* J Neurosci, 2011. **31**(22): p. 7991-8000.

53. Stephen, R., K. Palczewski, and M.C. Sousa, *The crystal structure of GCAP3 suggests molecular mechanism of GCAP-linked cone dystrophies.* J Mol Biol, 2006. **359**(2): p. 266-75.

54. Koch, K.W., *The guanylate cyclase signaling system in zebrafish photoreceptors.* FEBS Lett, 2013. **587**(13): p. 2055-9.

55. Koch, K.W., T. Duda, and R.K. Sharma, *Ca(2+)-modulated vision-linked ROS-GC guanylate cyclase transduction machinery.* Mol Cell Biochem, 2010. **334**(1-2): p. 105-15.

56. Hamasaki-Katagiri, N. and J.B. Ames, *Neuronal calcium sensor-1 (Ncs1p) is up-regulated by calcineurin to promote Ca2+ tolerance in fission yeast.* J Biol Chem, 2010. **285**(7): p. 4405-14.

57. Dason, J.S., *et al*., *Frequenin/NCS1 and the Ca2+-channel alpha1-subunit co-regulate synaptic transmission and nerve-terminal growth.* J Cell Sci, 2009. **122**(Pt 22): p. 4109-21.

58. Koh, P.O., *et al*., *Up-regulation of neuronal calcium sensor-1 (NCS1) in the prefrontal cortex of schizophrenic and bipolar patients.* Proc Natl Acad Sci U S A, 2003. **100**(1): p. 313-7.

59. Kuroda, Y., *et al*., *Refinement of the deletion in 8q22.2-q22.3: the minimum deletion size at 8q22.3 related to intellectual disability and epilepsy.* Am J Med Genet A, 2014. **164A**(8): p. 2104-8.

60. Piton, A., *et al*., *Mutations in the calcium-related gene IL1RAPL1 are associated with autism.* Hum Mol Genet, 2008. **17**(24): p. 3965-74.

61. Zhu, Y., *et al*., *R102Q mutation shifts the salt-bridge network and reduces the structural flexibility of human neuronal calcium sensor-1 protein.* J Phys Chem B, 2014. **118**(46): p. 13112-22.

62. Makino, C.L., *et al*., *Recoverin regulates light-dependent phosphodiesterase activity in retinal rods.* J Gen Physiol, 2004. **123**(6): p. 729-41.

63. Zang, J., *et al*., *Recoverin depletion accelerates cone photoresponse recovery.* Open Biol, 2015. **5**(8).

64. Grigoriev, II, *et al*., *Synergetic effect of recoverin and calmodulin on regulation of rhodopsin kinase.* Front Mol Neurosci, 2012. **5**: p. 28.

65. Polans, A.S., *et al*., *Recoverin, a photoreceptor-specific calcium-binding protein, is expressed by the tumor of a patient with cancer-associated retinopathy.* Proc Natl Acad Sci U S A, 1995. **92**(20): p. 9176-80.

66. Thirkill, C.E., *et al*., *The cancer-associated retinopathy antigen is a recoverin-like protein.* Invest Ophthalmol Vis Sci, 1992. **33**(10): p. 2768-72.

67. Dizhoor, A.M. and J.B. Hurley, *Inactivation of EF-hands makes GCAP-2 (p24) a constitutive activator of photoreceptor guanylyl cyclase by preventing a Ca2+-induced "activator-to-inhibitor" transition.* J Biol Chem, 1996. **271**(32): p. 19346-50.

68. Peshenko, I.V. and A.M. Dizhoor, *Ca2+ and Mg2+ binding properties of GCAP-1. Evidence that Mg2+-bound form is the physiological activator of photoreceptor guanylyl cyclase.* J Biol Chem, 2006. **281**(33): p. 23830-41.

69. Peshenko, I.V. and A.M. Dizhoor, *Guanylyl cyclase-activating proteins (GCAPs) are Ca2+/Mg2+ sensors: implications for photoreceptor guanylyl cyclase (RetGC) regulation in mammalian photoreceptors.* J Biol Chem, 2004. **279**(17): p. 16903-6.

70. Lim, S., A.M. Dizhoor, and J.B. Ames, *Structural diversity of neuronal calcium sensor proteins and insights for activation of retinal guanylyl cyclase by GCAP1.* Front Mol Neurosci, 2014. **7**: p. 19.

71. Mendez, A., *et al*., *Role of guanylate cyclase-activating proteins (GCAPs) in setting the flash sensitivity of rod photoreceptors.* Proc Natl Acad Sci U S A, 2001. **98**(17): p. 9948-53.

72. Punta, M., *et al*., *Molecular modeling studies on CNG channel from bovine retinal rod: a structural model of the cyclic nucleotide-binding domain.* Proteins, 2003. **52**(3): p. 332-8.

73. Braunewell, K.H., *The darker side of Ca2+ signaling by neuronal Ca2+-sensor proteins: from Alzheimer's disease to cancer.* Trends Pharmacol Sci, 2005. **26**(7): p. 345-51.

74. Tucker, C.L., *et al*., *Biochemical analysis of a dimerization domain mutation in RetGC-1 associated with dominant cone-rod dystrophy.* Proc Natl Acad Sci U S A, 1999. **96**(16): p. 9039-44.

75. Pruunsild, P. and T. Timmusk, *Structure, alternative splicing, and expression of the human and mouse KCNIP gene family.* Genomics, 2005. **86**(5): p. 581-93.

76. An, W.F., *et al*., *Modulation of A-type potassium channels by a family of calcium sensors.* Nature, 2000. **403**(6769): p. 553-6.

77. Shibata, R., *et al*., *A fundamental role for KChIPs in determining the molecular properties and trafficking of Kv4.2 potassium channels.* J Biol Chem, 2003. **278**(38): p. 36445-54.

78. Scannevin, R.H., *et al*., *Two N-terminal domains of Kv4 K(+) channels regulate binding to and modulation by KChIP1.* Neuron, 2004. **41**(4): p. 587-98.

79. Mellstrom, B. and J.R. Naranjo, *Ca2+-dependent transcriptional repression and derepression: DREAM, a direct effector.* Semin Cell Dev Biol, 2001. **12**(1): p. 59-63.

80. Mellstrom, B., *et al*., *Ca2+-operated transcriptional networks: molecular mechanisms and in vivo models.* Physiol Rev, 2008. **88**(2): p. 421-49.

81. Rhodes, K.J., *et al*., *KChIPs and Kv4 alpha subunits as integral components of A-type potassium channels in mammalian brain.* J Neurosci, 2004. **24**(36): p. 7903-15.

82. Dabrowska, J. and D.G. Rainnie, *Expression and distribution of Kv4 potassium channel subunits and potassium channel interacting proteins in subpopulations of interneurons in the basolateral amygdala.* Neuroscience, 2010. **171**(3): p. 721-33.

83. Hasdemir, B., *et al*., *Traffic of Kv4 K+ channels mediated by KChIP1 is via a novel post-ER vesicular pathway.* J Cell Biol, 2005. **171**(3): p. 459-69.

84. Boland, L.M., *et al*., *Functional properties of a brain-specific NH2-terminally spliced modulator of Kv4 channels.* Am J Physiol Cell Physiol, 2003. **285**(1): p. C161-70.

85. Van Hoorick, D., *et al*., *Differential modulation of Kv4 kinetics by KCHIP1 splice variants.* Mol Cell Neurosci, 2003. **24**(2): p. 357-66.

86. Braunewell, K.H. and A.J. Klein-Szanto, *Visinin-like proteins (VSNLs): interaction partners and emerging functions in signal transduction of a subfamily of neuronal Ca2+ -sensor proteins.* Cell Tissue Res, 2009. **335**(2): p. 301-16.

87. Buttgereit, J., *et al*., *Visinin-like protein 1 regulates natriuretic peptide receptor B in the heart.* Regul Pept, 2010. **161**(1-3): p. 51-7.

88. Paterlini, M., *et al*., *Expression of the neuronal calcium sensor protein family in the rat brain.* Neuroscience, 2000. **99**(2): p. 205-16.

89. Lin, L., *et al*., *The calcium sensor protein visinin-like protein-1 modulates the surface expression and agonist sensitivity of the alpha 4beta 2 nicotinic acetylcholine receptor.* J Biol Chem, 2002. **277**(44): p. 41872-8.

90. Dai, F.F., *et al*., *The neuronal Ca2+ sensor protein visinin-like protein-1 is expressed in pancreatic islets and regulates insulin secretion.* J Biol Chem, 2006. **281**(31): p. 21942-53.

91. Groblewska, M., *et al*., *The Role of Visinin-Like Protein-1 in the Pathophysiology of Alzheimer's Disease.* J Alzheimers Dis, 2015. **47**(1): p. 17-32.

92. Braunewell, K., *et al*., *Abnormal localization of two neuronal calcium sensor proteins, visinin-like proteins (vilips)-1 and -3, in neocortical brain areas of Alzheimer disease patients.* Dement Geriatr Cogn Disord, 2001. **12**(2): p. 110-6.

93. Schnurra, I., *et al*., *The neuronal calcium sensor protein VILIP1 is associated with amyloid plaques and extracellular tangles in Alzheimer's disease and promotes cell death and tau phosphorylation in vitro: a link between calcium sensors and Alzheimer's disease?* Neurobiol Dis, 2001. **8**(5): p. 900-9.

94. Tarawneh, R., *et al*., *Visinin-like protein-1: diagnostic and prognostic biomarker in Alzheimer disease.* Ann Neurol, 2011. **70**(2): p. 274-85.

95. Fagan, A.M., *et al*., *Longitudinal change in CSF biomarkers in autosomal-dominant Alzheimer's disease.* Sci Transl Med, 2014. **6**(226): p. 226ra30.

96. Mroczko, B., *et al*., *Evaluation of visinin-like protein 1 concentrations in the cerebrospinal fluid of patients with mild cognitive impairment as a dynamic biomarker of Alzheimer's disease.* J Alzheimers Dis, 2015. **43**(3): p. 1031-7.

97. Kester, M.I., *et al*., *Cerebrospinal fluid VILIP1 and YKL-40, candidate biomarkers to diagnose, predict and monitor Alzheimer's disease in a memory clinic cohort.* Alzheimers Res Ther, 2015. **7**(1): p. 59.

98. Zhao, C. and K.H. Braunewell, *Expression of the neuronal calcium sensor visinin-like protein-1 in the rat hippocampus.* Neuroscience, 2008. **153**(4): p. 1202-12.

99. Few, A.P., *et al*., *Differential regulation of CaV2.1 channels by calcium-binding protein 1 and visinin-like protein-2 requires N-terminal myristoylation.* J Neurosci, 2005. **25**(30): p. 7071-80.

100. Jheng, F.F., *et al*., *Functional contribution of Ca2+ and Mg2+ to the intermolecular interaction of visinin-like proteins.* Protein J, 2006. **25**(4): p. 250-6.

101. Spilker, C., *et al*., *The neuronal EF-hand calcium-binding protein visinin-like protein-3 is expressed in cerebellar Purkinje cells and shows a calcium-dependent membrane association.* Neuroscience, 2000. **96**(1): p. 121-9.

102. Spilker, C. and K.H. Braunewell, *Calcium-myristoyl switch, subcellular localization, and calcium-dependent translocation of the neuronal calcium sensor protein VILIP3, and comparison with VILIP1 in hippocampal neurons.* Mol Cell Neurosci, 2003. **24**(3): p. 766-78.

103. Hidaka, H. and K. Okazaki, *Neurocalcin family: a novel calcium-binding protein abundant in bovine central nervous system.* Neurosci Res, 1993. **16**(2): p. 73-7.

104. Duda, T., *et al*., *A novel calcium-regulated membrane guanylate cyclase transduction system in the olfactory neuroepithelium.* Biochemistry, 2001. **40**(40): p. 12067-77.

105. Venkataraman, V., *et al*., *Neurocalcin delta modulation of ROS-GC1, a new model of Ca(2+) signaling.* Biochemistry, 2008. **47**(25): p. 6590-601.

106. Kumar, V.D., *et al*., *A second calcium regulator of rod outer segment membrane guanylate cyclase, ROS-GC1: neurocalcin.* Biochemistry, 1999. **38**(39): p. 12614-20.

107. Ivings, L., *et al*., *Identification of Ca2+-dependent binding partners for the neuronal calcium sensor protein neurocalcin delta: interaction with actin, clathrin and tubulin.* Biochem J, 2002. **363**(Pt 3): p. 599-608.

108. Kuechler, A., *et al*., *Five patients with novel overlapping interstitial deletions in 8q22.2q22.3.* Am J Med Genet A, 2011. **155A**(8): p. 1857-64.

109. Isaksson, H.S., B. Sorbe, and T.K. Nilsson, *Whole genome expression profiling of blood cells in ovarian cancer patients -prognostic impact of the CYP1B1, MTSS1, NCALD, and NOP14.* Oncotarget, 2014. **5**(12): p. 4040-9.

110. Shi, X., *et al*., *Upregulation of long intergenic noncoding RNA 00673 promotes tumor proliferation via LSD1 interaction and repression of NCALD in non-small-cell lung cancer.* Oncotarget, 2016.

111. Takamatsu, K. and T. Noguchi, *Hippocalcin: a calcium-binding protein of the EF-hand superfamily dominantly expressed in the hippocampus.* Neurosci Res, 1993. **17**(4): p. 291-5.

112. Kobayashi, M., *et al*., *Hippocalcin-deficient mice display a defect in cAMP response element-binding protein activation associated with impaired spatial and associative memory.* Neuroscience, 2005. **133**(2): p. 471-84.

113. Charlesworth, G., *et al*., *Mutations in HPCA Cause Autosomal-Recessive Primary Isolated Dystonia.* The American Journal of Human Genetics. **96**(4): p. 657-665.

114. Kim, K.S., *et al*., *Hippocalcin and KCNQ channels contribute to the kinetics of the slow afterhyperpolarization.* Biophys J, 2012. **103**(12): p. 2446-54.

115. Moon, C., *et al*., *Calcium-sensitive particulate guanylyl cyclase as a modulator of cAMP in olfactory receptor neurons.* J Neurosci, 1998. **18**(9): p. 3195-205.

116. Mercer, E.A., *et al*., *NAIP interacts with hippocalcin and protects neurons against calcium-induced cell death through caspase-3-dependent and -independent pathways.* EMBO J, 2000. **19**(14): p. 3597-607.

117. Kobayashi, M., *et al*., *Hippocalcin mediates calcium-dependent translocation of brain-type creatine kinase (BB-CK) in hippocampal neurons.* Biochem Biophys Res Commun, 2012. **429**(3-4): p. 142-7.

118. Haynes, L.P., *et al*., *Analysis of the interacting partners of the neuronal calcium-binding proteins L-CaBP1, hippocalcin, NCS1 and neurocalcin delta.* Proteomics, 2006. **6**(6): p. 1822-32.

119. Kajimoto, Y., *et al*., *Molecular cloning of two additional members of the neural visinin-like Ca(2+)-binding protein gene family.* J Neurochem, 1993. **61**(3): p. 1091-6.

120. Cox, J.A., *et al*., *Cation binding and conformational changes in VILIP and NCS1, two neuron-specific calcium-binding proteins.* J Biol Chem, 1994. **269**(52): p. 32807-13.

121. Ladant, D., *Calcium and membrane binding properties of bovine neurocalcin delta expressed in Escherichia coli.* J Biol Chem, 1995. **270**(7): p. 3179-85.

122. O'Callaghan, D.W., A.V. Tepikin, and R.D. Burgoyne, *Dynamics and calcium sensitivity of the Ca2+/myristoyl switch protein hippocalcin in living cells.* J Cell Biol, 2003. **163**(4): p. 715-21.

123. Peshenko, I.V., *et al*., *Enzymatic properties and regulation of the native isozymes of retinal membrane guanylyl cyclase (RetGC) from mouse photoreceptors.* Biochemistry, 2011. **50**(25): p. 5590-600.

124. Viviano, J., *et al*., *Electrophoretic mobility shift in native gels indicates calcium-dependent structural changes of neuronal calcium sensor proteins.* Anal Biochem, 2016. **494**(February 1): p. 93-100.

125. Brunelle, J.L. and R. Green, *One-dimensional SDS-polyacrylamide gel electrophoresis (1D SDS-PAGE).* Methods Enzymol, 2014. **541**: p. 151-9.

126. Laemmli, U.K., *Cleavage of structural proteins during the assembly of the head of bacteriophage T4.* Nature, 1970. **227**(5259): p. 680-5.

127. Hruz, T., *et al*., *Genevestigator v3: a reference expression database for the meta-analysis of transcriptomes.* Adv Bioinformatics, 2008. **2008**: p. 420747.

128. Su, A.I., *et al*., *A gene atlas of the mouse and human protein-encoding transcriptomes.* Proc Natl Acad Sci U S A, 2004. **101**(16): p. 6062-7.

129. Uhlen, M., *et al*., *Towards a knowledge-based Human Protein Atlas.* Nat Biotechnol, 2010. **28**(12): p. 1248-50.

130. Uhlen, M., *et al*., *A human protein atlas for normal and cancer tissues based on antibody proteomics.* Mol Cell Proteomics, 2005. **4**(12): p. 1920-32.

131. Ponten, F., *et al*., *A global view of protein expression in human cells, tissues, and organs.* Mol Syst Biol, 2009. **5**: p. 337.

132. Wang, M., *et al*., *PaxDb, a database of protein abundance averages across all three domains of life.* Mol Cell Proteomics, 2012. **11**(8): p. 492-500.

133. Maruyama, K., T. Mikawa, and S. Ebashi, *Detection of calcium binding proteins by 45Ca autoradiography on nitrocellulose membrane after sodium dodecyl sulfate gel electrophoresis.* J Biochem, 1984. **95**(2): p. 511-9.

134. Detwiler, P., *Open the loop: dissecting feedback regulation of a second messenger transduction cascade.* Neuron, 2002. **36**(1): p. 3-4.

135. Pugh, E.N., Jr. and T.D. Lamb, *Cyclic GMP and calcium: the internal messengers of excitation and adaptation in vertebrate photoreceptors.* Vision Res, 1990. **30**(12): p. 1923-48.

136. Pertzev, A., T. Duda, and R.K. Sharma, *Ca(2+) sensor GCAP1: A constitutive element of the ONE-GC-modulated odorant signal transduction pathway.* Biochemistry, 2010. **49**(34): p. 7303-13.

137. Brackmann, M., *et al*., *Neuronal Ca2+ sensor protein VILIP1 affects cGMP signalling of guanylyl cyclase B by regulating clathrin-dependent receptor recycling in hippocampal neurons.* J Cell Sci, 2005. **118**(Pt 11): p. 2495-505.

138. Fik-Rymarkiewicz, E., T. Duda, and R.K. Sharma, *Novel frequenin-modulated Ca2+-signaling membrane guanylate cyclase (ROS-GC) transduction pathway in bovine hippocampus.* Mol Cell Biochem, 2006. **291**(1-2): p. 187-204.

139. Wang, K., *Modulation by clamping: Kv4 and KChIP interactions.* Neurochem Res, 2008. **33**(10): p. 1964-9.

140. Link, W.A., *et al*., *Day-night changes in downstream regulatory element antagonist modulator/potassium channel interacting protein activity contribute to circadian gene expression in pineal gland.* J Neurosci, 2004. **24**(23): p. 5346-55.

141. Chen, C.K., *Recoverin and rhodopsin kinase.* Adv Exp Med Biol, 2002. **514**: p. 101-7.

142. Koch, K.W., *Biophysical investigation of retinal calcium sensor function.* Biochim Biophys Acta, 2012. **1820**(8): p. 1228-33.

143. Ermilov, A.N., E.V. Olshevskaya, and A.M. Dizhoor, *Instead of binding calcium, one of the EF-hand structures in guanylyl cyclase activating protein-2 is required for targeting photoreceptor guanylyl cyclase.* J Biol Chem, 2001. **276**(51): p. 48143-8.

144. Imanishi, Y., *et al*., *Diversity of guanylate cyclase-activating proteins (GCAPs) in teleost fish: characterization of three novel GCAPs (GCAP4, GCAP5, GCAP7) from zebrafish (Danio rerio) and prediction of eight GCAPs (GCAP1-8) in pufferfish (Fugu rubripes).* J Mol Evol, 2004. **59**(2): p. 204-17.

145. Lusin, J.D., *et al*., *NMR structure of DREAM: Implications for Ca(2+)-dependent DNA binding and protein dimerization.* Biochemistry, 2008. **47**(8): p. 2252-64.

146. Fisher, J.R., *et al*., *Purification of myristoylated and nonmyristoylated neuronal calcium sensor-1 using single-step hydrophobic interaction chromatography.* Protein Expr Purif, 2000. **20**(1): p. 66-72.

147. Kobayashi, M., *et al*., *Molecular cloning of hippocalcin, a novel calcium-binding protein of the recoverin family exclusively expressed in hippocampus.* Biochem Biophys Res Commun, 1992. **189**(1): p. 511-7.

148. Peshenko, I.V., *et al*., *Calcium-myristoyl Tug is a new mechanism for intramolecular tuning of calcium sensitivity and target enzyme interaction for guanylyl cyclase-activating protein 1: dynamic connection between N-fatty acyl group and EF-hand controls calcium sensitivity.* J Biol Chem, 2012. **287**(17): p. 13972-84.

149. Viviano, J., Krishnan, A., Wu, H., Venkataraman, V., *Electrophoretic Mobility Shift in Native Gels Indicates Calcium-dependent Structural Changes of Neuronal Calcium Sensor Proteins.* Analytical Biochemistry, 2015. **In Press**.

150. Viviano, J., Krishnan, A., Scully, J., Wu, H., Venkataraman, V., *Mobility retardation of NCS proteins is specifically induced by Calcium, but not Magnesium, Barium or Strontium.* Data in Brief, 2015. **In Press**.

151. Viviano, J., Wu, H.,Krishnan, A., Venkataraman, V., *Myristoylation enhances, but is not essential for, calcium-induced mobility shift of neurocalcin delta on native gels.* Data in Brief, 2015: p. In Press.

152. Kobayashi, M., *et al*., *Myristoylation of hippocalcin is linked to its calcium-dependent membrane association properties.* J Biol Chem, 1993. **268**(25): p. 18898-904.

153. Palmer, C.L., *et al*., *Hippocalcin functions as a calcium sensor in hippocampal LTD.* Neuron, 2005. **47**(4): p. 487-94.

154. Ohshima, H., *Electrophoresis of soft particles: analytic approximations.* Electrophoresis, 2006. **27**(3): p. 526-33.

155. Chae, K.S. and A.M. Lenhoff, *Computation of the electrophoretic mobility of proteins.* Biophys J, 1995. **68**(3): p. 1120-7.

156. Kim, J.Y., *et al*., *Electrophoretic mobility equation for protein with molecular shape and charge multipole effects.* J Colloid Interface Sci, 2006. **299**(1): p. 486-92.

157. Winzor, D.J., S. Jones, and S.E. Harding, *Determination of protein charge by capillary zone electrophoresis.* Anal Biochem, 2004. **333**(2): p. 225-9.

158. Weber, K. and M. Osborn, *The reliability of molecular weight determinations by dodecyl sulfate-polyacrylamide gel electrophoresis.* J Biol Chem, 1969. **244**(16): p. 4406-12.

159. Burgoyne, J.R. and P. Eaton, *Contemporary techniques for detecting and identifying proteins susceptible to reversible thiol oxidation.* Biochem Soc Trans, 2011. **39**(5): p. 1260-7.

160. Gianazza, E., J. Crawford, and I. Miller, *Detecting oxidative post-translational modifications in proteins.* Amino Acids, 2007. **33**(1): p. 51-6.

161. Miksik, I. and Z. Deyl, *Post-translational non-enzymatic modification of proteins. II. Separation of selected protein species after glycation and other*

carbonyl-mediated modifications. J Chromatogr B Biomed Sci Appl, 1997. **699**(1-2): p. 311-45.

162. Kinoshita-Kikuta, E., E. Kinoshita, and T. Koike, *Separation and identification of four distinct serine-phosphorylation states of ovalbumin by Phos-tag affinity electrophoresis.* Electrophoresis, 2012. **33**(5): p. 849-55.

163. Frins, S., *et al*., *Functional characterization of a guanylyl cyclase-activating protein from vertebrate rods. Cloning, heterologous expression, and localization.* J Biol Chem, 1996. **271**(14): p. 8022-7.

164. Helten, A. and K.W. Koch, *Calcium-dependent conformational changes in guanylate cyclase-activating protein 2 monitored by cysteine accessibility.* Biochem Biophys Res Commun, 2007. **356**(3): p. 687-92.

165. Hwang, J.Y. and K.W. Koch, *The myristoylation of the neuronal Ca2+ -sensors guanylate cyclase-activating protein 1 and 2.* Biochim Biophys Acta, 2002. **1600**(1-2): p. 111-7.

166. Viviano, J., Krishnan, A., Scully, J., Wu, H., Venkataraman, V., *Mobility Retardation of NCS proteins is specifically induced by Calcium, but not Magnesium, Barium or Strontium.* Analytical Biochemistry, 2015. **In Press**.

167. Marshak, D.R., D.M. Watterson, and L.J. Van Eldik, *Calcium-dependent interaction of S100b, troponin C, and calmodulin with an immobilized phenothiazine.* Proc Natl Acad Sci U S A, 1981. **78**(11): p. 6793-7.

168. Baudier, J., N. Glasser, and D. Gerard, *Ions binding to S100 proteins. I. Calcium- and zinc-binding properties of bovine brain S100 alpha alpha, S100a (alpha beta), and S100b (beta beta) protein: Zn2+ regulates Ca2+ binding on S100b protein.* J Biol Chem, 1986. **261**(18): p. 8192-203.

169. Gilli, R., *et al*., *Thermodynamic analysis of calcium and magnesium binding to calmodulin.* Biochemistry, 1998. **37**(16): p. 5450-6.

170. Haiech, J., C.B. Klee, and J.G. Demaille, *Effects of cations on affinity of calmodulin for calcium: ordered binding of calcium ions allows the specific activation of calmodulin-stimulated enzymes.* Biochemistry, 1981. **20**(13): p. 3890-7.

171. Linse, S., A. Helmersson, and S. Forsen, *Calcium binding to calmodulin and its globular domains.* J Biol Chem, 1991. **266**(13): p. 8050-4.

172. Gifford, J.L., M.P. Walsh, and H.J. Vogel, *Structures and metal-ion-binding properties of the Ca2+-binding helix-loop-helix EF-hand motifs.* Biochem J, 2007. **405**(2): p. 199-221.

173. Mikhaylova, M., J. Hradsky, and M.R. Kreutz, *Between promiscuity and specificity: novel roles of EF-hand calcium sensors in neuronal Ca2+ signalling.* J Neurochem, 2011. **118**(5): p. 695-713.

174. Ikura, M., *Calcium binding and conformational response in EF-hand proteins.* Trends Biochem Sci, 1996. **21**(1): p. 14-7.

175. Zozulya, S., D. Ladant, and L. Stryer, *Expression and characterization of calcium-myristoyl switch proteins.* Methods Enzymol, 1995. **250**: p. 383-93.

176. Viviano, J., Wu, H.,Krishnan, A., Venkataraman, V., *Myristoylation enhances, but is not essential for, calcium-induced mobility shift of neurocalcin delta on native gels.* Analytical Biochemistry, 2015: p. In Press.

177. Ferguson, K.A., *Starch-Gel Electrophoresis--Application to the Classification of Pituitary Proteins and Polypeptides.* Metabolism, 1964. **13**: p. SUPPL:985-1002.

178. Vijay-Kumar, S. and V.D. Kumar, *Crystal structure of recombinant bovine neurocalcin.* Nat Struct Biol, 1999. **6**(1): p. 80-8.

179. Dovgan, A.V., *et al*., *Decoding glutamate receptor activation by the Ca2+ sensor protein hippocalcin in rat hippocampal neurons.* Eur J Neurosci, 2010. **32**(3): p. 347-58.

180. Markova, O., *et al*., *Hippocalcin signaling via site-specific translocation in hippocampal neurons.* Neurosci Lett, 2008. **442**(2): p. 152-7.

181. Ohki, S., M. Ikura, and M. Zhang, *Identification of Mg2+-binding sites and the role of Mg2+ on target recognition by calmodulin.* Biochemistry, 1997. **36**(14): p. 4309-16.

182. Senguen, F.T. and Z. Grabarek, *X-ray structures of magnesium and manganese complexes with the N-terminal domain of calmodulin: insights into the mechanism and specificity of metal ion binding to an EF-hand.* Biochemistry, 2012. **51**(31): p. 6182-94.

183. Peshenko, I.V., E.V. Olshevskaya, and A.M. Dizhoor, *Binding of guanylyl cyclase activating protein 1 (GCAP1) to retinal guanylyl cyclase (RetGC1). The role of individual EF-hands.* J Biol Chem, 2008. **283**(31): p. 21747-57.

184. Lim, S., *et al*., *Effects of Ca2+, Mg2+, and myristoylation on guanylyl cyclase activating protein 1 structure and stability.* Biochemistry, 2009. **48**(5): p. 850-62.

185. Peshenko, I.V. and A.M. Dizhoor, *Activation and inhibition of photoreceptor guanylyl cyclase by guanylyl cyclase activating protein 1 (GCAP-1): the functional role of Mg2+/Ca2+ exchange in EF-hand domains.* J Biol Chem, 2007. **282**(30): p. 21645-52.

186. Burgess, W.H., D.K. Jemiolo, and R.H. Kretsinger, *Interaction of calcium and calmodulin in the presence of sodium dodecyl sulfate.* Biochim Biophys Acta, 1980. **623**(2): p. 257-70.

187. Kuo, H.C., *et al*., *A defect in the Kv channel-interacting protein 2 (KChIP2) gene leads to a complete loss of I(to) and confers susceptibility to ventricular tachycardia.* Cell, 2001. **107**(6): p. 801-13.

188. Balint, B. and K.P. Bhatia, *Dystonia: an update on phenomenology, classification, pathogenesis and treatment.* Curr Opin Neurol, 2014. **27**(4): p. 468-76.

189. Surgeons, A.A.o.N. *Dystonia*. 2016; Available from: http://www.aans.org/patient information/conditions and treatments/dystonia.aspx.

Abbreviations

aa- Amino Acid
CALM- Calmodulin
cAMP - adenylyl cyclase monophosphate
cGMP- 3',5'-cyclic guanosine monophosphate
DRE- Downstream Regulatory Element
FRQN- Frequenin
GCAP-1-Guanylyl-Cyclase Activating Protein 1
GCAP-2- Guanylyl-Cyclase Activating Protein 2
GCAP-3- Guanylyl-Cyclase Activating Protein 3
GCAPs- Guanylyl-Cyclase Activating Proteins
GCs- Guanylate cyclases
GTP- guanosine triphosphate
HPCA- Hippocalcin
HPCL1- Hippocalcin-like protein 1
HPCL4- Hippocalcin-like protein 1
KChIP1- Potassium Channel-Interacting Protein 1
KChIP2- Potassium Channel-Interacting Protein 2
KChIP3- Potassium Channel-Interacting Protein 3
KChIP4- Potassium Channel-Interacting Protein 4
Mry- Myristoyl
nAChR- α4β2 nicotinic acetylcholine receptors
NAIP- Neuronal Apoptosis Inhibitor Protein
NCALD-Neurocalcin Delta
NCS- Neuronal Calcium Sensor
NCS1 (Frequnin)- Neuronal calcium sensor 1
ONE-GC- Olfactory Neuro-Epithelial Guanylate cyclases
RCVRN-Recoverin
ROSGC- Retinal outer segment Guanylate cyclases
VILIPs- Visinin-Like Proteins
VSNL1- Visinin-Like Proteins-1

Attributes

Chapter 4.1

Figure 4.1-1- Jeffrey Viviano, Hao Wu
Figure 4.1-2- Jeffrey Viviano
Figure 4.1-3- Jeffrey Viviano
Figure 4.1-4- Jeffrey Viviano
Figure 4.1-5- Jeffrey Viviano , Hao Wu

Chapter 4.2

Figure 4.2-1- Jeffrey Viviano
Figure 4.2-2- Jeffrey Viviano, Anu Krishnan
Figure 4.2-3- Jeffrey Viviano, Yaroslav Morotov
Table 4.2-1- Jeffrey Viviano
Figure 4.2-4- Jeffrey Viviano
Figure 4.2-5-Anu Krishnan, Jeffrey Viviano

Chapter 4.3

Table 4.3-1- Jeffrey Viviano
Figure 4.3-1- Jeffrey Viviano
Figure 4.3-2- Jeffrey Viviano
Figure 4.3-3- Jeffrey Viviano
Figure 4.3-4- Jeffrey Viviano
Figure 4.3-5- Jeffrey Viviano
Figure 4.3-6- Jeffrey Viviano,
Figure 4.3-7- Jeffrey Viviano
Figure 4.3-8- Jeffrey Viviano
Figure 4.3-9- Jeffrey Viviano
Table 4.3-2- Jeffrey Viviano
Figure 4.3-10- Jeffrey Viviano
Figure 4.3-11- Jeffrey Viviano
Figure 4.3-12- Jeffrey Viviano
Figure 4.3-13- Jeffrey Viviano

Chapter 4.4

Table 4.4-1- Jeffrey Viviano
Figure 4.4-1- Jeffrey Viviano
Figure 4.4-2- Jeffrey Viviano
Figure 4.4-3- Jeffrey Viviano, Venkat Venkataraman
Figure 4.4-4- Jeffrey Viviano
Figure 4.4-5- Jeffrey Viviano

Figure 4.4-6- Jeffrey Viviano, Anu Krishnan
Figure 4.4-7- Jeffrey Viviano
Figure 4.4-8- Jeffrey Viviano, Anu Krishnan

Chapter 4.5

Figure 4.5-1- Jeffrey Viviano
Figure 4.5-2- Jeffrey Viviano, Sunkesula Sagar
Figure 4.5-3- Jeffrey Viviano
Figure 4.5-4- Jeffrey Viviano
Figure 4.5-5- Jeffrey Viviano
Figure 4.5-6- Jeffrey Viviano
Figure 4.5-7- Jeffrey Viviano

Chapter 4.6

Figure 4.6-1- Jeffrey Viviano
Figure 4.6-2- Jeffrey Viviano
Figure 4.6-3- Jeffrey Viviano
Figure 4.6-4- Jeffrey Viviano
Figure 4.6-5- Jeffrey Viviano
Figure 4.6-6- Jeffrey Viviano,
Figure 4.6-7- Jeffrey Viviano, Jingyi Zhang
Figure 4.6-8- Jeffrey Viviano, Jingyi Zhang

Chapter 5.4

5.4-1- Jeffrey Viviano

Chapter 5.7

5.7-1- Jeffrey Viviano